Synthesis and Experimental Investigation of Copper Matrix Hybrid Composite Reinforced with Sic/Gr/Cr and Optimization of Extrusion Parameter for Further Property Enhancement

Mekonnen Girma Dimbushe

A Thesis Submitted to Department of Mechanical Engineering
School of Mechanical, Chemical and Materials Engineering

Presented in Partial Fulfillment of the Requirement for the Degree of Master's in Manufacturing Engineering

Office of Graduate Studies
Adama Science and Technology University

July-2023
Adama, Ethiopia

Synthesis and Experimental Investigation of Copper Matrix Hybrid Composite Reinforced with Sic/Gr/Cr and Optimization of Extrusion Parameter for Further Property Enhancement

Mekonnen Girma Dimbushe

Advisor: Moera Gutu Jiru (Associate professor)

A Thesis Submitted to Department of Mechanical Engineering School of Mechanical, Chemical and Materials Engineering

Presented in Partial Fulfillment of the Requirement for the Degree of Master's in Manufacturing Engineering

Office of Graduate Studies
Adama Science and Technology University

July-2023
Adama, Ethiopia

DECLARATION

I hereby declare that this Master Thesis entitled "**Synthesis and Experimental Investigation of Copper Matrix Hybrid Composite Reinforced with Sic/Gr/Cr and Optimization of Extrusion Parameter for Further Property Enhancement**" is my original work. That is, it has not been submitted for the award of any academic degree, diploma or certificate in any other university. All sources of materials that are used for this thesis have been duly acknowledged through citation.

Mekonnen Girma Dimbushe	______________	__________
Name	Signature	Date

RECOMMENDATION

We, the advisors of this thesis, hereby certify that we have read the final version of the thesis entitled "**Synthesis and Experimental Investigation of Copper Matrix Hybrid Composite Reinforced with Sic/Gr/Cr and Optimization of Extrusion Parameter for Further Property Enhancement**" Prepared under our guidance by Mekonnen Girma Dimbushe submitted in partial fulfillment of the requirements for the degree of Mater's of Science in Manufacturing Engineering. Therefore, we recommend the submission of the final revised version of the thesis to the department following the applicable procedures.

______________________	______________________	______________
Advisor	**Signature**	**Date**
______________________	______________________	______________
Co-advisor	**Signature**	**Date**

APPROVAL SHEET

I, the advisors of the thesis entitled "**Synthesis and Experimental Investigation of Copper Matrix Hybrid Composite Reinforced with Sic/Gr/Cr and Optimization of Extrusion Parameter for Further Property Enhancement**" and developed by **Mekonnen Girma Dimbushe**, hereby certify that the recommendation and suggestions made by the board of examiners are appropriately incorporated into the final version of the thesis.

______________________	______________________	______________
Major Advisor/Supervisor	Signature	Date

We, the undersigned, members of the Board of Examiners of the thesis by **Mekonnen Girma** have read and evaluated the thesis entitled "**Synthesis and Experimental Investigation of Copper Matrix Hybrid Composite Reinforced with Sic/Gr/Cr and Optimization of Extrusion Parameter for Further Property Enhancement**" and examined the candidate during open defense. This is, therefore, to certify that the thesis is accepted for partial fulfillment of the requirement of the degree of Master of Science in **Manufacturing Engineering.**

______________________	______________________	______________
Chairperson	Signature	Date
______________________	______________________	______________
Internal Examiner	Signature	Date
Mestin Gizaw (PhD)		15 August/2023
Eternal Examiner	Signature	Date

Finally, approval and acceptance of the thesis is contingent upon the submission of its final copy to the Office of Postgraduate Studies (OPGS) through the Department Graduate Council (DGC) and School Graduate Committee (SGC).

______________________	______________________	______________
Department Head	Signature	Date
______________________	______________________	______________
School Dean	Signature	Date
______________________	______________________	______________
Office of Postgraduate Studies, Dean	Signature	Date

ACKNOWLEDGEMENT

I would like to thank and praise the Almighty Lord for all the blessing and patience he gives me to successfully complete this thesis. I would like to express my deepest gratitude to my advisor, Dr. Moera Gutu Jiru, for his guidance, support, encouragement, and patience throughout my study at Adama Science and Technology University. I would also like to thank Dr. Davendra Kumahar Sihna for helpful discussions, Supports and suggestions. I am very grateful to my brother too, Mr. Cherinet Girma for his valuable supports, suggestions and comments. Special thanks to Mr. Kuba Defaru for all of his untapped support and guidance in all aspects. I would like to extend my sincere appreciation to the mechanical engineering department head Mr. Bariso Bino for his endless support. I would like to thank Material Science and Engineering Department of Adama Science and Technology University for providing experimental work. Special thanks to Mr. Kanate Sanbaba and Mr. Biruk Sisay from material science and engineering department for their technical support and encouragement during experimental work.

I would like to express my immense gratitude and profound thanks to all those who have helped me in different ways during the tenure of my MSc. work at Adama Science and Technology University. My sincere apologies, if I have inadvertently missed out a few names.

TABLE OF CONTENTS

DECLARATION i

RECOMMENDATION ii

APPROVAL SHEET iii

ACKNOWLEDGEMENT iv

TABLE OF CONTENTS v

LIST OF FIGURES ix

LIST OF TABLES x

LIST OF ACRONYMS xi

ABSTRACT xii

CHAPTER ONE 1

INTRODUCTION 1

1.1 Background 1

1.2 Application area of copper matrix composites 3

1.3 Motivation of research 3

1.4 Problem Statement 4

1.5 Objectives of this study 5

1.5.1 General Objective 5

1.5.2 Specific Objective 5

1.6 Significance of the study 5

1.7 Scope of the study 6

1.8 Thesis organization 6

CHAPTER TWO 7

LITERATURE REVIEW 7

2.1 Introduction to Composite. 7

2.1.1 Classification of composite 7

2.1.2 Metal matrix composite 8

2.1.3 Copper matrix composite 8

2.2 Fabrication process 9

2.2.1 Solid state processing 9
2.2.2 Liquid state processing 9
2.2.3 Stir casting processing parameters 10
2.3 Selection of reinforcement 12
2.3.1 Graphite reinforced composite 12
2.3.2 Chromium reinforced composite 13
2.3.3 Silicon carbide reinforced composites 13
2.4 Effect of reinforcement on mechanical properties 14
2.5 Wear performance of copper matrix composite 17
2.6 Electrical and corrosion behavior of CuMMC's 19
2.7 Secondary Process 21
2.7.1 Extrusion 22
2.7.2 Classification of extrusion 22
2.7.3 Effect of extrusion on mechanical properties 23
2.8 Finite Element Analysis 24
2.9 Multi response optimization 25
2.10 Literature Summary 26
2.11 Research Gap 26
CHAPTER THREE 28
MATERIALS AND METHODOLOGY 28
3.1 Introduction 28
3.2 Materials 28
3.2.1 Copper alloy 28
3.2.2 Silicon Carbide (SiC) Reinforcement 29
3.2.3 Graphite 30
3.2.4 Chromium 30
3.2.5 Die Material (H13 Tool Steel) 31
3.3 Research Methodology Flow Chart 32
3.3.1 Identifying matrix and reinforcement 34
3.3.2 Experimental design for fabrication of composite 34
3.3.3 Weight (in mass) estimation for matrix and reinforcement inquires 35
3.3.4 Tools and Equipment 38

3.3.5 Fabrication Composite Procedure 39
3.3.6 Specimen preparation for tests 40
3.3.7 Microstructural characterization of composite 41
3.3.8 Density and Porosity Measurement 42
3.3.9 Hardness test 44
3.3.10 Compression test 44
3.3.11 Corrosion test 45
3.3.12 Electrical conductivity test 46
3.4 Finite element analysis of hot deformation 47
3.4.1 Input material data 48
3.4.2 Experimental design for simulation 50
3.5 Secondary process operation 51
3.5.1 Design and Fabrication of die parts 51
3.5.2 Hot extrusion process 52
3.6 Analysis of material behavior and optimization of material properties as per L16 orthogonal array 53
3.6.1 Taguchi based Grey relational analysis method 53
3.6.2 Taguchi's Orthogonal Array 54
3.6.3 Signal-Noise Ratio Analysis 54
3.6.4 Analysis of Variance (ANOVA) 55
3.6.5 Optimization Steps Used in Grey Relational Analysis 55
CHAPTER 4 57
RESULTS AND DISCUSSION 57
4.1 Introduction 57
4.2 Analysis of density and Porosity of Composite 57
4.3 Electrical behavior analysis 59
4.4 Analysis of hardness for composite 60
4.5 Compression test 61
4.6 Microstructure of casted composite 63
4.6.1 Optical microscopy 64
4.6.2 Scanning electron microscopy 65
4.7 Analysis of corrosion rate 66
4.8 Selection of sample for hot extrusion 69

4.9 Simulation result for hot extrusion 71
4.9.1 Analysis of damage percentage 72
4.9.2 Analysis of Extrusion Load 77
4.10 Analysis of results after extrusion process 89
CONCLUSION AND RECOMMENDATION 93
5.1 Conclusion 93
5.2 Recommendation 94
REFERENCES 96
Appendix II: Microstructural image of composite from SEM 108
Appendix III: Microstructural image of composite from optical microscope 109
Appendix IV: calculation of current density from Tafel plot 110
Appendix V: damage distribution of Cu-6SiC-1Gr-2Cr via numerical simulation of hot extrusion 111
Appendix VI: predicted extrusion load of Cu-6SiC-1Gr-2Cr via numerical simulation of hot extrusion 112
Appendix VII: IV curve characteristics for electrical conductivity test 113
Appendix VIII: Percentage value of f distribution 114

LIST OF FIGURES

Figure 2-1 Schematic diagram of stir casting 10
Figure 3-1Research methodology flow chart 33
Figure 3-2 Fabrication of composites (a) stir casting setup (b) fabricated sample 39
Figure 3-3 Lathe machine setup for sample preparation 40
Figure 3-4 Sample preparation for microstructure 42
Figure 3-5 Vickers hardness testing machine set up 44
Figure 3-6 Universal testing machine (UTM) setup for compression test 45
Figure 3-7 Corrosion test set up........ 46
Figure 3-8 Precision source measuring unit set up for electrical conductivity test 46
Figure 3-9 Meshed model of simulation setup 51
Figure 3-10 simulation setup at different step 51
Figure 3-11 Die fabrication setup and fabricated die 52
Figure 3-12 Hot extrusion setup 53
Figure 4-1 Actual and theoretical density of Cu-SiC-Gr-Cr hybrid composite........ 58
Figure 4-2 Electrical conductivity of Cu-SiC-Gr-Cr hybrid composite 60
Figure 4-3 Hardness value of Cu/SiC/Gr/Cr hybrid composite........ 61
Figure 4-4 Compression strength of copper matrix hybrid composites 63
Figure 4-5 Stress-strain diagrams for Cu-6SiC-2Cr-1Gr hybrid composite........ 63
Figure 4-6 Image of optical microscopy for........ 65
Figure 4-7 SEM image for selected samples 66
Figure 4-8Tafel plot of copper matrix hybrid composite 68
Figure 4-9 Main effect plot for SN ratio........ 74
Figure 4-10 Damage distribution over the surface of composite 76
Figure 4-11 Normal probability plot of damage........ 76
Figure 4-12 Main effect plot for SN ratios for extrusion load parameters 79
Figure 4-13 extrusion load distribution over surface of composites 81
Figure 4-14 Normal probability plot of extrusion load 82
Figure 4-15 Main effect plot for SN ratios for multi-response parameters 87
Figure 4-16 Simulation result for confirmation result 88
Figure 4-17 Hardness of extruded. 90

LIST OF TABLES

Table 3.1 Properties of C15100 29
Table 3.2 Properties of Silicon Carbide (SiC) 29
Table 3.3 Properties of Graphite 30
Table 3.4 Properties of chromium 31
Table 3.5 Properties of H13 tool steel 31
Table 3.6 Composition of H13 tool steel 32
Table 3.7 Process parameter and their levels 34
Table 3.8 Experimental design for fabrication 35
Table 3.9 List of equipment and tools used in research 38
Table 3.10 Theoretical and Actual density of composites 43
Table 3.11 Extrusion parameter and their levels 50
Table 4.1 Composition and sample designation of composite 57
Table 4.2 Porosity level and variations in theoretical and actual density values 59
Table 4.3 Hardness values of Cu/SiC/Gr/Cr hybrid composite 61
Table 4.4 Electrochemical corrosion for casted specimens in 3.5% NaCl solution 67
Table 4.5 Experimental data and S/N ratio for response of Cu-SiC-Cr-Gr composites 69
Table 4.6 Normalized data of multi-responses 70
Table 4.7 Deviation sequence of normalized data 70
Table 4.8 Grey relational coefficient and grey relational grade with $\boldsymbol{\delta} = 0.5$ 70
Table 4.9 data required to define material and assumption made for simulation 71
Table 4.10 Simulation result for damage percentage 72
Table 4.11 Signal to Noise Ratios for the damage percentage (smaller the better) 73
Table 4.12 The optimum conditions for damage result prediction-settings 74
Table 4.13 ANOVA result on the damage percentage 75
Table 4.14 Numerical simulation result for extrusion load 77
Table 4.15 Signal to Noise Ratios for the damage percentage (smaller the better) 78
Table 4.16 The optimum conditions for extrusion load result prediction-settings 80
Table 4.17 Analysis of Variance of tensile toughness of Composite 80
Table 4.18 Simulation responses at different levels of extrusion process parameter 83
Table 4.19 Experimental results and S/N ratio of response values 84
Table 4.20 Normalized data of the experimental results 84
Table 4.21 Deviation sequence and Grey relational coefficient with $\boldsymbol{\delta} = 0.5$ 85
Table 4.22 Signal to Noise Ratios for GRG for larger is better 86
Table 4.23 density and hardness of extruded sample 90

LIST OF ACRONYMS

Al MMC	Aluminum Metal Matrix Composite
ANOVA	Analysis of variance
ASTM	American Society for Testing and Materials
Co	Cobalt
Cr	Chromium
Cu	Copper
CuMMC	Copper Metal Matrix composite
Gr	Graphite
H2SO4	Sulfuric Acid
MMC	Metal Matrix Composite
MoS2	Molybdenum disulphide
Ni	Nickel
S/N	Signal to Noise Ratio
SEM	Scanning Electron Microscopy
SiC	Silicon Carbide
Ti	Titanium
TiB	Titanium Boride
TiB2	Titanium Diboride
TiC	Titanium carbide
TiO2	Titanium oxide
WC	Tungsten Carbide
XRD	X-ray diffraction

ABSTRACT

Copper matrix composites (CuMMC) overcome the constraints of pure copper by providing high strength, wear resistance, and corrosion resistance while maintaining excellent electrical and thermal conductivity. CuMMC is thus a promising material for a wide range of applications including heat exchangers, resistance welding electrodes, and maritime components. This study was aimed to fabricate silicon carbide reinforced copper matrix hybrid composite with addition of 1%Gr and 2%Cr to enhance good wettability between molten copper and solid reinforcement. Five samples were synthesized using stir casting with varying weight percentage of silicon carbide (0,3, 6, 9 and 12 wt.%) at 500rpm stirring speed, 30-minute stirring time and 1200 stirring temperature. Porosity percentage, hardness, electrical conductivity, compression strength and corrosion resistance properties of fabricated samples were investigated and analyzed. Test results demonstrated that the addition of SiC-Gr-Cr improved hardness and corrosion resistance when compared to commercial copper, however increasing the amount of reinforcement lowered electrical conductivity. The addition of SiC-Gr-Cr up to 12%wt enhanced compression strength, although when the amount of reinforcement approaches 15% wt., the compressive strength of the composite decreased due to an increased in brittleness. Cu-6SiC-2Cr-1Gr with overall enhanced properties was selected using Grey Relational analysis (GRA) technique for secondary process for further enhancement of properties. DEFORM 3D was employed for numerical simulation of hot extrusion at varying extrusion ratio (2,3,4 and 5), ram speed (1,2,3 and 4 mm/s) and billet temperature (800, 850, 900 and 950°C). Damage percentage and extrusion load were measured and analyzed as single response characteristics using Taguchi's S/N ratio and as multi-response characteristics using Hybrid Taguchi Grey Relational Analysis (HTGRA). The findings revealed that both damage and extrusion load was increased with increasing extrusion ratio of cosine dieCu-6SiC-2Cr-1Gr composite was finally extruded with optimum combination of parameter using extruder machine. Finding obtained after extrusion shows that porosity percentage was decreased from 2.71% to 1.57% when compared to sample before extrusion. Compression strength and hardness of Cu-6SiC-2Cr-1Gr were improved by 21.4% and 17.4% following extrusion although electrical conductivity showed slight decrement. This research work is expected to help all industries and researchers working in this area of focus.

Key words: copper matrix composite, stir casting, Grey relational analysis, numerical simulation, hot extrusion

CHAPTER ONE

INTRODUCTION

1.1 Background

Composite is defined as combination of two or more material differing in form and composition to achieve unattained properties in individual materials (Anil Kumar et al., 2016).based on their fundamental material or matrix, composite materials can be divided into three categories: polymer, metal-based, or ceramic-based. metal matrix composites are type of material where a standard metal or alloy serves as the base and is strengthened by another material(Sankhla and Patel, 2021). Composites fabricated using metal matrix (MMC) has currently a lot of interest in by researchers, due to their higher mechanical properties. Metal matrices in a composite materials provide more strength, fracture toughness, and stiffness than their polymer equivalents (Anil Kumar et al., 2016). Magnesium, Aluminum, and Titanium are the most popular metals utilized as matrix in MMC(Sankhla and Patel, 2021). Hybrid Metal Matrix Composites (HMMCs) are a type of metal-matrix composite in which homogeneous reinforcements with different particle sizes or heterogeneous particles with identical particle size or heterogeneous with different particle size are used in their structure to improve metal mechanical, electrical, and tribological properties. When dual reinforcements are used in a metal matrix, the elastic modulus, tensile strength, hardness, and tribological properties improve more than when single reinforcement is used, while the thermal expansion coefficient decreases (Akbarpour et al., 2019).

Copper and its alloys are widely employed in a variety of industries due to major qualities such as superior thermal and electrical conductivity, corrosion resistance, non-magneticity, stability at high temperatures, and so on. An additional reinforcement must be applied to the copper matrix to improve strength and wear resistance (Balamurugan and Uthayakumar,2015). The development of Cu-MMC is based on the use of ceramics as reinforcements, with alumina, silicon carbide, titanium carbide, and graphite being the most commonly used. The importance of ceramic particles in enhancing copper performance cannot be overstated. The copper matrix is pinched by the reinforced phase particles, inhibiting copper grain development and ultimately producing the effect of grain refining. According to the Hall-Petch formula's empirical relationship between strength and grain size, an increase in the number of grain boundaries slows the movement of dislocations and boosts material strength (Qin et al., 2020).

Mechanical properties, wear resistance, corrosion, cost advantage, availability, and refractoriness heavily influence the selection of reinforcement materials(Gupta et al., 2013). Copper exhibits very poor wetting for ceramic reinforcements, resulting in poor interface strength and adhesion between the copper and reinforced materials. The mechanical properties of Cu-MMC are affected by the poor interface bonding between copper and reinforcement(Zhan and Zhang, 2003). Poor wettability of copper can be improved by optimizing process parameter and using wetting agent during fabrication.

There are numerous methods for preparing metal matrix composites. The majority of these processes involve liquid and solid-state processing. Some processes may employ a variety of deposition techniques or an in situ process incorporating a reinforcement phase(Chawla, 2012). The stir casting method is a liquid state fabrication of Metal Matrix Composites that includes a discontinuous phase to the molten matrix metal. One of the simplest and most effective methods in metal matrix composites. This methodology is appropriate for a wide range of industrial applications that require complex shapes and sizes (Anandaraj et al., 2020). The powder metallurgy (PM) route is solid state processing technique which is most suitable and easiest to produce copper matrix composites, and it offers numerous advantages such as reducing the metal removing process to a minimum and lowering manufacturing costs.

Because of poor wettability of copper with ceramic reinforcement porosity can be formed during fabrication. The secondary operation can improve the porosity level, surface polish and dimensional tolerances of the finished product. When there are ceramic reinforcements, secondary processes like extrusion, rolling, and forging serve to strengthen the link between the metal and the ceramic, which enhances the product's characteristics(Mohapatra, 2016). Finite element modelling and simulation techniques are now required to determine the effect of variable factors on the metal forming process before the actual manufacturing process in order to reduce the number of experimental attempts. This is because they are both cost and time-effective. There are a variety of commercial finite element codes, including Forge, Hyper extrude, LS-DYNA, SUPERFORM, DEFORM, and ABACUS, etc., that can simulate the metal forming process. The DEFORM 3D Finite Element Analysis (FEA) was the most effective simulation for metal forming(Nizam et al., 2020). DEFORM-3D, with its conventional application and adaptive geometric shape, demonstrates better practicability and performance advantages in terms of forming load, stress/strain distribution, material distortion, temperature distribution, and velocity field, and is thus used in investigation(Hsia, 2013).

1.2 Application area of copper matrix composites

Due to important characteristics including strong thermal and electrical conductivity, corrosion resistance, non-magnetism, stability at high temperatures, etc., copper and its alloys are widely used in a variety of industries (Suman et al., 2021). Enhancing the mechanical characteristics of a composite material requires the use of reinforcement. They can be utilized for heat exchangers, resistance welding electrodes, electronic casing and contacts, and other applications because copper metal matrix composites have outstanding mechanical and electrical properties (Gautam et al., 2018). Due to important characteristics including strong thermal and electrical conductivity, corrosion resistance, non-magnetism, stability at high temperatures, etc., copper and its alloys are widely used in a variety of industries (Suman et al., 2021). Enhancing the mechanical characteristics of a composite material requires the use of reinforcement. They can be utilized for heat exchangers, resistance welding electrodes, electronic casing and contacts, and other applications because copper metal matrix composites have outstanding mechanical and electrical properties (Gautam et al., 2018).

1.3 Motivation of research

Copper matrix composites (CMCs) have sparked considerable attention due to their promising mechanical qualities, excellent electrical and thermal conductivity, and superior corrosion resistance. However, CMCs can be restricted by poor wettability between the matrix and the reinforcement, which causes residual porosity, weak interfacial bonding, and, as a result, mechanical property loss for targeted application. In order to overcome this constraint, different alternatives have been developed, such as the use of wetting agents, surface modification techniques, and the optimization of processing conditions. Among these options, adding wetting agents has been found to be an effective method for increasing wettability and decreasing porosity in CMCs.

In recent research, silicon carbide (SiC) particles were used as a reinforcing material in copper matrix composites, resulting in improved mechanical qualities such as increased hardness and wear resistance. Furthermore, heated extrusion has been recommended as a useful consolidation approach for producing CMCs with better density and uniformity. As a result, the combination of reinforcing chemicals like SiC and new processing techniques like stir casting and hot extrusion offers an appealing way to create copper matrix composites with better capabilities while overcoming restrictions. The proposed study will look into the effects of wetting agents and SiC reinforcement on the wettability and mechanical properties of copper matrix composites via stir casting, followed by hot extrusion to consolidate and refine the microstructure. The ultimate goal is to create novel materials with improved properties that can be used in a variety of industrial applications such as aerospace, automotive, maritime, spot welding, heat exchangers and electronics.

1.4 Problem Statement

Nowadays, copper matrix composite materials are widely employed in a variety of industrial applications, including marine, aerospace, and automotive applications, as well as resistant welding electrodes and heat exchangers. Copper matrix composites have been developed through various fabricating system mainly stir casting and powder metallurgy. Most papers addressed composite material fabricated through stir casting have problem of bonding between reinforcement and matrix due to poor wettability which tends to reduce ultimate strength of the composite. There is also high particle segregation at bottom and floats over surface of molten metals causing porosity that resulted in heterogeneous mechanical properties leading difficulty during machining(Duong et al., 2016).

Most researchers illustrate addition of high weight percentage of hard reinforcement will increase hardness and strength of composite material but most researchers haven't considered addition of SiC as hard reinforcement is highly decrease electrical conductivity which limit application of copper matrix composite (Meher & Chaira, 2017). There is a gap on improving mechanical and tribological properties of base metal through post fabrication metal forming process and effect of using soft reinforcement as hybrid along hard reinforcement in improving wettability is not well discussed in previous studies. This thesis was aimed to fill those requirement properties for application in marine and resistant welding electrode by using optimum process parameter to enhance properties by varying weight percentage of hard and soft reinforcement and further enhancement of properties through secondary process.

1.5 Objectives of this study

This study is focused to addresses the following general and specific objectives.

1.5.1 General Objective

The main objective of this thesis was to experimental investigation of Cu matrix composite reinforced with SiC/Gr/Cr that was developed through stir casting process and to optimize hot extrusion parameter for further property enhancement.

1.5.2 Specific Objective

To achieve the main objective of this thesis proposal, the following specific objectives are designed:

- To synthesis copper matrix composite reinforced with SiC, Gr and Cr via stir casting.
- To study microstructural, phase and particle distribution of synthesized composite (using SEM and Optical microscopy).
- To study physical, electrical and corrosion behavior of developed composite.
- To investigate mechanical properties (hardness and compression strength) of the developed composite material.
- To Investigate deformation behavior of optimum composite using Numerical simulation of hot extrusion and parameter optimization of composite for extrusion.
- To Extrude composite and study physical, mechanical and electrical behavior of composite after extrusion.

1.6 Significance of the study

This study work was focused to fabricate and investigate properties of Cu/SiC/Gr/Cr hybrid composites and optimizing process parameter of stir casting. In practical aspect it will helps industries in determining high strength, corrosion resistant and electrically conductive copper matrix for resistance welding electrode application. this work will used as input for next researchers as a reference and for industries to develop copper matrix composites for resistant welding electrode application. It used to investigate a property lost in base matrix as weight percentage of reinforcement is increase. Beside investigation of properties this study was addressed enhancement of properties through metal forming to fit targeted application.

1.7 Scope of the study

This research concerned on synthesis, characterization and investigation of mechanical, electrical and corrosion properties of copper matrix reinforced with SiC, Gr and Cr via stir casting and optimization of process parameter. A variety of experiments conducted for this study including fabrication of Cu/SiC/Gr/Cr hybrid composite via stir casting with varied SiC and constant Gr and Cr weight composition, as well as investigation of hardness test, compression strength tests and electrical conductivity tests. In addition, characterization of composite material was conducted with optical microscopy and SEM. Among fabricated samples optimum sample was selected for numerical simulation of hot extrusion with DEFORM 3D to investigate deformation behavior composite with varying extrusion parameter. S/N ratio and ANOVA was conducted to show which parameter is significant while HTGRA was used for multi response optimization of extrusion. Enhancement properties of developed material with optimized parameter was then conducted through metal forming (extrusion).

1.8 Thesis organization

This research paper consists of five chapters. The first chapter is about the introduction and background of the study, problem statement, objectives of the study, significance of the study, the scope of the study, and thesis organization. The second chapter is about the theoretical and empirical review of copper-based reinforced MMC, literature summary, and gap. The third chapter is about materials and methodologies like copper-matrix and wt.% of SiC, Gr and Cr reinforcements and fabrication method and investigation. The fourth chapter is about detailed discussion and analysis based on the experimental result of mechanical and tribological properties, the microstructure of developed materials, and also hot deformation of synthesized composite. Finally, the fifth chapter presents the conclusion and recommendations for future works.

CHAPTER TWO

LITERATURE REVIEW

2.1 Introduction to Composite.

The composite material is a mixture of two or more insoluble materials that have qualities that are superior to any of the component components. The key component is the macroscopic examination of a substance in which the component can be seen with the naked eye. Although different materials can be combined on a microscopic level, as in the alloying of metals, the resulting material is, for all practical purposes, macroscopically homogenous. The benefit of composite materials is that, when well developed, they typically display the best characteristics of their component(Anil Kumar et al., 2016). By developing composite materials, some qualities can be enhanced, including:

- Stiffness
- Strength
- Thermal conductivity
- Wear resistance
- Corrosion resistance
- Strength to weight ratio
- Attractiveness
- Improved fatigue life
- Thermal insulation

2.1.1 Classification of composite

Composite materials can be classified in to two main categories:

- Based on nature of matrix metal (matrix material)
- Based on dispersed phase (geometry of reinforcement.

Metal Matrix Composites (MMCs), Ceramic Matrix Composites (CMCs), and Polymer Matrix Composites (PMCs) are the three categories that are based on the matrix material (Ramanathan et al., 2019). Based on the geometry of the reinforcements (dispersed phase), composite materials can also be categorized as particle reinforced composites, fiber reinforced composites, and structural composites.

2.1.2 Metal matrix composite

Metal matrix composites are materials in which a standard metal or alloy serves as the base material and is reinforced by a secondary material. Metal matrix composites are combinations of two or more different materials, with at least one being metal and another substance such as ceramics. Hybrid composites are those that have at least two or more reinforcements (Aktar Zahid Sohag et al., 2020). A metallic complex, metals in powder or fiber form, oxides, or ceramic particles can all be used as secondary or reinforcing materials (Sankhla and Patel, 2021). Titanium, aluminum, iron, copper, and magnesium are the most used matrix metals right now, and they are very helpful for aircraft applications and automotive sectors. Silicon carbide and alumina are the primary reinforcements used. Metal matrix composites are classified as either having continuous or discontinuous fiber reinforcement(Chawla, 2012). MMCs have gained interest as high-quality materials in many applications because to their appealing property range. As a result, they are currently preferred over traditional metallic alloys in a number of applications, including those related to sports and recreation, construction and civil constructions, electrical, electronic, and computer systems, security and surveillance, industrial thermal facilities, and transportation (Alaneme et al., 2019).

2.1.3 Copper matrix composite

Copper and its alloys are widely employed in a variety of industries due to major qualities such as superior thermal and electrical conductivity, corrosion resistance, non-magneticity, stability at high temperatures, and so on. An additional reinforcement must be applied to the copper matrix to boost strength and wear resistance (Balamurugan and Uthayakumar, 2015). Copper alloys with hybrid reinforcements outperform the base alloy. Hybrid reinforcement enhances qualities like as hardness, wear resistance, and tensile strength (Jamwal, Mittal, et al., 2020). As a result, developing an effective strengthening process that allows copper to increase its strength and high-temperature tolerance can encourage a wide range of copper applications. To increase the mechanical properties of copper, one effective way is to introduce ceramic particles as a reinforcement phase(Qin et al., 2020). Copper matrix composites' high electrical and thermal conductivity, as well as their quite acceptable mechanical properties, have attracted the attention of many scientists in recent years. Cu-based composites are suitable for applications such as electrical slide contacts, spot welding electrodes, connectors, heat sinks, and so on due to their qualities. According to studies, ceramics have greater mechanical qualities than other types of reinforcements, especially at high temperatures (Bagheri, 2016).

2.2 Fabrication process

There are numerous methods to fabricate metal matrix composites. The majority of these procedures include liquid and solid-state processing. Some processes may employ a variety of deposition techniques or an in-situ process incorporating a reinforcement phase(Chawla, 2012).

2.2.1 Solid state processing

Solid state fabrication of metal matrix composites is the process by which MMCs are formed as a result of bonding matrix metal and dispersed phase due to mutual diffusion occurring between them in solid states at elevated and low temperatures. Many techniques have been developed for producing particulate reinforced MMCs. P/M has been used for several years as a low-cost manufacturing method for producing near-net form composites; thus, P/M may be a cost-effective approach for producing metal matrix composites. Because of the ease of incorporating a hard phase into a metal phase via powder mixing, P/M technology is the best solid state processing route as a processing method(Akhtar et al., 2009).

2.2.2 Liquid state processing

They are interesting to various sectors since they are simple and cost-effective. These processes include liquid metal infiltration methods into preforms or fiber packs, as well as casting methods such as molten metal mixing with reinforcing particles (Ramanathan et al., 2019). Casting of metal matrix composites with particulate or fiber reinforcement may appear to be superficially similar to casting of metals. Because of their low melt viscosities, metals can be cast into nearly net-shape product forms. When a metal is heated above its melting point (or, in the case of an alloy, over its liquidus temperature), possible to get a low-viscosity liquid with good fluid flow characteristics that can be utilized to infiltrate a fibrous or particle preform(Chawla, 2012). MMCs produced by liquid metal processing are gaining popularity due to their inexpensive cost, but they have the following drawbacks (Moustafa et al., 2002).:

i no uniform distribution of ceramic particles or fibers due to agglomeration and dendritic segregation, and
ii undesired chemical reaction at the interface due to the melt's high temperature

2.2.3 Stir casting processing parameters

Stir casting for MMC: Stir casting is one of the typical processing techniques that may be used to process composite materials while they are still in the liquid state. By melting the matrix material and shaping it into the desired shape, the matrix material is cast traditionally. The reinforcement material is added to the liquid metal primarily in the particle or whisker form, and mechanical agitating is continuously used to achieve uniform distribution of reinforcement because the reinforcement material is chosen to have a melting point that is always higher than the matrix material (Sankhla and Patel, 2021). (Dasgupta, 2012) synthesized MMC utilizing a stir-casting technique in which the initial reinforcement was added in liquid metal and stirred continuously for homogeneous dispersion before being poured into preheated metal molds. Stirring velocity, stirrer geometry, stirring time, melt temperature, liquid metal density, wettability, surface energy of reinforcement particles, liquid metal surface tension, and scope of the chemical reaction are all factors that influence MMC's goal attributes (Sankhla and Patel, 2021).

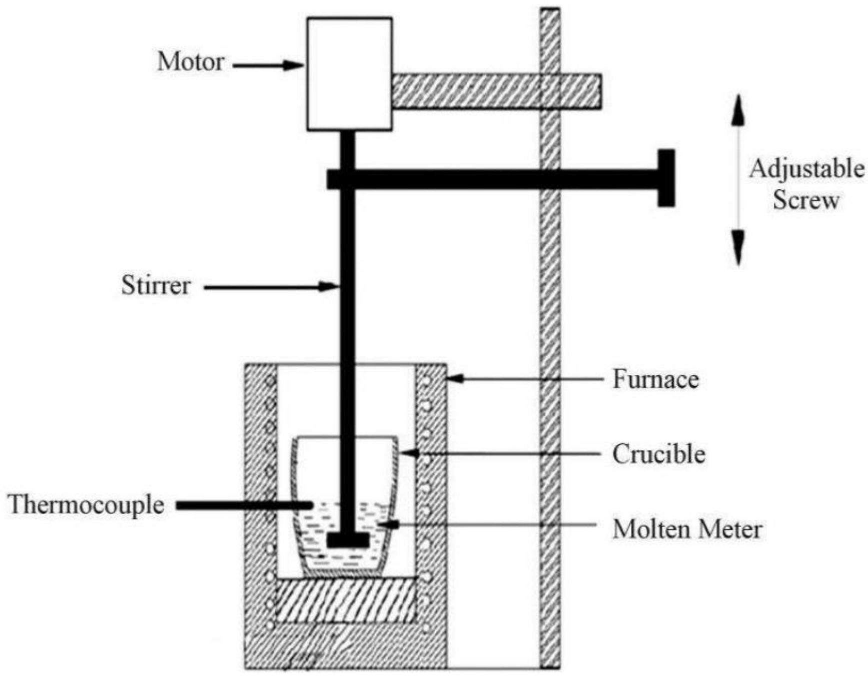

Figure 2-1 Schematic diagram of stir casting (Anil Kumar et al., 2016)

Some studies have reported changing the stir-casting process to create a hybrid stir-casting procedure. Idusuyi and Olayinka,(2019)made a four-bladed impeller and stirrer out of mild steel. They maintained a 45° blade angle. The major goal of maintaining the blades at 45 degrees is to keep 65% of the material above the stirrer and the remaining 35% above the impeller to provide the most shear possible during stirring. To achieve uniform distribution of reinforcement, the impeller must overcome the viscosity resistance of liquid metal. To ensure that the melt has a lower viscosity, it is important to monitor metal temperature and keep it consistently higher than the melting point of the matrix material.

Viswanath et al., (2015)reported to produce a vortex in the melt pool and swirl with a steel impeller at 750 rpm for 10 minutes to get optimum homogeneity. While (Brabazon et al., 2002)suggested a groove-based impeller design that was proven to be successful in creating higher shear during metal stirring. Reaction Bonded Silicon Nitride (RSBN), which was used to make the stirrer, demonstrated acceptable stress resistance as well as strength at high temperatures and inertness to melting. Particle dispersion number (PDN) has been reported to be important for achieving uniform mixing when stirring. According to them, axial velocity is greater than settling velocity and particles are moved from bottom to top if PDN is more significant when there are multiples present. A PDN of at least four will always guarantee uniform dispersion. A faster rotational speed can liberate the trapped liquid and increase the solids fraction, breaking up the agglomeration and resulting in more even mixing. Due to increased shear rate, the greater impeller speed has the effect of reducing the apparent viscosity of the composite slurry (Hashim et al., 2002). To increase the flow of molten metal, (Thomas et al., 2014)created a stirrer with twisted blades. Additionally, they discovered that a bigger stirring force may be produced by increasing the blade area, which decreased the attraction between the reinforcement or SiC particles. Stainless steel can be the best option for impeller or stirrer material, according to the microstructure of MMC that they acquired. This microstructure revealed no local explanation for the interfacial region (Poddar et al., 2007). (Ghosh et al., 1984)Suggested that the height ratio is a crucial parameter to determine the uniformity of reinforcement while generating an MMC slurry, in addition to the type of impeller and its rotating speed. They recommended a ratio of 0.81 h/H, where h is the impeller's height above the melting pot's bottom and H is the total depth of liquid slurry.

Dehghan Hamedan and Shahmiri (2012) demonstrated that the SiC-reinforced A356 alloy's compressive strength was highly dependent on the rate of stirring, and they noted a diminishing effect when the stirrer's speed was increased. Atuanya and Aigbodion (2014) reported on the impact of fewer graphite particles in the stir-casting process for a lower melt temperature. The performance was unaffected by the stirrer's constant speed, but the procedure was shown to be severely impacted by the melt's increasing viscosity. But it was reported that preheating the mold and graphite powder would help keep the reinforcement in place. Sankhla and Patel (2021) used a double-feeding stir-casting process to create and test an Al-Cu-Mg alloy enhanced with nanoparticles. Preheating LM6 alloy with SiC particles at high stirring speeds resulted in consistent particle dispersion, and MMC was found to be robust and machinable.

2.3 Selection of reinforcement

The mechanical characteristics of the reinforcing materials, such as wear resistance, hardness, cost effectiveness, availability, and refractoriness, have a significant impact on the choice of those materials (Jamwal et al., 2019). Soft and hard reinforcements are added to the matrix to improve the mechanical and wear characteristics of metal. The soft reinforcement has qualities such as low friction, chemical inertness, lack of inherent abrasiveness, film forming ability on metal surfaces, and is relatively inoffensive to nature. However, there was a loss in hardness and flexural strength as well. The use of hard ceramic reinforcements along with soft reinforcements may solve these problems and increase mechanical and tribological qualities (Jojith and Radhika, 2019). Some common reinforcements include silicon carbide and alumina. Discontinuous reinforced MMCs appear to provide more because of their simplicity of production. Discontinuous fibers can exist in a variety of forms, including short fibers, whiskers, platelets, and particles (Gautam et al., 2018).

2.3.1 Graphite reinforced composite

Lubricants are commonly used to reduce friction and wear between contacting surfaces. While liquid lubricants are commonly utilized in most industrial and technical applications, solid lubricants such as graphite(Gr) and molybdenum disulphide (MoS_2) are used in tribo-systems when liquid lubrication is restricted due to operational or environmental concerns (Moazami-Goudarzi and Nemati, 2018). However, because to the strong reactivity of MoS_2 particles with molten copper, liquid metallurgical processing methods such as stir casting could not be used to developed Cu and MoS_2 composites. The use of low-density particles in reinforcement reduces the density of composites. The addition of graphite as reinforcement also aids in the lowering of composite density, which aids in the development of composite materials for light weight applications such as vehicle and aircraft applications (Jamwal, Seth, et al., 2020).

2.3.2 Chromium reinforced composite

Because copper is considered to have comparatively superior wettability for metals compared to ceramics, the poor wetting of ceramic materials by copper generated the idea of a metal-based reinforcement in this research. Chromium is also a member of the refractory metals group, which includes those metals with a melting point higher than platinum (Lunk, 2015). Wettability of cast metal matrix composites can be greatly influenced by reactive wetting by adding alloying elements such as Ti, Mg, Cr, Ca, Sr, Mn, Ce, Cu, and Zr to a melt matrix, which improves wettability by lowering surface tension and reinforcement- matrix interfacial energy(Malaki et al., 2021). Chromium is commonly used as an alloying element, such as in Cu/graphite systems to increase wettability. The contact angle between pure copper and graphite has been measured to be around 140, showing that the copper matrix does not wet the graphite particles; however, adding 1.0 wt.% Cr to the graphite/Cu composite reduces the wetting angle from 140 to 43 at 1573 K (Kennedy et al., 2000). Wetting agents form a temporary layer between the matrix and the reinforcement; coating of reinforcement particles has also been proven to be beneficial in promoting interfacial reactions; surface energy is altered, resulting in better wettability (Sankhla and Patel, 2021). Singh et al.(2019) reported the development of hybrid copper-highly strained stainless steel (HSSS)-tungsten carbide (WC) composites. To improve the fluidity of the molten metal, Cr (2% wt.) is added during the fabrication of all composites.

2.3.3 Silicon carbide reinforced composites

The addition of ceramic-based reinforcements has enabled MMCs to attain the majority of the outstanding properties. Mostly metal matrices are reinforced with ceramic materials such as aluminum oxide (Al_2O_3), silicon carbide (SiC), titanium oxide (TiO_2), graphite (C), and boron carbide (B4C). Among these reinforcements, SiC particles are added to the copper matrix due to their low cost, high hardness, high thermal conductivity, good wear and corrosion resistance, and ability to significantly increase the strength and wear properties without compromising the matrix metal's electrical and thermal properties (Akbarpour et al., 2019). (Akbarpour et al., 2019)Were prepared nanostructured Cu, Cu reinforced with hybrid SiC (4 vol.% Nano-size and 4 vol.% micro-size SiC), and Cu-8vol.% SiC micro composite by high energy mechanical milling and hot-pressing process. in comparison to the nanostructured Cu sample, the introduction of hybrid particles significantly reduced the matrix grain size by 61%, reduced the wear track width by 53%, and increased compressive strength by 35%.Any material's compression strength is influenced by two different sorts of mechanisms: hardening of the reinforcing particles due to dispersion and strengthening of the grain size (Jamwal, Seth, et al., 2020). The Orowan mechanism often explains the high yield strength of particles scattered in matrix material. This explains how dislocation interacts with insoluble dispersoids. (Jamwal et al., 2019)Were developed copper matrix composites with SiC-graphite reinforcement (0, 2.5, 5, 7.5, and 10% wt.) through stir casting to investigate the effect of SiC-graphite reinforcement on pure copper characteristics. The hardness of a hybrid composite reinforced with graphite and SiC is lower than that of a pure casted Cu matrix.

2.4 Effect of reinforcement on mechanical properties

Wagih et al. (2019) were developed Electro-less deposition of GNPs and Al_2O_3 coated Ag reinforced Cu matrix nanocomposites, followed by ultrasonic mixing and hot compaction, resulted in the effective fabrication of GNPs and Al_2O_3 coated Ag reinforced Cu matrix nanocomposites. The effects of GNPs coated Ag volume fractions (0%, 0.3%, 0.6%, 0.9%, and 1.2%) on the microstructures, density, compressive, hardness, thermal, and electrical properties of Cu-Al_2O_3/GNPs hybrid nanocomposites were studied. The microhardness of Cu-Al_2O_3/GNPs hybrid nanocomposites increases with increasing GNPs content, reaching 496.8 HV for samples containing 1.2% GNPs as opposed to 319.2 for pure Cu. The compressive strength of Cu- Al_2O_3/GNPs hybrid nanocomposites increase with increasing GNPs content, reaching 786 MPa for samples containing 1.2% GNPs as opposed to 416 MPa for pure Cu.

Shehata et al. (2009) were successfully prepared Cu-Al_2O_3 nanocomposites by two chemical routes, namely route-A: through decomposition of Al (NO_3)3 to Al_2O_3 by calcinations of the paste of CuO-Al (NO_3)3 followed by H2 reduction and sintering; and route-B: through hydrolysis of Al (NO_3)3 by ammonia in a slurry of CuO in Al (NO_3)3 solution followed by calcinations, reduction and sintering. The micro hardness of the sintered samples was examined as a measure of reinforcement of the highly conducting copper matrix, and the results demonstrate that the increase in micro hardness value is a function of the rise in Al_2O_3 concentration for both pathways A and B. The micro hardness evaluation results are the result of a rather equal distribution of Al_2O_3 dispersed in the copper matrix. As the Al_2O_3 content rises, the composite becomes harder and has smaller crystal grains due to the stronger strengthening effects of nano-Al_2O_3 dispersion and grain refining.

Alaneme and Odoni (2016) were fabricated copper matrix composites with 5, 7.5, and 10 wt.% of the chips as reinforcement were created using steel machining chips with chip size ranges of 105 nm and below. Investigated that an increase in the weight percentage of steel machining chips is observed to increase the hardness of copper matrix composites. The hardness of the steel chip reinforced composite grades was somewhat higher than that of the alumina reinforced composite grade, which was used as the control sample. In comparison to the control samples (unreinforced copper and 10 wt.% alumina reinforced copper matrix composite), the 5 wt.% steel machining chips reinforced copper composite grade exhibits improved ultimate tensile strength, percent elongation, and tensile toughness. The strong interface bonding between the copper matrix and the steel machining chips, which enables the transmission and distribution of load from the matrix to the reinforcement, is thought to be the cause of the increase in strength.

Moustafa et al.(2002) successfully developed copper matrix reinforced with either Ni-coated or uncoated SiC and Al_2O_3 particulate composites through powder metallurgy. This study sheds light on the compression and densification characteristics of Cu-20% coated SiC, Cu-20% coated Al_2O_3, and Cu-20% Al_2O_3 composites. The results show that the yield and breaking (fracturing) strengths of coated composites are significantly higher than those of uncoated composites. Furthermore, the compression strains of coated composites are greater than those of uncoated composites. The improved compression capabilities of the coated composites might be due to the good adherence of the coated particles to the Cu-matrix, as well as the higher density and decreased porosity.

Jamaati and Toroghinejad (2010) were fabricated high-strength, finely dispersed and highly uniform copper/alumina metal matrix composite (MMC) through an efficient alternative technique, known as the accumulative roll bonding (ARB) process. The Cu/15 vol% Al_2O_3 composite's microstructural development and mechanical characteristics during different ARB cycles are presented. The tensile strength of the Cu/15 vol.% Al_2O_3 MMC was 2.5 and 1.2 times higher than that of the annealed and ARBed pure copper strips, respectively. It was discovered that the copper/alumina composite exhibited a higher tensile strength than the annealed and ARBed pure copper strips. When the number of cycles was increased, the composites' tensile strength and elongation improved. The hardness of the generated MMC was higher than that of the annealed and ARBed pure copper strips, so that the hardness value of the copper/alumina composite was 3 and 1.17 times higher than that of the annealed and ARBed copper, respectively.

A Powder Metallurgy (P/M) route was used to reinforce Copper (Cu) with low density material Fly Ash (FA) to form Cu-FA composite material (Rajan et al., 2019). Samples of FA in Cu matrix with weight percentages of 3, 6, and 9 were prepared. Investigated that the Vickers hardness of Cu-FA composite material increases as FA reinforcement is added. The uniform distribution of FA in the Cu matrix reduces the intergranular space. Also, the increase in hardness indicates a strong physical bond between the Cu-FA composite materials.

Jabinth and Selvakumar (2021) were fabricated Copper Matrix Composite, secondary hybrid reinforcements such as Vanadium (V) and Graphene-L (Gr-L) in various proportions such as pure Cu, Cu-2V, Cu-2V-0.5Gr, Cu-2V-1Gr, and Cu-2V-1.5Gr were applied Investigated that the size of the grain reduces as vanadium and Gr-L content increases. The strength of hybrid composites is increased as a result of the fine grain refining. The combination of 2%V6 and 1.5% Gr-L results in a maximum increase in copper's tensile strength of 138.75%. The hardness value of the hybrid composite rises when the grain size is reduced. According to the experiment, the hardness value increases to about 53% when 2%V and 1.5% Gr-L are added compared to pure matrix phase. Impact strength also rises to roughly 178.84% for hybrid CMC compared to pure copper, along with hardness.

Nageswaran et al. (2018) were developed copper metal matrix composites reinforced with 0, 3, 6 and 9 wt. % TiO_2 and 1% Gr. The refining of the Cu phase with the function of reinforcing particles in the hybrid composite has been made possible by the formation of nucleation sites and the reduction in grain expansion. Due to homogeneous distribution and grain refinement, the use of 9% reinforcement boosted the composite's hardness, tensile strength, and wear resistance. As a result, the Cu - 9% TiO_2 and 1% Gr hybrid composite can be considered a viable material for improving the performance of condenser tubes.

Singh and Gautam (2017) were successfully fabricated hybrid copper matrix composite reinforced with alumina (Al_2O_3) of grade 6, zirconia (ZrO_2), tungsten carbide (WC) and chromium (Cr) using stir casting. It is observed that in comparison to ZrO_2 based hybrid composites and its matrix, the Al_2O_3 based hybrid composites exhibit much higher Brinell hardness, compressive strength, and tensile strength. This is explained by how harder

Al_2O_3 strengthens particles and transfers loads. The created hybrid composites' overall electrical property, as determined by a four-probe technique, diminishes with reinforcement.

Rizi (2019) were prepared copper matrix composite reinforced with vanadium of 0%, 0.5%, 1.0%, 1.5% & 2% weight percentage. Investigated that the size of the grain decreases as the vanadium component increases. The tensile strength of the material increases as grain size decreases. The addition of 2% vanadium to copper improves its tensile strength by 81% maximum, allowing it to be employed in applications requiring high strength in addition to its usual features. Copper's increased strength is also owing to its increased hardness. It is also discovered that the addition of vanadium increases the hardness value by 25% in Cu-2%V when compared to matrix phase.

2.5 Wear performance of copper matrix composite

The study and practice of friction, lubrication, and wear under applied loads are all included in tribology. In general, wear is defined as mechanically induced surface damage that causes material to gradually be removed as a result of relative motion between that surface and the substance or substances it is in contact with. In the wear test, the reinforcing particles operate as a lubricating coating on the counter surface, lowering the coefficient of friction and reducing wear rates. As the reinforcing content of the composites increases, the wear rates of the composites decrease. However, compared to low loading circumstances, wear rates are higher with high loads (Jamwal, Seth, et al., 2020). Ti_2AlC, Gr and MoS_2 could act as solid lubricants and hence be smeared over the worn surface during sliding wear tests, preventing the BM from attaching to the counterpart. As a result, the adhesive wear mechanism is restricted in the case of nan-composites (Mazaheri et al., 2021). Due to the huge grain size, lack of mechanical characteristics, absence of second phase particles, and agglomeration action, unreinforced composites have a very high wear rate value. This is because they have weak resistance to deformation on the worn surface (Nageswaran et al., 2018). Soft and hard reinforcements are inserted into the matrix to improve the mechanical and wear characteristics of copper alloy. Soft reinforcement has qualities such as minimal friction, chemical inertness, lack of inherent abrasiveness, capacity to form films on metal surfaces, and is relatively inoffensive to nature. However, there was a loss in hardness and flexural strength. The use of hard ceramic reinforcements in conjunction with soft reinforcements can solve this problem and increase mechanical and tribological qualities (Jojith and Radhika, 2019).

Mazaheri et al.(2021) were successfully prepared pure copper matrix surface Nano-composites reinforced with Ti_2AlC and MoS_2 nanoparticles by multiple passes of the friction stir processing (FSP). Investigated that the mass losses of the Cu/MoS_2 and Cu/Ti_2AlC nano-composites may be reduced by around 55% and 60%, respectively, based on the wear characteristics of the samples worn by the AISI 52100 steel equivalent. Additionally, upon the FSP, the friction coefficients of the Cu/Ti_2AlC and Cu/MoS_2 nano-composites dropped by roughly 20% and 32%, respectively. According to SEM analysis of the worn surface and debris left behind by the wearing of the samples, adhesion was the primary wear mechanism of pure copper. The wear mechanism, however, changed to the delamination mechanism after performing the FSP. Both nano-composites were found to exhibit the abrasion wear mechanism.

By using powder technique, three copper base matrix composites with TiC reinforcement were created. Al, Ti, Ni, and Co alloying elements were added to improve the mechanical and sintering properties(Akhtar et al., 2009). High speed steel was used to compare the composite materials' wear resistance. The predominant wear mechanism was discovered to be micro ploughing of the copper base matrix. Less micro ploughing and wear loss was seen with higher volumes of TiC particles and lower loads. The material demonstrated good wear performance as long as the mean free path of the binder was greater than the average grain size of the TiC. The matrix phase's plastic ploughing, grooving, and cutting was the predominant wear mechanism when this ratio was reduced to less than the average TiC grain size, and substantial wear loss was noted.

Dong et al. (2001) looked at the wear and friction characteristics of a carbon nanotube-reinforced Cu-matrix composite (Nanotube/Cu composite). According to research, the principal wear mechanism for the Nanotube/Cu composite under dry sliding conditions is oxidation wear. The rate of friction and wear can be decreased by the creation of carbon coating. The Nanotube/Cu composite weighs less and has a lower coefficient of friction than CF/Cu composite. The composite's coefficient of friction and wear rate can both be markedly reduced by increasing the nanotube volume fraction. The ideal concentration of nanotubes is between 12 and 15%.

Uzun and Usca (2018) Analyze the impact of various Cr particle reinforcement ratios on the toughness and wear resistance of Cu matrix composites made using the (P/M) method.

In pure Cu dust, Cr particles were introduced at various weight ratios of 5, 10, and 15%. According to the results obtained, the Cr reinforcement increased the hardness of pure copper. Furthermore, it was discovered during the wear test that the Cr reinforcement created wear resistance by lowering the friction coefficient, weight loss, wear diameter, and wear depth.

Bagheri(2016) synthesized copper matrix composites reinforced with different amounts of titanium carbide particles by mechanical milling and in-situ formation of reinforcements. It is clear that as the volume fraction of reinforcement increased, the wear resistance of the samples improved. Ceramic particles increase the hardness of the matrix, reducing the real area of the wear surface. Real area is defined as the normal load to hardness ratio. As a result, the wear rate decreases as the TiC hard particle content increases.

The friction and wear characteristics of the Cu-TiB_2 composites were determined by performing dry sliding tests on a pin-on-disk machine with varying loads, sliding speeds, and sliding distances(Zou et al., 2017). A comparison of the volume wear losses of the composites under different conditions reveals a significant improvement in wear property of the composites over pure copper. The presence of TiB2 improves the wear performance of Cu-TiB_2 composites significantly, and the volume wear loss at different loads, sliding distance, and sliding speed of the composite decrease with increasing TiB_2 content.

Material hardness affects wear resistance, but this is not always the case. The wear rate of a material is also influenced by its toughness. The dispersion strengthening and solid bonding between the matrix and reinforcement phases cause a reduction in wear rate (Jamwal et al., 2019). Although it is understood that increasing applied load causes an increase in wear rate, the hybrid composite has a lower wear rate than the unreinforced alloy. The presence of TiO_2 and MoS_2 particles in the metal matrix can explain this. With the addition of hard ceramic and soft reinforcements, the wear coefficient and volumetric wear loss are reduced (Jojith and Radhika, 2019).

2.6 Electrical and corrosion behavior of CuMMC's

Copper matrix composites are widely used in structural materials, electronic devices, and thermal devices due to their good mechanical qualities, strong electrical conductivity, and thermal conductivity(Gao et al., 2016). Copper alloy with reinforcement is far superior to base alloy. By including reinforcements, properties such as tensile strength, hardness, impact strength, wear strength, and corrosion resistance are increased. Additionally, it is established that base metal's electrical and thermal conductivity properties improve following reinforcement(Gautam et al., 2018). The cubic structure of copper is face centered. It is widely used as an electrical conductor; it has excellent thermal conductivity. It is simple to cast and work with. One of the most important applications of copper as a matrix material in a composite is in niobium-based superconductors(Chawla, 2012). By altering the sintering temperature, it was shown that the graphene loading into the Cu matrix clearly affected the mechanical and electrical conductivity. For instance, as compared to the pure Cu sample, the graphene-loaded Cu composites sintered at 600°C showed a minimal change in the mechanical characteristic and a much higher electrical conductivity(Salvo et al., 2019).

Akhtar et al. (2009) were successfully fabricated three TiC reinforced copper base matrix composites reinforced with Alloying elements (Al, Ti, Ni and Co) using powder technology. It was observed that adding alloying materials to the copper base matrix boosted electrical conductivity. This is owing to the absence of porosity in the composite. Ideally, alloying element additions (Ni, Co, Ti, Al) reduce electrical conductivity. When the electrical conductivities of composites using Cu-Ti-Al (66 at. % Cu) and Cu-Ni-Co (84.5 at. % Cu) as binders are compared, Cu-Ni-Co composites have higher electrical conductivity. This is owing to the higher concentration of copper.

The electrical conductivity of Cu/ZrO_2 nanocomposite specimens sintered at 750 or 850°C for 1 hour in an argon environment is demonstrated. It has been noted that the related reduction in porosity causes the electrical conductivity of sintered composite to increase dramatically with increasing sintering temperature. Electrical conductivity of the composites increases as sintering temperature rises to 850 °C and reaches 9.57 104 S/m for composite having 12 wt% ZrO_2 (Taha & Zawrah, 2017).

Electrical conductivity values as the standard electrical conductivity (IACs) were investigated in green and sintered Cu-CNT nanocomposites. When the weight percentage (wt. %) of Cu-CNT nanocomposites was increased from 0.5 to 5wt%, the electrical conductivity values of green Cu-CNT nanocomposites declined. Green 0.5wt% Cu-CNT nanocomposites have an electrical conductivity of 55.3 IACs. Sintered 2wt% Cu-CNT nanocomposites had an electrical conductivity of 46.26 IACs, compared to 5.9 IACs for green 2wt% Cu-CNT nanocomposites(Varo and Canakci, 2015).

Apart from electronic applications, copper and its alloys exhibit exceptional corrosion resistance and are employed in corrosive situations due to its superior electrical and mechanical qualities. Investigating how reinforcements impact copper corrosion qualities appears to be both important and necessary. Although extensive research has been undertaken on the corrosion behavior of pure copper, understanding the impact of reinforcement on the corrosion behavior of Cu-based composites is an issue that has not been thoroughly investigated (Akbarpour et al., 2020). The flake powder metallurgy and spark plasma sintering methods were used to create nanostructured Cu and Cu/CNT+SiC hybrid nanocomposite. Polarization testing revealed that the anodic dissolution of copper was suppressed and the oxygen reduction reaction was hampered. Additionally, a 62.5% improvement in corrosion rate for composite material was estimated. Furthermore, EIS studies validated the hybrid composite sample's superior corrosion resistance when compared to monolithic Cu.

The EIS(Electrochemical impedance spectroscopy) technique is used to evaluate the corrosion behaviors of copper and Copper-WC composites in 0.5 M H_2SO_4 solutions(Kumar Singh et al., 2018). It was discovered that the corrosion behavior of copper was greatly enhanced as a result of the reinforcement of WC particles. Furthermore, the comparison of Cu-WC micro composite and Cu-WC Nano composite revealed that the size of WC particles was critical in improving copper characteristics. The smaller size of the reinforcing WC particles resulted in improved interaction between matrix and filler martial. As a result, the mechanical characteristics and corrosion behavior of Cu-WC nano composite improved above Cu-WC micro composite.

Investigations have been done into the mechanical characteristics, wear, and corrosion behavior of copper matrix composites reinforced with steel machining chips (Alaneme and Odoni, 2016). The corrosion susceptibility in 3.5 wt.% NaCl solution was greater for the unreinforced copper and alumina reinforced composite grades than for the steel chips reinforced copper matrix composites. However, no consistent corrosion trend was seen in 0.3 M H_2SO_4 solution, despite the fact that the corrosion resistance of all composite grades created was superior to unreinforced copper. MMCs have demonstrated contradictory corrosion behavior in chloride environments(Hannula et al., 2018).

2.7 Secondary Process

To enhance the product's tribo-mechanical capabilities, several heat treatments and forming techniques are used as secondary operations. Different forming procedures are typically offered as the secondary strengthening mechanisms for materials that cannot be heat treated. Severe plastic deformation (SPD) is a broad term for metal-working techniques that cause a significant strain without affecting the object's overall dimensions. In other words, tools with high strengths and unique geometries make it difficult for materials to flow smoothly. As a result, hydrostatic pressure builds up, which pushes materials down their intended paths while experiencing severe shear strain. Fine grains are produced as a result of the procedure, which also results in crystal defects with increased dislocation density. the bending of tools or dies(Mishra et al., 2019).

2.7.1 Extrusion

Extrusion is a relatively new metalworking process, while being one of the most significant industrial processes in use today. Commercial extrusion of lead pipes began in the early 19th century, but it wasn't until the latter half of that century that even brass could be extruded(Tiernan et al., 2005). Extrusion is a compression process that forces work metal through a die opening to produce a desired cross-sectional shape(Ma et al., 2016). This modern technique has various advantages: In cold and warm extrusion grain structure and strength qualities are improved, fairly close tolerances are attainable, especially in cold extrusion; and in some extrusion procedures, little to no waste material is produced. The cross section of the extruded part must be constant along its whole length, which is a restriction.

2.7.2 Classification of extrusion

Extrusion can be accomplished in a variety of ways. One important distinction is between direct and indirect extrusion. Another classification is based on the working temperature: cold, warm, or hot extrusion. Finally, extrusion can be either continuous or discrete(Ma et al., 2016). Direct extrusion (also known as forward extrusion) is a process in which a metal billet is loaded into a container and a ram compresses it, forcing it to flow through one or more openings in a die at the opposite end of the container. A small portion of the billet remains as the ram approaches the die and cannot be forced through the die opening. This extra portion, known as the butt, is removed from the product by cutting it just beyond the die's exit. Indirect extrusion, also known as backward extrusion and reverse extrusion, mounts the die to the ram as opposed to the other end of the container. Metal is compelled to flow through the clearance in a direction counter to the ram's motion as it is driven further into the job. The ram force is smaller than in direct extrusion because there is no friction at the container walls where the billet would otherwise be pushed to move in relation to it. The hollow ram's lesser stiffness and the challenge of supporting the extruded product as it emerges from the die are constraints placed on indirect extrusion.

Extrusion can be done either hot or cold, depending on the work metal and the amount of strain applied during deformation. Aluminum, copper, magnesium, zinc, tin, and their alloys are typical hot extruded metals. Prior to hot extrusion, the billet is heated to a temperature above Its temperature of recrystallization. This reduces the metal's strength while increasing its ductility, allowing for more extreme size reductions and complex shapes to be achieved in the process. Cold and warm extrusion are processes that use a billet that has been heated below its recrystallization temperature to produce discrete parts, often in finished (or near finished) form.

2.7.3 Effect of extrusion on mechanical properties

The friction extrusion process successfully produced bulk-sized copper-carbon composite wires(X. Li et al., 2021). The severe in-plane shear deformation caused by the rotating die dispersed carbon filler material uniformly in the copper matrix. At the same time, the processing temperature is below 600 °C, which is much lower than the copper casting or sintering temperature. The friction-extrusion copper-carbon composite wires have a superior heat capacity when compared to pure copper, as well as superior electrical conductivity and mechanical properties when compared to other copper-carbon composites.

Hot extrusion and T6 heat treatment of high-pressure gas-atomized and mechanically milled powders resulted in a composite with a fine-grained AA6005A matrix and 3 vol% TiC nanoparticles. The effect of grain refinement on the composite's microstructure and mechanical properties was investigated (Feijoo et al., 2020). Microstructural and mechanical analyses revealed that the consolidated nanocomposite responded moderately to heat treatment. In any case, the composites produced in this study, which combine the use of nanoparticles TiC and T6 heat treatment, exhibit high strength and hardness, even though they have a significant drop in ductility, as would be expected when adding a brittle component, and a slight recuperation after the T6 heat treatment.

0% HEA strengthened Cu matrix composite was created by SPS, which was then preheated at 850 °C for varying lengths of time and hot extruded. Microstructure characterization and performance tests were used to analyze the 10 vol.% HEA/Cu composites while they were extruded (Liu et al., 2021). The mechanical characteristics of HEA/Cu composites can be greatly improved with the right preheating period. The 10 vol% HEA/Cu composite has a yield strength of 317 MPa and an elongation of 11.7% at the 6 h preheating time, which can be attributed to the reinforcements' lower hardness and smaller diameter during the preheating process.

A hot hydrostatic extrusion process was used to manufacture an Al/Cu clad composite at 320 °C. In the process of hydrostatic extrusion, the influence of the extrusion ratio and die angle on the extrusion pressure was measured experimentally (Rhee et al., 2004). SEM and EDS investigations were used to examine the bonding condition at the contact between aluminum and copper. TTC4 particles, when surrounded by PDZs during hot extrusion, can aid in the nucleation of DRX of Mg alloy matrix(Wang et al., 2020).

2.8 Finite Element Analysis

Finite element modelling and simulation techniques are now required to determine the effect of variable factors on the metal forming process before the actual manufacturing process in order to reduce the number of experimental attempts. This is because they are both cost and time-effective. There are a variety of commercial finite element codes, including Forge, Hyper extrude, LS-DYNA, SUPERFORM, DEFORM, and ABACUS, etc., that can simulate the metal forming process (Mohapatra and Maity, 2016). The only method for digitally visualizing and analyzing the changes that occur in the inaccessible zone during deformation is to use FEM. Prior to the experiment, it is possible to better understand the stress, strain, temperature, and other factors created throughout the deformation zone. With software analysis, it is feasible to minimize the most crucial data, which is the maximum load demand for the operation, by customizing variable parameters as well as die modification. Modelling and simulation are helpful tools for deformation processes because they allow for the investigation of state variables that have a significant impact on the extruded profiles. The DEFORM 3D Finite Element Analysis (FEA) was the most effective simulation for metal forming(Nizam et al., 2020). DEFORM-3D, with its conventional application and adaptive geometric shape, demonstrates better practicability and performance advantages in terms of forming load, stress/strain distribution, material distortion, temperature distribution, and velocity field, and is thus used in investigation(Hsia, 2013). The calculation attempts to satisfy the equilibrium equation, the constitutive equation, the geometric compatibility equation, the yield criterion, and the boundary conditions. Because metal forming is a complex deforming action, the assumption of boundary conditions and material properties in Finite Element Analysis is necessary.

The method of extrusion may seem simple, but it greatly depends on geometrical factors such die angle, ram speed, material, die land height, extrusion ratio, product form, coefficient of friction, and cross-sectional area (Kothasiri and Chalamalasetti, 2022). validated hot extrusion procedure for AA6061. The DEFORMTM-3D simulation software, which is based on FEM, was used to simulate the effects of the extrusion load, exit temperature, displacement, and damage on process parameters and design. Process parameters for extrusion load, exit-temperature, displacement, and damage were optimized using the Taguchi method contemporaneous with GRA (a multi performance response optimization).

2.9 Multi response optimization

The goal of optimization approaches is to identify the "best" operating parameters of a system that can produce the highest levels of performance possible for the system given the current restrictions. Based on process design concerns, several optimization techniques can be employed for a variety of applications. These techniques can be classified into two major categories: deterministic techniques and probabilistic techniques. Only a few estimations of the outcome may be achievable with probabilistic approaches, in contrast to deterministic methods where the outcome may be precisely anticipated. By using the Taguchi approach, a single performance characteristic can be easily optimized. The task of analyzing and resolving several performance criteria is difficult, though. One method for improving control variables with several performance levels is GRA. The majority of previous works focused on developing optimized designs for various forming processes of different materials using various optimization techniques, and some investigated the effect of forming process parameters using simulation software (DEFORM-3D. In recent days, most advancements in Al extrusion have been seen through numerical models. In this study, FEM modelling and Taguchi's DOE with GRA (method for multi-response optimization) were used to optimize the AA6061 alloy hot extrusion process (Jajimoggala et al., 2019). A neural network model and multi-objective meta-heuristic optimization techniques were used to optimize the twist extrusion process. As a result, three well-known multi-objective algorithms were used: non-dominated sorting genetic algorithm, strength pareto evolutionary algorithm, and multi-objective particle swarm optimization (MOPSO). The results showed that the

MOPSO method outperformed other algorithms in finding optimal zones (Bakhtiari et al., 2016)

2.10 Literature Summary

Several studies have been conducted on the production and characterization of copper matrix composites with various types of reinforcement, particle sizes of reinforcement, fabrication processes, and testing circumstances. The above literature analysis clearly reveals that numerous manufacturing processes, primarily liquid state processing techniques, and the effect of processing conditions, as well as the effect of reinforcement, have been extensively explored. CuMMC's are reinforced with varied particulate ceramic reinforcements and the influence of weight composition and particle size of reinforcement on the mechanical and tribological behavior of developed composite has been studied. Ceramic particles were commonly used as reinforcements in the manufacture of copper matrix composites. According to the literature, the addition of various particle reinforcements greatly improves the mechanical and tribological properties of copper alloy matrix. Secondary operations, particularly metal forming, can improve the mechanical and tribological performance of fabricated composites. Extrusion is an efficient metal forming method for reinforcing composite materials. Extrusion has the advantage of assisting in the alignment of the reinforcement within the composite material, increasing the overall strength of the finished product. To reduce the number of experimental tries, finite element modelling and simulation techniques are required to identify the effect of variable factors on the metal forming process prior to the real manufacturing process. This is due to the fact that they are both cost and time effective. The DEFORM 3D Finite Element Analysis (FEA) was the most effective simulation for metal forming. DEFORM-3D, with its traditional application and adaptive geometric shape, displays improved practicability and performance advantages in terms of forming load, stress/strain distribution, material distortion, temperature distribution, and velocity field, and is thus employed in study.

2.11 Research Gap

There have been many studies conducted on metal matrix composites. Metal matrices in a composite material provide more strength, fracture toughness, and stiffness than their polymer equivalent. Magnesium, copper, Aluminum, and Titanium are the most popular metals utilized as matrix in MMC. Researchers have fabricated metal matrix through various process such as stir casting, slurry casting, powder metallurgy and so on. The stir casting process is simplest, economical and most commercially used technique in liquid state processing. Researchers are focused on improving mechanical and tribological properties with addition of hard and soft reinforcements without considering less degree of enhancement due to poor wettability of copper with solid reinforcement. There was limitation on improving fabricated composite with secondary process like metal forming which was used as strengthening mechanism by refining grain size. This thesis work is proposed to fabricate copper matrix hybrid composite via stir casting and to improve poor wettability between reinforcement and molten matrix with addition of dry lubricant and metallic reinforcement. Mechanical property was enhanced with hot extrusion to fit a property required for application of resistant welding electrode.

CHAPTER THREE
MATERIALS AND METHODOLOGY

3.1 Introduction

This chapter discusses the materials utilized in the prepare of copper-based hybrid metal matrix composites, the fabrication methodology and procedures for sample preparation, the experimental procedure, and the testing setups. the devices and equipment used, as well as the methods for data analysis organized under current chapter. Overall setup of the experiment and characterization is also specified with certain precise parameters. The stages for the optimization process, formulas, and standards for various experiments and tests are also discussed in the chapter.

3.2 Materials

To select the materials, a proper understanding of the composite properties necessary for application of resistant welding electrode is essential. It is important to understand the necessary characteristics of the composite utilized in resistant welding electrode and heat exchangers applications. All analyses relating to mechanical properties, microstructural properties, electrical properties, corrosion behavior and fracture mechanics was included in this list of properties. This makes choosing the materials for the metal matrix and reinforcement matrix phases easier. After determining the properties of composites required for the application, the materials used in this research was, as metal matrix (copper alloy) and as reinforcement matrix (silicon carbide and chromium) materials that yield the required properties, as well as a small amount of graphite for self-lubrication properties. Cost, properties, and availability all need to be taken into consideration when making this decision. All particles size was ranged from 50µm to 200µm.

3.2.1 Copper alloy

C15100 is a CuZr alloy that can be toughened by cold forming and moderately by CuZr-phase precipitation during heat treatment. It is bendable, has great hot and cold forming capabilities, is strong, and has superior corrosion resistance. Because of the low diffusion of Zr in Cu, the softening resistance and relaxation qualities are excellent even at temperatures up to 150°C. Electrical and thermal conductivity are both excellent. Welding and brazing properties are satisfactory, but soldering properties are exceptional. This heat treatable alloy, which has a nominal composition of 99.85% copper and 0.15%

zirconium. Table 3.1 shows physical, thermal, electrical and mechanical properties of C1500

Table 3.1 Properties of C15100(Astm et al., 2013)

property	**Value**
code	C15100
Thermal conductivity	371W/mK
density	8.89g/cm^3
Electrical conductivity	55.1 MS/m
Electrical resistivity	1.81 microhm-cm
Melting point	1097℃
Elastic of modulus	123 GPa
Hardness	HRB 65
Tensile strength, yield	415 MPa
Tensile strength, ultimate	430 MPa

3.2.2 Silicon Carbide (SiC) Reinforcement

After diamond and boron nitride, silicon carbide (SiC) is the third hardest material, which gives SiC its exceptional qualities like high-temperature stability. To improve the composite's characteristics, silicon carbide is employed as reinforcement in the form of fibers and particles. SiC surely increases the overall strength and corrosion and wear resistance of metal matrix composites when it is introduced. Compared to an unreinforced matrix alloy, copper MMC-S reinforced with SiC particles has improved yield strength, a decreased coefficient of thermal expansion, a higher elastic modulus, and greater wear resistance.

Table 3.2 Properties of Silicon Carbide (SiC)(Street, 2016)

Density	3.1 g/cm^3
Elastic modulus	410 GPa
Flexural strength	550 MPa
Compression strength	3900 MPa
Hardness	2800kg/mm^2
Poisson’s Ratio	0.14
Thermal Conductivity	120 W/mK

3.2.3 Graphite

Carbon exists in its crystalline form as graphite. Graphene is layered in layers to make it. Under normal circumstances, graphite is the most stable form of carbon and it is found in nature. Both natural and synthetic graphite are extensively used in pencils, lubricants, and electrodes. It turns into diamond at high pressures and temperatures. It is a poor heat- and electricity-conductor. The addition of graphite to the Cu matrix reduces the density of the composite, which is advantageous in light-weight applications. It has also been discovered that the particle shape and size of reinforcement determine the density of the composite material. The lubricating coating that graphite particles provide on both surfaces increases the wear resistance of counterparts and composites (Jamwal et al., 2019).

Table 3.3 Properties of Graphite(J. Singh & Sharma, 2016)

Property	Value
Density	2.25g/cm^3
Thermal conductivity	1.50 W/mK
Heat capacity	710 J/(kg.K)
Electrical conductivity	0.03 $\mu\Omega^{-1}$ cm^{-1}
Melting point	3652 °C
Hardness	5 BHN

3.2.4 Chromium

Chromium is a chemical element, with the symbol Cr, the metal chromium is a hard, brittle, steely-gray color. It has a high level of corrosion resistance. It may be polished to create a very shiny surface that is used to plate other metals to create a cover that is both protective and attractive. As an alloying component, chromium enhances the steel's strength, hardness, and elastic limit. starting with thermal treatments and the temperature effect on adhesion and affinity in MMCs or MMNCs, pre- or post-mechanical treatments including stir casting or ultrasonication, reactive wetting processes to improve wetting conditions by chemical agents, and strategies based on coating reinforcements to provide composites with stronger interfacial and mechanical properties (Malaki et al., 2021). Wettability of cast metal matrix composites can be considerably modified by reactive wetting by adding alloying elements to a molten matrix such as Ti, Mg, Cr, Ca, Sr, Mn, Ce, Cu, and Zr, which improves wettability by decreasing surface tension and lowering reinforcement-matrix interfacial energy in the matrix. Chromium is commonly used as an alloying element, such as in Cu/graphite systems to increase wettability. The contact angle between pure copper and graphite has been measured to be around 140, showing that the copper matrix does not wet the graphite particles; however, adding 1.0 wt.% Cr to the graphite/Cu composite reduces the wetting angle from 140 to 43 at 1573 K (Kennedy et al., 2000).

Table 3.4 Properties of chromium(Barnhart, 1997)

Property	value
Density	7.19g/cm^3
Boiling point	2672℃
Melting point	1907℃
Poisson’s ratio	0.31
Hardness	HRB 48
Modulus of elasticity	248GPa
Thermal conductivity	69.1 W/mK

3.2.5 Die Material (H13 Tool Steel)

H13 Tool Steel is a versatile chromium-molybdenum hot work steel utilized in both hot and cold work tooling applications. H13's hot hardness (hot strength) resists thermal fatigue cracking caused by cyclic heating and cooling cycles in hot work tooling applications. H13 is utilized for more hot work tooling applications than any other tool steel due to its exceptional combination of high toughness and resistance to thermal fatigue cracking (also known as heat checking).

Table 3.5 Properties of H13 tool steel(Work & Steel, n.d.)

Properties	Value
Density	7.80g/cm^3
Melting point	1427℃
Tensile strength, ultimate	1200 - 1590 MPa
Tensile strength, yield	1000 - 1380 MPa
Modulus of elasticity	215 GPa
Poisson’s ratio	0.27-0.30

Table 3.6 Composition of H13 tool steel (Markforged, 2018)

Composition	Fe	Mn	Si	Cr	Mo	C	V
Weight percentage (. wt.%)	91.26	0.34	0.9	5.07	1.22	0.40	0.81

3.3 Research Methodology Flow Chart

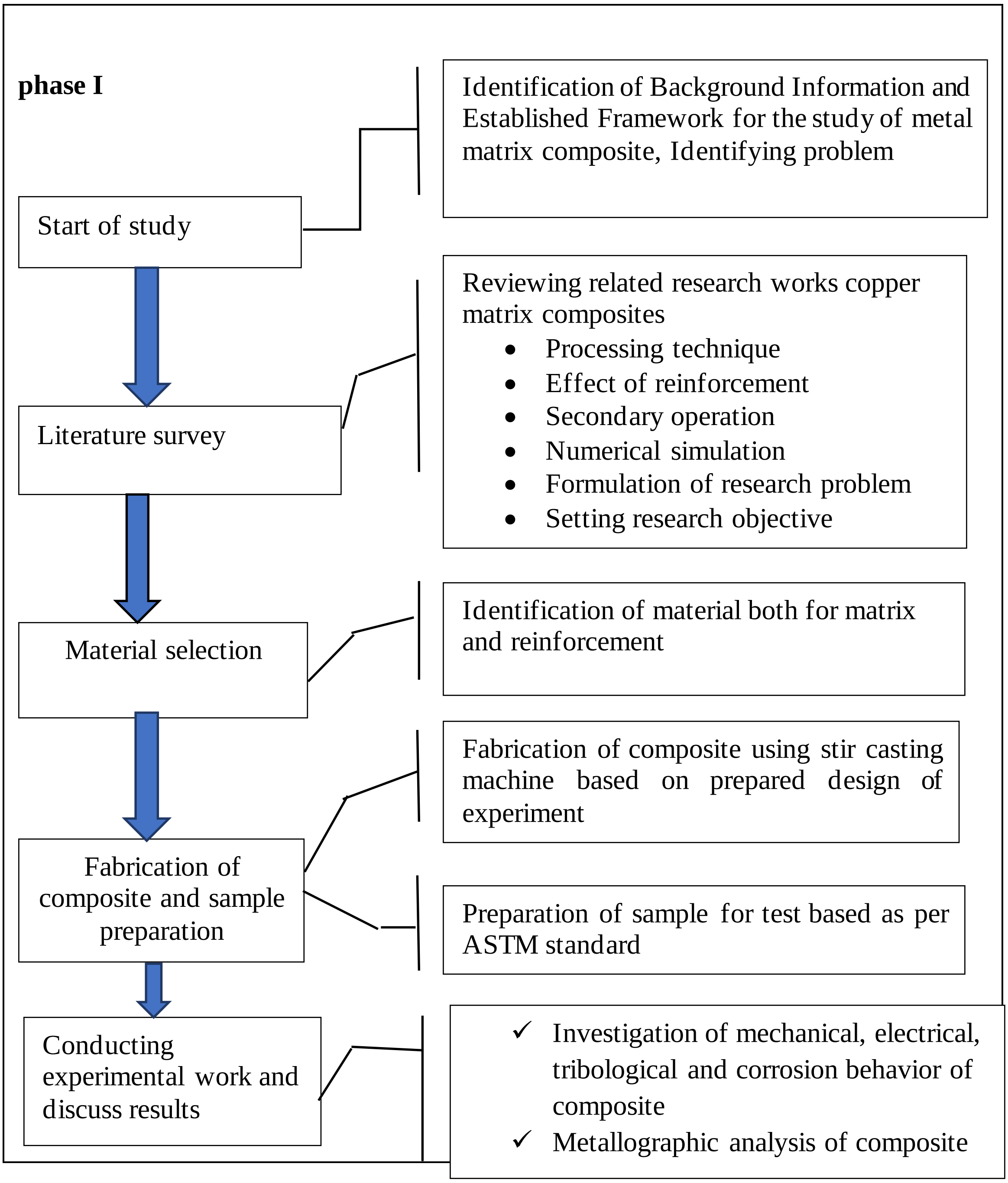

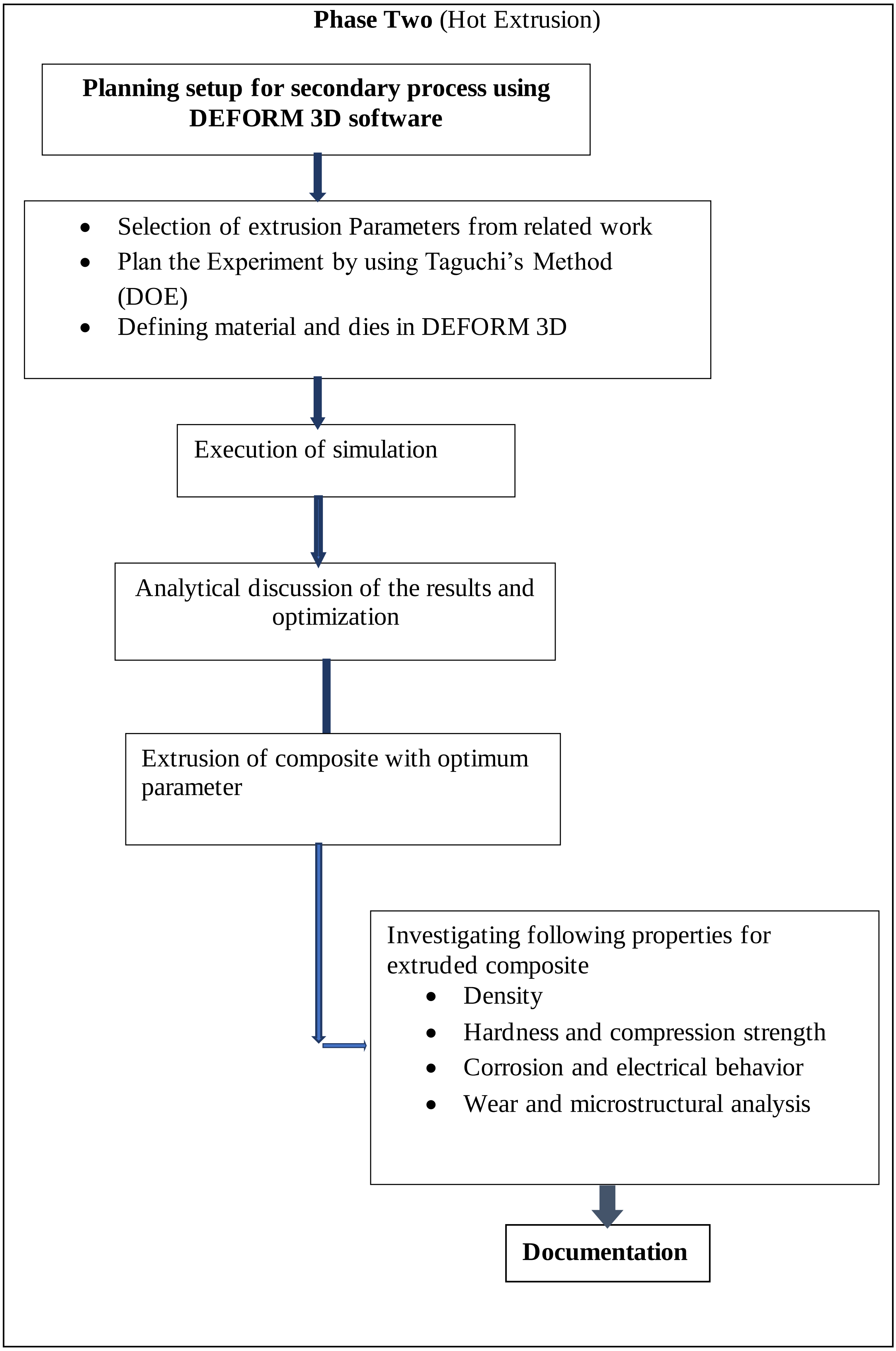

Figure 3-1Research methodology flow chart (a) phase I (b) phase II

3.3.1 Identifying matrix and reinforcement

The materials utilized in this research was (copper alloy) as matrix and silicon carbide used as reinforcement materials that yield the required properties, as well as a small amount of graphite for self-lubrication properties and chromium was added to improve wettability between molten metal and solid reinforcement, after determining the properties of composites required for the application. When making this choice, it is important to take into account the cost, properties, and availability of each option.

3.3.2 Experimental design for fabrication of composite

The composite was prepared using a stir casting machine with an experimental design constructed based on basic input variables of process parameters (stirring speed, stirring time, and reinforcement weight percentage) at the same pouring temperature of 1200℃ for each fabrication. Experimental design is constructed with constant stirring speed, stirring time and pouring temperature based on optimum condition suggested by researcher to fabricate copper matrix via stir casting. Weight percentage of silicon carbide is varying to yield required properties for application of resistant welding electrode. 1% wt. of graphite is used to improve wear performance of copper, as well as 2% wt. Chromium is added to improve wettability of molten copper with reinforcement by decreasing contact angle between matrix and reinforcements.

Table 3.7 Process parameter and their levels

<table>
<tr><th>S. No</th><th colspan="2">Parameters</th><th>levels</th><th>unit</th></tr>
<tr><td>1</td><td colspan="2">Pouring temperature</td><td>1200</td><td>℃</td></tr>
<tr><td>2</td><td colspan="2">Stirring speed</td><td>300</td><td>rpm</td></tr>
<tr><td>3</td><td colspan="2">Stirring time</td><td>30</td><td>minute</td></tr>
<tr><td rowspan="3">4</td><td rowspan="3">Weight percentage of reinforcement</td><td>Graphite</td><td>1</td><td rowspan="3">Wt.%</td></tr>
<tr><td>Chromium</td><td>2</td></tr>
<tr><td>Silicon carbide</td><td>0, 3, 6, 9, 12</td></tr>
</table>

Table 3.8 Experimental design for fabrication

Samples	Composition	Weigh percentage
S1-Sample 1	Copper	97%
	Silicon carbide	0%
	Graphite	1%
	Chromium	2%
S2-Sample 2	Copper	94%
	Silicon carbide	3%
	Graphite	1%
	Chromium	2%
S3-Sample 3	Copper	91%
	Silicon carbide	6%
	Graphite	1%
	Chromium	2%
S4-Sample 4	Copper	88%
	Silicon carbide	9%
	Graphite	1%
	Chromium	2%
S5-Sample 5	Copper	85%
	Silicon carbide	12%
	Graphite	1%
	Chromium	2%

3.3.3 Weight (in mass) estimation for matrix and reinforcement inquires

Total weight mass of matrix and reinforcement required for Cu/SiC/Cr/Gr composite samples production is found from the total specimens require for hardness, compression test, microstructural, wear test and for hot deformation (extrusion) process. All samples were prepared with diameter of 20mm and length of 30cm. The mechanical and tribological properties of the produced composite materials are largely reliant on the reinforcing weight percentage (wt.%). As a result, the weight percent composition of SiC, Gr and Cr employed in this research work was determined based on a survey of the literature. The wt.% composition of any reinforcement addition should not exceed 30% to minimize porosity formation in the composite, for better uniform reinforcement distribution, and for good densification of the fabricated composite(Ramanathan et al., 2019). therefore, the maximum reinforcement for this research study was 15 wt% (12%SiC, 1%Gr and 2%Cr).

The required volume of material for a cylindrical sample is calculated using eqn. (3.1)

$$v = \frac{\pi}{4} D^2 * L \tag{3.1}$$

Where,

V= volume of sample in mm^3,

L=length of sample in mm, and

D=diameter sample in mm

For the hardness and microstructure test, the sample size required was L=15mm, D=20mm, for the compression test as per ASTM standard specimen size required was 18mm length and 6mm diameter for the wear test, depending on the ASTM G99-05 standard the sample size required was L=12mm, D=6mm the calculation to get the required material for fabrication used are within the consideration sample preparation. The amount of material removed by hand saw, file/rasp and grinding (machining and grinding allowance) 2mm per specimen was considered. 100mm length and 20mm diameter was utilized for hot extrusion.

Length = 15 (hardness) + 18(comp) + 12 (wear) + 30 (sample preparation) +30 (electrical conductivity) +100(hot extrusion) +20 (machining allowance for each specimen) = 213mm

Diameter = 20mm

V_T= the total volume of material required for each sample in mm^3

$$v = \frac{\pi}{4} D^2 * L = \frac{\pi}{4} 20^2 * 213 = 66{,}915.92 mm^3 = 66.915 cm^3$$

V_T = (66.915 cm^3 *5) =334.575 cm^3 for five sample fabrication.

The required amount of matrix and reinforcement to fabricate each sample are estimated based on weight percentage set on experimental design. Mass of matrix (copper alloy) and reinforcements (SiC, Gr and Cr) in each sample for the given composition are estimated using Eq (3.2).

$$m_x = V_T * \rho_x * y \tag{3.2}$$

Where m_x is mass of reinforcement or matrix, ρ_x is density of matrix and reinforcement and "y" is weight percentage of reinforcement and matrix. Since weight percentage of graphite and chromium remains constant in all samples it is calculated as follows.

Mass of graphite= $m_x = V_T * \rho_x * y$ = 66.915 cm^3*2.25g/cm^3 *0.01 = 1.5g

Mass of chromium = 66.915 *7.19 *0.02 = 9.62g

I. Weight used for copper **sample 1** is:

Weight (in mass), $m_{(Cu)}$ = 66.915cm^3 *8.89g/cm^3 *0.97 = 577g

II. Weight for copper and silicon carbide used in **sample 2** are:

$m_{(Cu)}$ = 66.915cm^3 *8.89g/cm^3 *0.94 = 559g

$m_{(SiC)}$ = 66.915cm^3 *3.1g/cm^3 *0.03 = 6.22g

III. Weight for copper and silicon carbide used in **sample 3** are:

$m_{(Cu)}$ = 66.915cm^3 *8.89g/cm^3 *0.91 = 541.33g

$m_{(SiC)}$ = 66.915cm^3 *3.1g/cm^3 *0.06= 12.45g

IV. Weight for copper and silicon carbide used in **sample 4** are:

$m_{(Cu)}$ = 66.915cm^3 *8.89g/cm^3 *0.88 = 523.5g

$m_{(SiC)}$ = 66.915cm^3 *3.1g/cm^3 *0.09 =18.57g

V. Weight for copper and silicon carbide used in **sample 5 are:**

$m_{(Cu)}$ = 66.915cm^3 *8.89g/cm^3 *0.85 = 505.6g

$m_{(SiC)}$ = 66.915cm^3 *3.1g/cm^3 *0.12 = 24.89g

Total weight, m_T (in mass) of matrix and reinforcement used for fabrication are calculated as follows:

m_T (Cu) = m_{Cu} in (S1 +S2 +S3+S4+S5) = (577+559+541.33+523.5+505.6) g = 2,706.43g

m_T (SiC) = m_{SiC}) in (S2+S3+S4+S5) = (6.22+12.45+18.57+24.89) g =62.13g

m_T (Cr) = m_{Cr} * (5 sample) = 9.62 g *5 =48.1g

m_T (Gr) = m_{Gr} * (5 sample) = 1.5g *5 =7.5g

3.3.4 Tools and Equipment

Table 3.9 List of equipment and tools used in research

S. No	**Tools**	**Function**
1	Stir casting machine	To fabricate composite
2	Lathe machine	To prepare testing specimen as per ASTM standard
3	Grinder/polisher	To obtain a flat mirror-like surface
4	Abrasive cutter	To sectioning sample while preparing testing specimen
5	Chemical (Keller 's etchant) solution (Ammonia hydroxide, hydrogen peroxide and distilled water)	To keep away from any particles, dust, debris…. etc. from the fabricated specimen for micro structural characterization
6	Optical Microscope	To investigate microstructural analysis of developed composite
7	Universal testing machine	To determine compression strength of prepared composite
8	Vickery hardness machine	To determine hardness of composite's
9	Pin On Disk Apparatus	To determine wear rate of composite's
10	Precision source measuring unit	To determine electrical behavior of composite's
11	Extruder machine	To extrude selected composite with optimum parameter
12	Minitab 21 software	Minitab is a software package used for the analysis of data and optimization using tools in it surface response (S/N ratio, ANOVA)

13	DEFORM 3D v11	It is software used for simulation of deformation behavior of materials that predict load, damage and stress developed
14	ImageJ Software	To analyze porosity level and grain size of composite using OM image
15	potentiator	To determine corrosion behavior of composite

3.3.5 Fabrication Composite Procedure

To achieve optimal properties in metal matrix composites, the distribution of reinforcement material in the matrix alloy must be uniform, the wettability or bonding between these substances must be optimized, and porosity levels must be minimized. Steps involved in the fabrication of copper metal matrix composites are as follows; experimental procedure involves graphite crucible, tungsten coil to heat base metal at required temperature and stirrer road made of tungsten is used to mix reinforcement with matrix. In this work stir casting was used to fabricate metal matrix composites, copper alloy (C15100) circular bar is used as matrix and SiC, graphite and chromium are used as reinforcement. First crucible and reinforcements are preheated at 300°C to remove moisture from crucible and reinforcements.

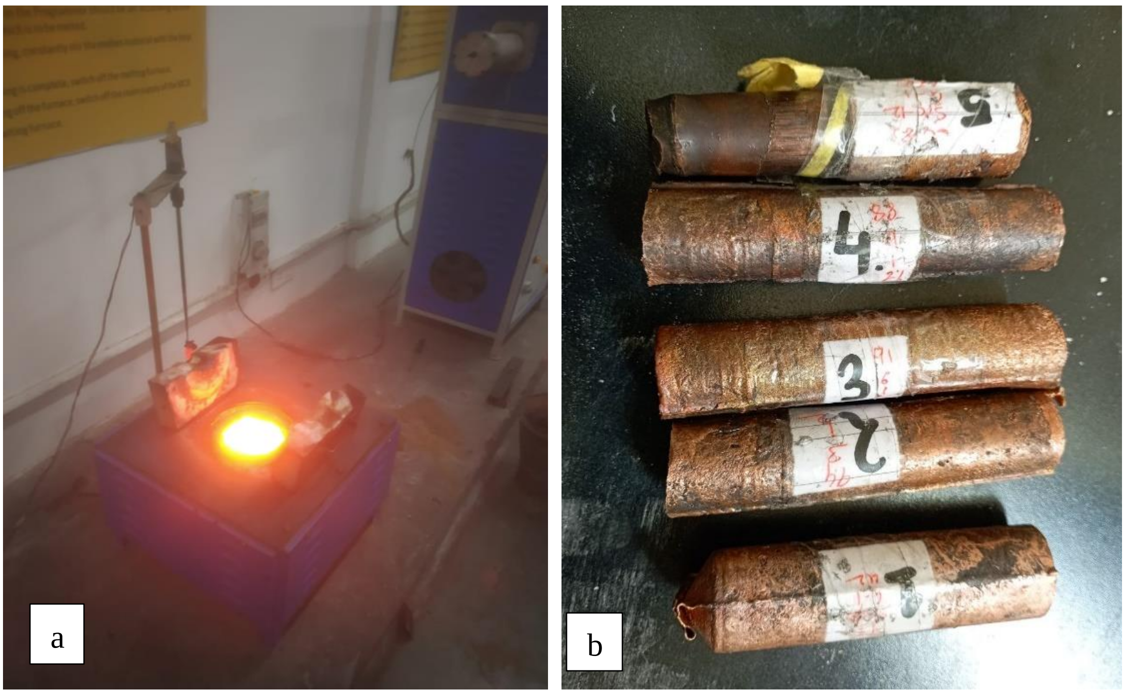

Figure 3-2 Fabrication of composites (a) stir casting setup (b) fabricated sample

Copper alloy at different weight percentage as per experimental design added to graphite crucible in furnace. Then crucible with copper alloy is heated to 1200°C while preheated reinforcements (SiC, Gr and Cr) is added to crucible and mechanical mixed with tungsten rod below their melting point. Stirring of materials takes place at 300rpm (Ali et al., 2020)stirring rate for 30 minute, thereby uniformly dispersing the additive powders in the copper alloy matrix. Pouring of mixed material has been done in ceramic mold. Fabrication is repeatedly carried out with varied composition of materials used in fabrication of composite as per experimental design.

3.3.6 Specimen preparation for tests

Following the successful fabrication of the composite material using the stir casting method, the composite was prepared for mechanical testing, physical testing, microstructural characterization, and tribological testing. The specimen was machined on a lathe to the required shape and size for physical, mechanical, and tribological tests in accordance with ASTM standards.

I. Machining and cutting

The produced composite's surfaces were quite uneven and had undesired components on them. Machining on a lathe was carried out to obtain the necessary shape and size in accordance with ASTM standards, as well as to reduce surface roughness and prevent undesired parts.

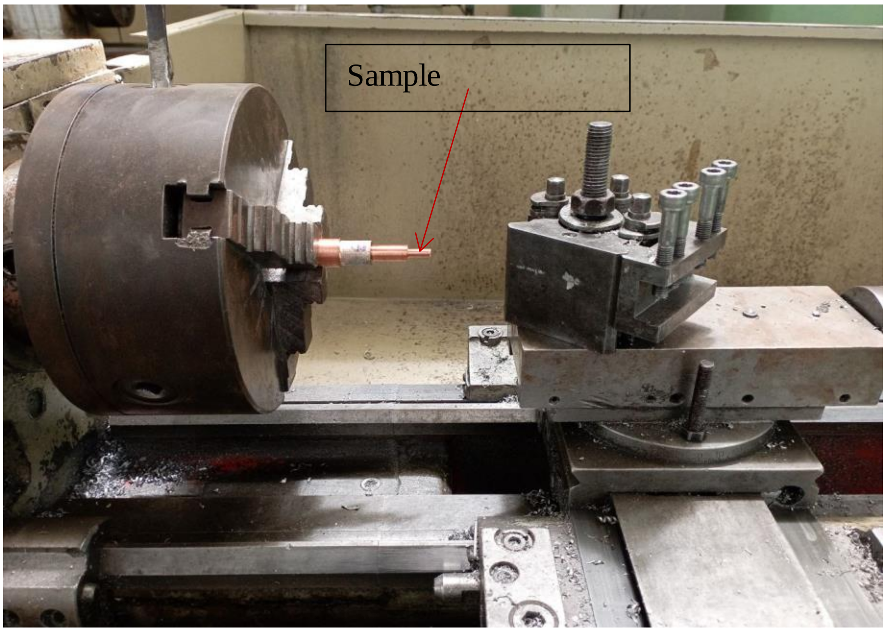

Figure 3-3 Lathe machine setup for sample preparation

3.3.7 Microstructural characterization of composite

The microstructural analysis is performed on each combination of fabricated composite and hybrid composites using an optical microscope to analyze the fair distribution of reinforcement and to determine the volume fraction of grain particle size. It provides information about the specimen under investigation, such as the size and shape of the grains (crystallites), the presence of micro defects (such as segregation and non-metallic inclusions), and the nature and distribution of secondary phases. Specimen is prepared through following steps.

(i) Sectioning

It has two functions: it generates a cross-section of the specimen to be examined; it reduces the size of a specimen to be placed on optical microscope stage; and it reduces the size of a specimen to be embedded in mounting media for further preparation processes. Abrasive cutting is used for sectioning synthesized copper matrix hybrid composites. Specimens are sectioned by a thin rotating disc in which abrasive particles are supported by suitable media.

(ii) Grinding

Grinding is the process of flattening the surface to be examined and removing any damage caused by sectioning. The surface of the specimen to be examined is abraded using a graded sequence of abrasives, beginning with a coarse grit. Synthesized copper matrix hybrid composites are grinded using the sand paper of gradually increasing scale 400, 800, and 2000 grits.

(iii) Polishing

Polishing is the process of creating a smooth and shiny surface by rubbing the sample using a diamond suspension with a gradual reduction of the pressure to keep the specimen from plastic deformations and the sand wheel rotation speed using the RB 204 Metpol-II Model polishing process was used.

(iv) Etching

Chemical etching is a technique for producing contrast between microstructural features on specimen surfaces. Etching is a controlled corrosion process that occurs between surface areas with different electrochemical potentials. Before performing the recommended microstructural characterization, the polished samples of the Cu/SiC/Gr/Cr composites were etched using the recommended mixed etchants solution (25 ml of ammonia hydroxide, 20 ml of hydrogen peroxide and25ml of distilled water). Etching was simply performed by submerging the samples in the solution for 30 seconds.

Figure 3-4 Sample preparation for microstructure (a) sectioning (b) grinding (c) polishing and (d) etching

3.3.8 Density and Porosity Measurement

The experimental density of each grade of composite manufactured was calculated by dividing the measured weight of a test sample by its measured volume on a digital weighing balance with a tolerance of 0.0001; the theoretical density was calculated equation (3.3) (Alaneme & Odoni, 2016).

$$\rho_{theo} = (\rho_{mat} * V_{mat}) + (\rho_{rein} * V_{rein}) \tag{3.3}$$

Where, V_{mat} and V_{rein} are represents volume fraction of matrix and reinforcement respectively. ρ_{theo}, ρ_{mat} and ρ_{rein} is represents theoretical density of composite, density of matrix and density of reinforcement respectively.

A. Actual or experimental density for the Cu/SiC/Gr/Cr hybrid composite was calculated as stated by Archimedes principles. First casted sample weighed in air (W_{air} and then weighted in the distilled water (W_{water}) by suspending samples in it. The actual density or experimental density of casted composite was calculated by equation (3.4) (Pradhan et al., 2020)

$$\rho_{actual} = \frac{m_{air}}{m_{air} - m_{water}} * \rho \tag{3.4}$$

Where, m_{air} = mass of composite in air and m_{water} = mass of composite in distilled water, and ρ = density of distilled water at 25°C 1g/cm3.

Table 3.10 Theoretical and Actual density of composites

samples	Theoretical density(g/cm^3)	Actual density(g/cm^3)
S1	8.79	8.7188
S2	8.62	8.4967
S3	8.44	8.211
S4	8.27	7.944
S5	8.095	7.668

B. porosity of all samples was fabricated by equation (3.5) (Alaneme & Odoni, 2016).

$$P = 1 - \frac{\rho_{act}}{\rho_{theo}} \tag{3.5}$$

Where P = the porosity of composite material, = the actual density of composite material, and = the theoretic density of composite material.

3.3.9 Hardness test

The hardness of a material usually implies its resistance to deformation. The primary goal of a hardness test is to determine the suitability of a produced composite material for a specific engineering application. The Vickers hardness tester was employed, with a square-base diamond pyramid serving as the indenter. This combined angle between the pyramid's opposing faces is 136°. The load divided by the surface area of the indentation yields the diamond-pyramid hardness number (DPH), sometimes known as the Vickers hardness number (VHN or VPH). The Vickers hardness test uses a diamond indenter and a light force to create an indentation on the subject being tested. The depth of indentation is transformed into the hardness value of the object.

Figure 3-5 Vickers hardness testing machine set up

3.3.10 Compression test

The capacity of a material or structure to withstand loads that tend to reduce size is referred to as compression strength. The ultimate tensile strength of a material, by definition, is the magnitude of uniaxial compressive stress achieved when the material fails completely. Compressive strength is often measured experimentally using a compressive test and a uniaxial compressive load. The compression test cylindrical specimen was prepared according to ASTM E-9 standard with a length to diameter ratio of 3mm (L= 18mm and 6mm diameter) and then conducted using a universal testing machine (UTM) with a load capability of 50KN. Load was applied until specimens fractured.

Figure 3-6 Universal testing machine (UTM) setup for compression test

3.3.11 Corrosion test

Corrosion tests were performed by immersing the specimens in a 3.5% NaCl bath for 30 minutes. The specimens for the testing were 15mm in diameter and 7mm in length. To remove any stray markings from the surface of the specimen and make it mirror polished, composite specimens were polished with emery polishing paper 800 no. and then with 12 m diamond paste on a double disc polishing machine. Working electrodes were copper-based composite specimens with an exposed area of 1cm2, an auxiliary (counter) electrode was graphite, and a reference electrode was standard calomel electrode (SCE) or mercury. Tafel curves were generated by automatically adjusting the electrode potential from -250 to +250 mV versus corrosion potential (Ecorr) at a scan rate of 1mVs-1. Experiments were carried out to investigate the effect of reinforcement content on the corrosion behavior of powder metallurgy-fabricated composites. Tafel polarization curves provide electrochemical data such as corrosion potential (Ecorr), corrosion current density (Icorr), and corrosion rate (Cr). The anodic and cathodic areas of Tafel plots were used to calculate corrosion potential (Ecorr) and corrosion current density (Icorr). Extrapolating linear portions of anodic and cathodic curves yielded corrosion potential and corrosion current densities (Icorr).

The corrosion rate was calculated using the conversion formula (3.6)

$$\textit{Corrosion rate(mpy)} = \frac{CEwIcorr}{d} \qquad (3.6)$$

Where C is the conversion constant (0.129), Ew is the equivalent weight of the specimen (g), d is the density of the specimen (g/cm^3)

Figure 3-7 Corrosion test set up (a) potentiator setup for corrosion test and (b) sample prepared for corrosion test

3.3.12 Electrical conductivity test

Electrical conductivity test was performed using precision source measuring unit of four probe terminal. The specimens for the testing were 15mm in diameter and 6mm in length. To remove any stray markings from the surface of the specimen and make it mirror polished, composite specimens were polished with emery polishing paper 800 no. and then with 12 m diamond paste on a double disc polishing machine.

Figure 3-8 Precision source measuring unit set up for electrical conductivity test

Precision source is used to show current–voltage characteristics (with IV-curve) which is used to determine resistance of material using slope of curve. Conductivity is calculate using equation (3.7) (Ren et al., 2015).

$$\sigma = \frac{l}{RA} \tag{3.7}$$

Where l is length of specimen, R is electrical resistance of specimen and A is cross section of specimen

3.4 Finite element analysis of hot deformation

Modelling an extrusion process to determine punch pressure, stress/strain distributions, material flow pattern, and so on is critical to the manufacturing process designer for a variety of reasons. It gives essential information not only for improved design of work equipment and process parameters, but also for refining existing extrusion processes or perhaps establishing new routes. DEFORM-3D v11 software was used for the current simulation investigation. FEM was used to implement simulations. It was typically intended to be used to analyze the forming process as well as for heat treatment. This simulation was currently involved with the process of hot extrusion for Cu/SiC/Gr/Cr hybrid composite. Unlike the general-purpose algorithms used for FEM, DEFORM was designed for modelling deformation with a user-friendly graphical interface that allows for simple data collection and preparation. DEFORM-3D consists of three key stages: a pre-processor, a simulation engine, and a post-processor(Miller & Vecchio, 2004)

pre-processor is used to create, put together, or modify the data needed to analyze the simulation and to create the necessary database file. The DEFORM pre-processor uses a graphical user interface to assemble the data required to run the simulation. Input data includes object description, material data, inter-object condition, simulation control and inner material data. **Simulation engine** that performs the numerical calculations necessary to analyze the process and writes the findings to a database file. The simulation engine reads the database file, computes the actual solution, and appends the solution data to the database file. When necessary, the simulation engine communicates with the Automatic Mesh Generation (AMG) system to build a new FEM mesh on the work piece. The simulation engine writes status information, including any error messages, to the message (.MSG) and log (.LOG) files while it is running. After the simulation has completed, the postprocessor is used to view the simulation data. A graphical user interface is provided by the postprocessor for viewing geometry, field data such as strain, temperature and stress, and other simulation data such as die loads. Additionally, the postprocessor can be used to extract graphic or numerical data for use in other applications.

This study applies commercial finite element code DEFORM-to simulate the plastic deformation behavior during the copper matrix hybrid composite hot extrusion process. The basic equation of rigid-plastic element are as follows(Yang, 2008):

Equilibrium condition:

$$\sigma_{ij,j} = 0 \tag{3.8}$$

Compatibility and incompressibility equations:

$$\dot{\varepsilon} = \frac{1}{2}(u_{i,j} + u_{j,i}) \qquad \varepsilon_{v,} = u_{i,j} = 0 \tag{3.9}$$

Constitutive equations;

$$\sigma'_{ij} = \frac{2\bar{\sigma}}{3\dot{\bar{\varepsilon}}}\dot{\varepsilon}_{ij} \qquad \bar{\sigma} = \sqrt{\frac{3}{2}(\sigma_{ij}\sigma_{ij})} \qquad \bar{\varepsilon} = \sqrt{\frac{3}{2}\dot{\varepsilon}_{ij}\varepsilon_{ij}} \tag{3.10}$$

Boundary condition:

$$\sigma_{ij} = F_j \text{ on } S_F, \qquad u_i = U_i \text{ on } S_U \tag{3.11}$$

Where σ_{ij} and $\dot{\varepsilon}_{ij}$ are the stress and strain rate, respectively, $\bar{\sigma}$ and $\dot{\bar{\varepsilon}}$ effective stress and effective stress rate, respectively, F_j is the force on boundary surface of S_F and U_i is deformation velocity on the boundary surface of S_{ij} . The weak form of rigid-plastic FEM can be determined by applying the variation method to equation (3.8) – (3.11).

$$\int_v^{-} \varepsilon\delta\bar{\varepsilon}dV + K\int_V \varepsilon_V\delta\varepsilon_V dV - \int_{SF} F_i\delta u_i dS = 0 \tag{3.12}$$

where V and S are the volume and the surface area of the material, respectively, and K is the penalty constant.

3.4.1 Input material data

To attain a high level of accuracy in a simulation, it is necessary to understand the material qualities required to specify a material in DEFORM. The material properties that the user is needed to specify are determined by the material types used in the simulation(Miller & Vecchio, 2004). For this simulation material was assumed as rigid-plastic workpiece whereas all dies assumed as rigid. As per guidelines of DEFORM 3D software for an isothermal forming problem with rigid dies and rigid-plastic workpiece flow stress should be determined only for workpiece. Flow stress data for selected composite is obtained from compression test. At room temperature, the flow stress of most metals is strain dependent. It was empirically found that the strain dependency of the flow stress can be expressed using Hollomon's equation (3.13) (Boulger, 2016).

$$\bar{\sigma} = K\dot{\varepsilon}^{n} \tag{3.13}$$

where $\bar{\sigma}$ is flow stress, $\dot{\varepsilon}$is true strain , K is material constant and n is strain hardening constant.

The flow stress is mostly driven by the strain rate at higher temperatures, above the recrystallization temperature, and it can be approximated as equation (3.14)

$$\bar{\sigma} = C\dot{\varepsilon}^{n} \tag{3.14}$$

DEFORM 3D provides several ways for defining flow stress. For simulation of copper matrix hybrid composite power law (equation 3.15) is employed as constitutive equation to determine flow stress developed during hot deformation.

$$\bar{\sigma} = C\bar{\varepsilon}^{n}\dot{\bar{\varepsilon}}^{m} + y \tag{3.15}$$

Where, $\bar{\sigma}$ is flow stress, $\bar{\varepsilon}$ is effective plastic strain, $\dot{\bar{\varepsilon}}$ effective strain rate, n is strain exponent, m is strain rate exponent, C is material constant and y represented initial yield value. Initial yield stress is obtained from stress-strain curve during compression test. Yield stress is a point of limit for elastic behavior and beginning of plastic behavior. true strain and true strain were calculated using equation (3.16) and (3.17) based on data obtained from compression test.

$$\varepsilon = \log(1+e) \tag{3.16}$$

$$\sigma = S(1+e) \tag{3.17}$$

where, ε and σ are represented true strain and true stress, respectively, while e and S are represented engineering strain and engineering stress respectively.

Following the yield point, further plastic deformation necessitates an increasing load but at a decreasing rate. Work hardening strengthens the material while lowering the area of cross section. The combination of these two phenomena produces a typical load progression curve. The strain hardening exponent (n) governs how the metal behaves during the formation process. Higher n value materials are more formable than lower n value materials. Metals' remaining work hardening capacity reduces as they harden(Argon, 2007). Stain hardening exponent and strain rate exponent is calculated by equation (3.18) and (3.19), respectively.

$$n = \frac{d\log(\sigma)}{d\log(\varepsilon)} \tag{3.18}$$

$$m = \frac{d\log(\sigma)}{d\log(\bar{\varepsilon})} \tag{3.19}$$

Strength coefficient K is calculated using following equation (3.20).

$$\log(\sigma) = \log(K) + n\log(\varepsilon) \tag{3.20}$$

3.4.2 Experimental design for simulation

The process parameters of each hot forming through extrusion were determined based on the desired qualities of the final products as well as various manufacturing concerns such as cost effectiveness. Based on the size of the sample to be fabricated, four hot extrusion process parameters were selected: extrusion speed, extrusion ratio, extrusion temperature and die length. Die length held constant to 20mm, and mesh size of billet was 90,000, while mesh size of each die was set to 80,000 As a result, the effect of these parameters on the on damage, and required load for extrusion was investigated utilizing multi objective optimization using Minitab 21 software to perform the GRA.

Table 3.11 Extrusion parameter and their levels

parameters	unit	levels			
		1	2	3	4
Extrusion speed	mm/s	1	2	3	4
Extrusion ratio	---	2	3	4	5
Temperature	℃	800	850	900	950

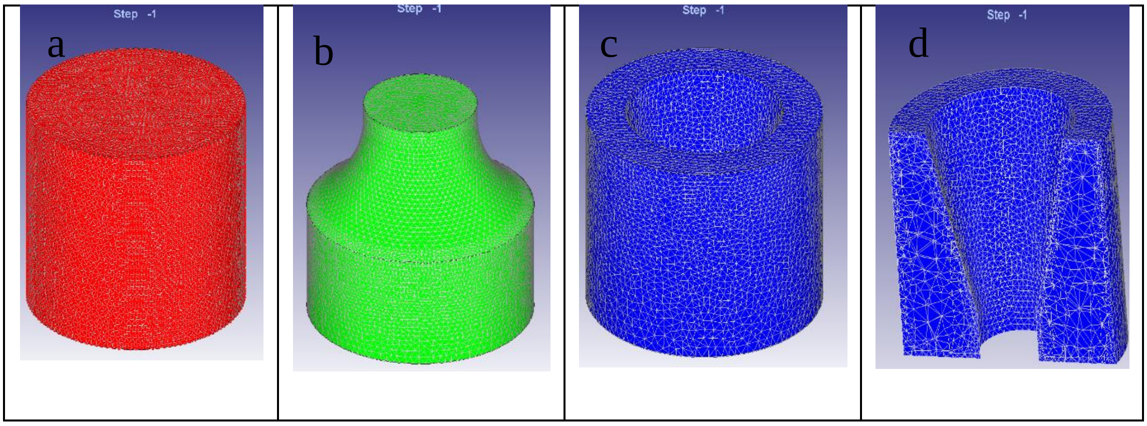

Figure 3-9 Meshed model of simulation setup (a) top die (b) material (c) full bottom die and (d) sectioned bottom die

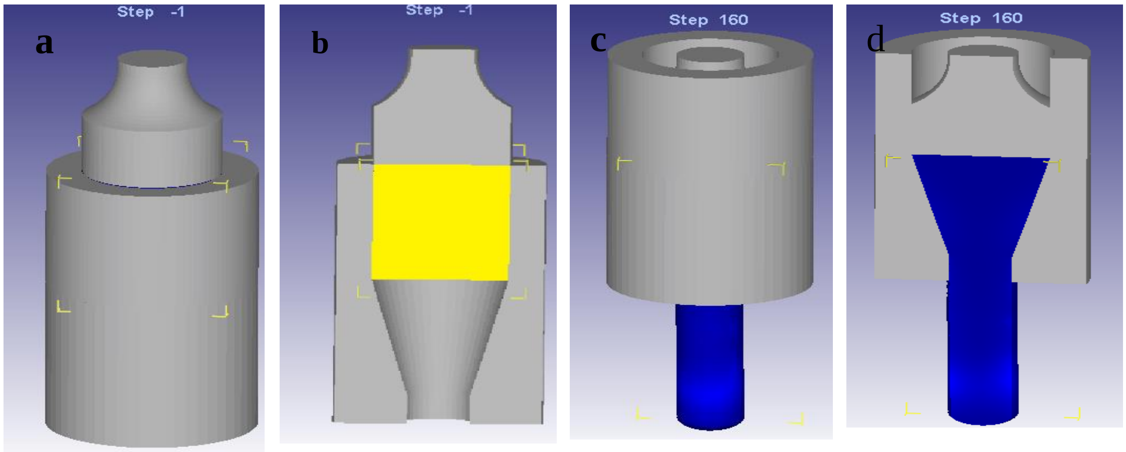

Figure 3-10 simulation setup at different step first step (a and b) and final step (c and d)

3.5 Secondary process operation

3.5.1 Design and Fabrication of die parts

The method employs a mathematically shaped cosine die designed for round to cylindrical shape extrusion. A H13 die steel stock of 95 mm diameter and 50 mm diameter was obtained from MIDI (Addis Ababa, Ethiopia) and power hacksaw cut to the desired size for die chamber punch and guide plate. The die chamber and punch were pre-machined on a lathe machine by facing, turning, drilling, and boring operations. After pre-machining, the die cylinder and punch set were heat treated in a muffle furnace in three steps: stress reliving, hardening, and tempering. Stress relief was performed at 650 °C for one hour and then gently cooled. The die components were hardened by directly placing them in a furnace preheated to 1000 °C, soaking for 25-30 minutes, and then quenching in still air. The pieces were placed in the furnace for tempering, and the furnace temperature was raised to the appropriate tempering temperature (900°C) and slowly cooled in the furnace. Finally, the surface polishing of die components was completed with a cylindrical grinder.

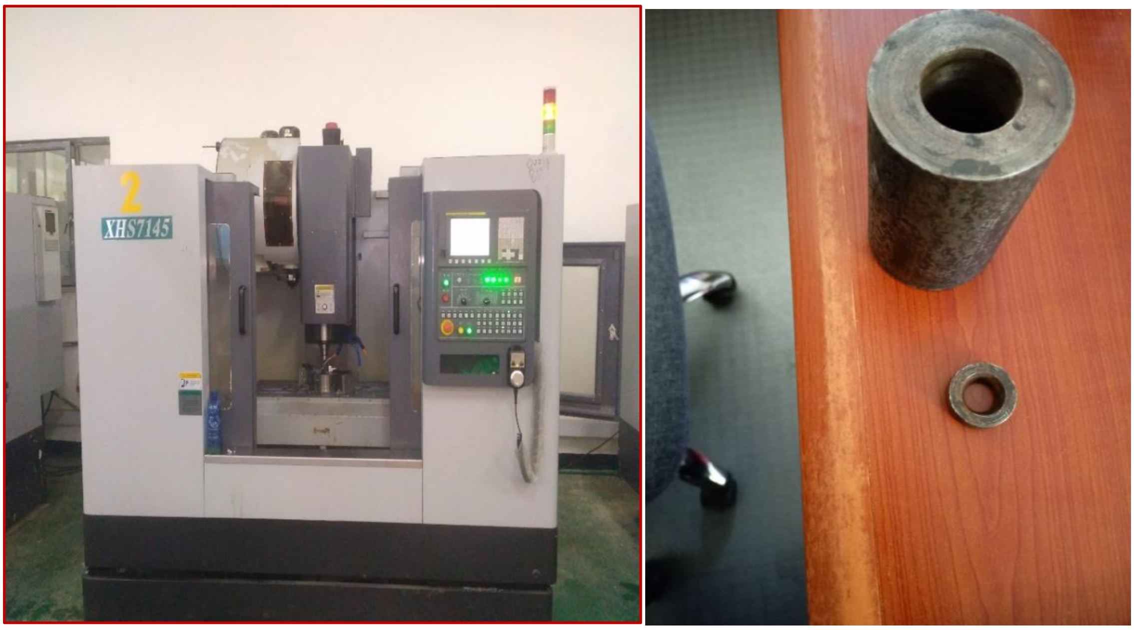

Figure 3-11 Die fabrication setup and fabricated die

3.5.2 Hot extrusion process

Before beginning the hot extrusion procedure, casted billet of copper matrix hybrid composite reinforced with SiC, Gr and Cr composites were preheated for 10 minutes 850°C to uniformly heat the sample volume. In order to reduce friction during the extrusion process, the solid lubricant graphite powder is combined with semi-solid lubricant grease and placed on the inner surface of the die. Due to its accessibility, affordability, and frequently low friction coefficient, graphite is frequently employed as a solid lubricant. Because humidity (such as air) lowers the material's shear strength to acceptable levels, it is a requirement for graphite to be lubricating. 30 mm-long specimens prepared using stir casting was followed by secondary processing hot extrusion. Then, using a 1500KN hydraulic press and a ram speed of 3 mm/min and an extrusion ratio of 2:1 (extrusion ratio = area of billet/area of shape), hot extrusion was performed. This is depicted in Figure 3.12 below. For hard metals, the maximum permitted extrusion ratio is 35:1, while for soft alloys, the maximum acceptable extrusion ratio is 100:1. For hard metals, the standard extrusion ratio is from 10:1 to 35:1, while for soft alloys, it ranges from 10:1 to 100:1. Since the actual shape of the extrusion can influence results, these restrictions shouldn't be taken as gospel, according to (Mohapatra, 2016) . Due to the greater resistance to metal flow, the harder the part is to extrude, the higher the extrusion ratio. Because of their poor surface properties, which necessitate the lowest billet temperature, hard alloys demand the highest extrusion pressure and are much more challenging. Because SiC, Gr and Cr in the Cu-SiC-Gr-Cr composite make it a hard material, the current work used a 2:1 extrusion ratio. The composite samples used in this work are hot-extruded and reduce in diameter from 20 mm to 10 mm.

Figure 3-12 Hot extrusion setup

3.6 Analysis of material behavior and optimization of material properties as per L16 orthogonal array

3.6.1 Taguchi based Grey relational analysis method

Taguchi Methods are an approach for developing and carrying out experiments to investigate processes where the outcome depends on numerous parameters (variables; inputs) without having to laboriously and uneconomically run the process using all possible combinations of values for those variables. Grey relational analysis is extensively used to quantify the degree of interaction among sequences using grey relational grades. Several researchers have used grey relational analysis to optimize control parameters with multiple responses via grey relational grade (Jajimoggala et al., 2019).The integrated Grey-based Taguchi approach integrates the Taguchi method's algorithms with grey relational analysis to determine the optimal value for process parameters with numerous performance criteria. The Taguchi method is used for optimization, but because it is a single response optimization strategy, it is applied together with grey relational methodology. Grey rational analysis reduces a multi-response to a single response, which is subsequently optimized using the Taguchi method.

Because hot extrusion simulation is time consuming, it is critical to conduct effective experiments with few runs to determine the most significant factors.

3.6.2 Taguchi's Orthogonal Array

Taguchi's Orthogonal Array specifies the generation of a pair of parameters from all levels at two column intervals in the experimental table, where each composition has the same frequency(Hsia, 2013). Orthogonal Array compromises on experimental cost and precision, and fewer experiments are required to obtain usable statistical information. Nonetheless, orthogonal array experiments are not full factorial experiments. The "bias" cannot be totally avoided, but it is acceptable because not all levels of composition appear on the orthogonal array. As a result, the optimal composition may not be in the experimental group.

3.6.3 Signal-Noise Ratio Analysis

To identify the optimum extrusion parameters, the Taguchi approach requires assessing the signal-to-noise ratio (S/N) of each extrusion parameter level for each output function. Analysis of the S/N ratio, that is, the lower-the-better, higher-the-better, and nominal the-better, is the performance characteristic. Based on the S/N analysis, the S/N ratio for each level of process parameters is derived. Regardless of the performance characteristic category, the higher the S/N ratio, the better the performance characteristic(Mohapatra & Maity, 2016). In Taguchi optimization, the S/N ratio represents a measure of quality features and is determined as follows (Kothasiri and Chalamalasetti, 2022).

$$\frac{S}{N} = -10\log\left[\frac{1}{n}\sum_{i=1}^{n} \mathrm{Yi}^2\right] \tag{3.21}$$

$$\frac{S}{N} = -10\log\left[\frac{1}{n}\sum_{i=1}^{n} \frac{1}{\mathrm{Yi}^2}\right] \tag{3.22}$$

where Y = observation n = total number of observations, Y = the average of observed data and Yi = ith response.

Eq. (3.20) is utilized for smaller the better S/N ratios, and Eq. (3.21) is appropriate for greater the better S/N ratios. To reduce extrusion force, damage, and time, the S/N ratio is estimated for damage, extrusion force, and time using the smaller-is-better criterion. To maximize displacement, the S/N ratio is determined for billet displacement using the larger-is-better criterion (Kothasiri and Chalamalasetti, 2022).

3.6.4 Analysis of Variance (ANOVA)

The analysis of variance (ANOVA) was used to determine which parameters have a significant influence on the quality attribute. The statistical approach of ANOVA is used to determine the influence of all control values. The percentage contributions of each control factor are used to measure the associated impacts on the performance characteristics in the analysis of variance. This analysis used a significance level of 5%, corresponding to a 95% level of confidence. The ANOVA findings show whether or not there is a statistically significant variation in output characteristics. ANOVA analysis is used when values are less than 0.05 and more than 0.05 are not significant.

3.6.5 Optimization Steps Used in Grey Relational Analysis

Step 1: Depending on the type of quality feature, convert the original response data into S/N ratio (Yij) using the relevant formula stated in equation (3.20 and 3.21).

Step 2: To prevent the effect of using various units and to reduce variability, normalize Yij as Zij (0 _ Zij _ 1) using the following formula. Normalization is a transformation done on a single input to uniformly distribute and scale the data into an acceptable range. Zij denotes the normalized value for the ith experiment/trial and the jth dependent variable/response.

$$\text{Zij} = \frac{Yij - Ymin}{Ymax - Ymin} \tag{3.23}$$

$$Zij = \frac{Ymax - Yij}{Ymax - Ymin} \tag{3.24}$$

When the original sequence's larger-the-better characteristic is considered, the original sequence should be normalized using equation (3.23). When the original sequence's smaller-the-better characteristic is considered, the original sequence should be normalized using equation (3.24).

Step 3: Compute the grey relational coefficient (GRC) for the normalized S/N ratio values.

$$GRCij = \frac{\Delta\text{min} + \partial\Delta\text{max}}{(\Delta ij + \partial\Delta\text{max})} \tag{3.25}$$

Where, i= 1, 2, ..., n-experiments and j== 1, 2, ..., m-responses

GRC*ij* = GRC for the *i*th experiment/trial and Δ= absolute difference between *Yoj* and *Yij*, Δmin = minimum value of Δ and Δmax = maximum value of Δ

∂ is the distinguishing coefficient which is defined in the range $0 \leq \partial \leq 1$ Step

Yoj = optimum performance value or the ideal normalized value of *j*th response

Yij = the *i*th normalized value of the *j*th response/dependent variable Δ

Step 4: Compute the grey relational grade (GRGi).

$$GRGi = \frac{1}{m}\sum GRCi \tag{3.26}$$

where m is the number of responses.

Step 5: Select optimal levels for the factors based on the maximum average GRGi value using the response graph method or ANOVA.

CHAPTER 4

RESULTS AND DISCUSSION

4.1 Introduction

In this analysis part, the results of the experimental work of the study have been addressed in detail in different sections and sub-sections in flow. Density determination, hardness test, compression test, electrical conductivity test, corrosion test and material characterization tests results for fabricated composite were reported and analyzed. Material with best properties was selected and extrude with DEFORM 3D to predict effect of extrusion process parameter on workpiece. The result was analyzed as a single response characteristic for (damage, effective stress and load) using Taguchi 's S/N ratio and as a multi-response characteristic using Hybrid Taguchi Grey Relational Analysis (HTGRA) for extrusion. Finally results of conducted test for extruded workpiece have been discussed in detail.

4.1.1 Analysis of synthesized samples behaviors

Table 4.1 below shows the composition and sample designation of five samples which synthesized with stir casting at constant stirring time, string temperature and stirring speed by varying weight percentage of reinforcement. The aim of fabricating those samples was to ensure manufacturability of Cu/SiC/Gr/Cr hybrid composite for application of resistant electrode welding and to investigate effect of silicon carbide as reinforcement.

Table 4.1 Composition and sample designation of composite

Samples code	composition
S1	Cu + 1%Gr +2%Cr
S2	Cu + 3% SiC + 1%Gr +2%Cr
S3	Cu + 6% SiC + 1%Gr +2%Cr
S4	Cu + 9% SiC + 1%Gr +2%Cr
S5	Cu + 12% SiC + 1%Gr +2%Cr

4.2 Analysis of density and Porosity of Composite

The plot of copper matrix hybrid composite with varying percentage of SiC for five specimens is shown in Figure 4.1. Because SiC, Gr and Cr have densities that are lower than those of Cu, their addition causes the material's density to decrease. The densities of copper matrix, SiC, Gr and Cr reinforcement are 8.89, 3.1, 2.26 and 7.19 g/cm3, respectively. It is thought that reinforcing metallic with ceramics causes voids in the microstructure due to ceramic aggregation, a considerable difference in surface energy between ceramics and metals, and arbitrary shape of the ceramics with sharp edges (Wagih et al., 2019).

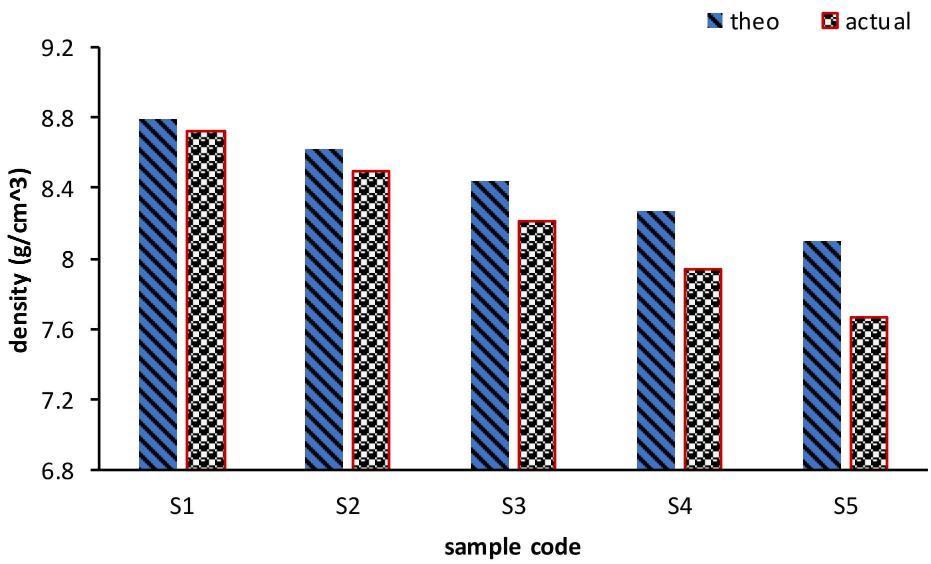

Figure 4-1 Actual and theoretical density of Cu-SiC-Gr-Cr hybrid composite

Porosity of synthesized composite material was determined by equation (3.5). The difference between the actual values and theoretical densities was a measure of voids and pores present in the composites. These voids severely pose a negative impact on the mechanical and thermal properties of composites and even affect the performance of the composite (Pradhan et al., 2020). So as shown in Table 4.2 porosity of copper-based composite was increased as weight percentage of reinforcement increased. Highest porosity percentage was found in sample 5 which was reinforced with 15% metallic and ceramic particles whereas minimum porosity level was found in sample 1 which was reinforced with 3%wt. Gr-Cr reinforcement. Due to a variety of conditions, adding reinforcement to a copper matrix composite might raise the porosity percentage. One reason for porosity increment is that the reinforcing particles may act as nucleation sites for gas bubbles during the manufacturing process, increasing porosity. Another reason is that the addition of reinforcement might cause the molten metal matrix to become more viscous, making it more difficult for gas bubbles to escape during solidification and resulting in blocked pores in the finished product. Furthermore, reinforcing particles might produce turbulence in molten copper, which could lead to gas bubble entrapment.

This was due to the presence of reinforcing particles, which obstruct the flow of molten metal and impede gas escape.

Table 4.2 Porosity level and variations in theoretical and actual density values

samples	Theoretical density(g/cm^3)	Actual density(g/cm^3)	Porosity (%)
S1	8.79	8.7188	0.81
S2	8.62	8.4967	1.43
S3	8.44	8.211	2.71
S4	8.27	7.944	3.94
S5	8.095	7.668	5.27

4.3 Electrical behavior analysis

The electrical conductivity of the samples was determined using a precision source measuring equipment. The instrument's four probes were held on the sample until the reading became stable. The voltage-current (IV curve) parameters of the examined sample were generated using an instrument. The IV curve slope was used to determine the resistance of each sample. Using an equation 3.7 the obtained resistance was utilized to calculate the conductivity of samples.

Figure 4.2 shows electrical conductivity value of pure copper and synthesized copper-based hybrid composite chart plotted using data acquired during testing. For Cu, Cu-1Gr-2Cr, Cu-3SiC-1Gr-2Cr, Cu-6SiC-1Gr-2Cr, Cu-9SiC-1Gr-2Cr and Cu-12SiC-1Gr-2Cr electrical conductivity is 55.1, 47.1, 39.3, 31.2, 26.9 and 18.3MS/m respectively. Even though graphite has excellent electrical conductivity, the addition of the alloying element chromium along solid lubricant graphite reduces the electrical conductivity of the copper-based composite in sample 1 reduced by 14.5% when compared to commercial copper. According to finding obtained from (Zuo et al., 2020) reduction of electrical conductivity is due to two reason Firstly, as Cr is added into the Cu matrix, the Cr_3C_2 phase forms, changing the local potential field inside the material and thus forming the scattering center, resulting in additional resistivity due to impurities; second, excess Cr may also act as a second phase, resulting in decreased electrical conductivity. S1 to S5 showed reduction in conductivity with increasing weight percentage of silicon carbide as reinforcement. Because silicon carbide is an insulator, the electrical conductivity of a copper matrix composite tends to decrease as the weight percentage of silicon carbide increases. When added to copper, it inhibits the flow of electricity through the composite material, potentially lowering overall conductivity. Furthermore, the presence of silicon carbide particles increased the possibility of voids and porosity development during processing, which might reduce electrical conductivity even further. Wagih et al. (2019) reported that the movement of free electrons is hindered by the presence of ceramic particles along the grain boundaries of copper, resulting in a higher electrical resistivity than for Cu. As composition of reinforcement increased porosity is increased because of poor wettability between base metal and reinforcement particles. the porosity in the samples led to a decline in electrical conductivity values with increasing content of reinforcement which had good agreement with investigation made by (Ayyappadas et al., 2017).

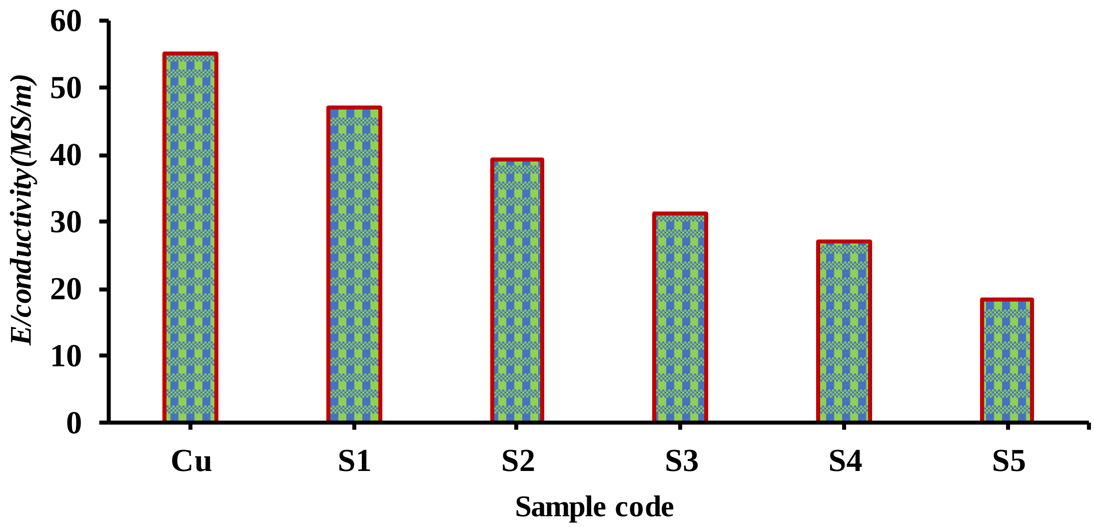

Figure 4-2 Electrical conductivity of Cu-SiC-Gr-Cr hybrid composite

4.4 Analysis of hardness for composite

Figure 4.3 shows Vickers hardness value of copper matrix composite reinforced with SiC/Cr/Gr. The maximum and minimum hardness value among five samples of Cu/SiC/Gr/Cr hybrid composite synthesized via stir casting was 102.7 and 184.93 respectively. In sample 1 hardness value of pure copper was improved by 23.4% with addition of chromium as reinforcement. According to the results obtained from (Uzun & Usca, 2018), the Cr reinforcement enhanced the hardness of pure copper. From sample 2 to sample 5 hardness of composite was increased with increasing composition of silicon carbide. According to finding obtained from (Shabani et al., 2016). The hardness of composite increases as the SiC particle content increased which will improve performance of the composite. Because SiC ceramic particles have a higher hardness value than the soft Cu matrix, therefore, the hardness of the composite was improved. Maximum hardness was obtained in sample 5 which was reinforced with 15%wt. reinforcement. Reinforcing particles enter the soft ductile metal matrix's lattice structure and hinder the mobility of atoms when there is a dislocation by providing greater resistance to plastic deformation. With increasing wt.% of reinforcements, grain boundary strength increases while dislocation density of atoms drops, giving strength to the matrix and hence an increase in hardness of the composite (Jojith and Radhika, 2019).

Table 4.3 Hardness values of Cu/SiC/Gr/Cr hybrid composite

Sample code	Harness value (HV)			Average hardness value
	Trial 1	Trial 2	Trial 3	
S1	93.4	106.5	108.2	102.7
S2	118.6	115.2	122.1	118.63
S3	119.6	124.3	132.0	125.3
S4	143.9	165.3	153.9	154.37
S5	177.7	183.5	193.6	184.93

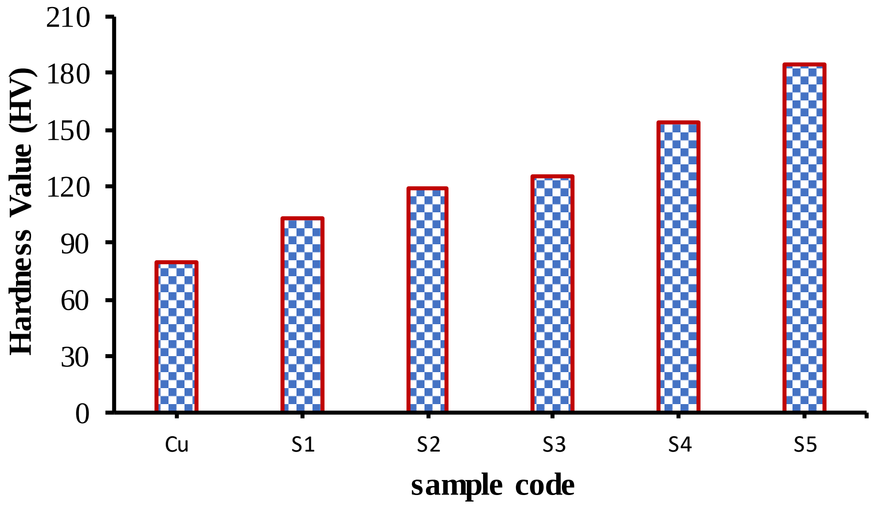

Figure 4-3 Hardness value of Cu/SiC/Gr/Cr hybrid composite

4.5 Compression test

Casted specimens were compressed using the universal testing equipment. Figure 4.4 shows compression strength bar chart plotted using data acquired during testing. For Cu, Cu-1Gr-2Cr, Cu-3SiC-1Gr-2Cr, Cu-6SiC-1Gr-2Cr, Cu-9SiC-1Gr-2Cr and Cu-12SiC-1Gr-2Cr the ultimate compressive is 225, 241, 275, 314, 278 and 207 MPa, respectively. The results show that adding reinforcement wt.% (SiC-Gr-Cr) up to 12% to copper matrix samples produces marginally better order yield strength than pure copper. When compared to the other samples, the addition of (15 SiC-Gr-Cr) wt.% did not significantly improve mechanical properties. The influence of these microstructural deteriorations was observed in the mechanical behavior of a sample containing 15% SiC-Gr-Cr in a compression test, where the sample failed in low loads and exhibited a very brittle fracture. The explanation for such a result could be due to the fact that as percentage of reinforcement was increase, the number of porosities in the microstructure and their impact on mechanical properties increased. The explanation for such a result could be attributed to the fact that the quantity of porosity in the microstructure and its effects on mechanical properties increased with the addition of more reinforcement. If these particles were uniformly and sufficiently added to the matrix, adding them up to a specific level, in this work 12wt.% of reinforcement, might favorably boost the compressive strength of composites. Prajapati and Chaira (2019) reported the same idea.

Maximum and minimum compressive strength was 314 MPa and 207MPa respectively, Addition of chromium in sample 1 slightly improved compressive strength when compared to pure copper which is agreed with investigation made by (Uzun & Usca, 2018).there is increment of compression strength from sample 2 to sample 4 with addition of silicon carbide as reinforcement. The compressive strength of the fabricated hybrid composites is found to be greater than that of its copper matrix. It is due to the reinforcement of harder ceramic materials into the matrix, where strengthening mechanisms such as Hall- Petch, load transfer effect, and mismatch of elastic moduli of the matrix and reinforcing particle involve improving the compressive strength of the hybrid composites materials (Singh and Gautam, 2017). When the amount of reinforcement approaches 15% wt, the compressive strength in sample 5 finally drops due to an increase in brittleness of the composite which is aligned with finding obtained from (Prajapati and Chaira, 2019)

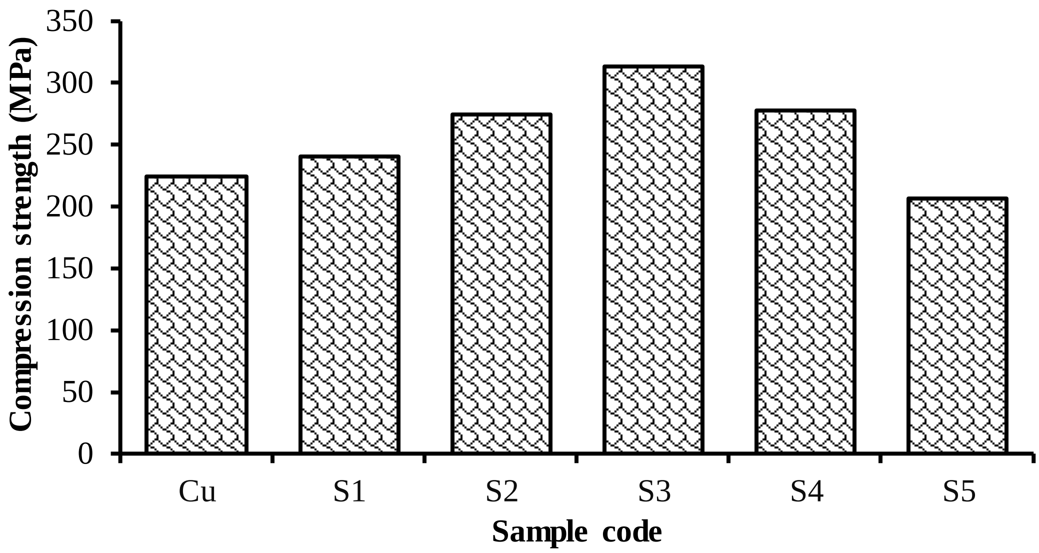

Figure 4-4 Compression strength of copper matrix hybrid composites

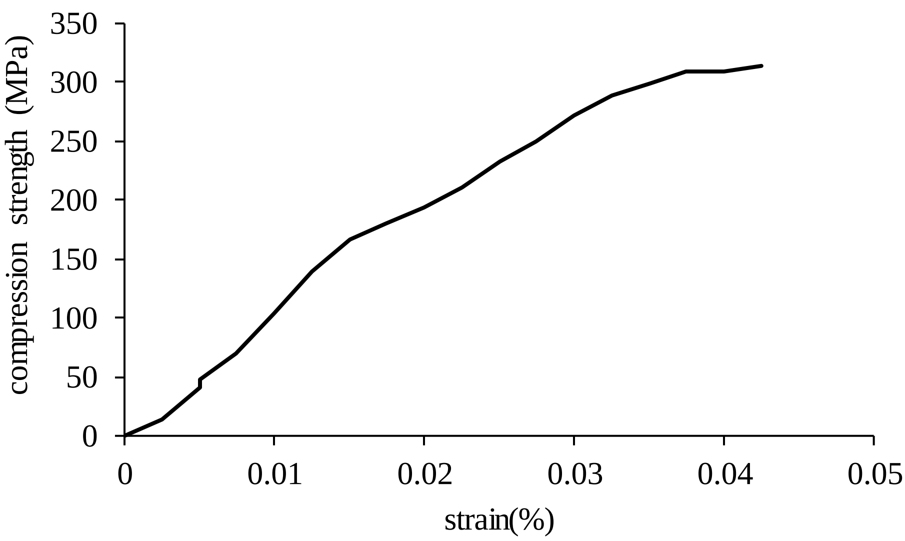

Figure 4-5 Stress-strain diagrams for Cu-6SiC-2Cr-1Gr hybrid composite

4.6 Microstructure of casted composite

The basic investigation during the material characterization process was the observation of the microstructure. It is feasible to reason about the real qualities of analyzed specimens based on observable patterns of microstructures. All synthesized specimen discussed in greater depth in the current study. The phase and microstructure of the composites were examined using optical microscopy and scanning electron microscopy.

4.6.1 Optical microscopy

The distribution of reinforcing particles in the copper matrix was studied using optical microscopy (OM), as illustrated in Figure 4.6. Using imaging software, the grain size was determined from an optical microscope image. The grain size was determined using the line intercept approach and ranged from 28.45µm to 162.4µm depending on the OM image. The average grain size determined from five trial values from different locations of the specimen image is 72.35µm.

ImageJ was used to analysis porosity level and grainsize of synthesized composite with varying weight percentage. Porosity percentage calculated for sample1, sample 3 and sample 5 are 0.92%, 2.46% and 5.78 respectively, which has good agreement with porosity level calculated using equation (3.4)

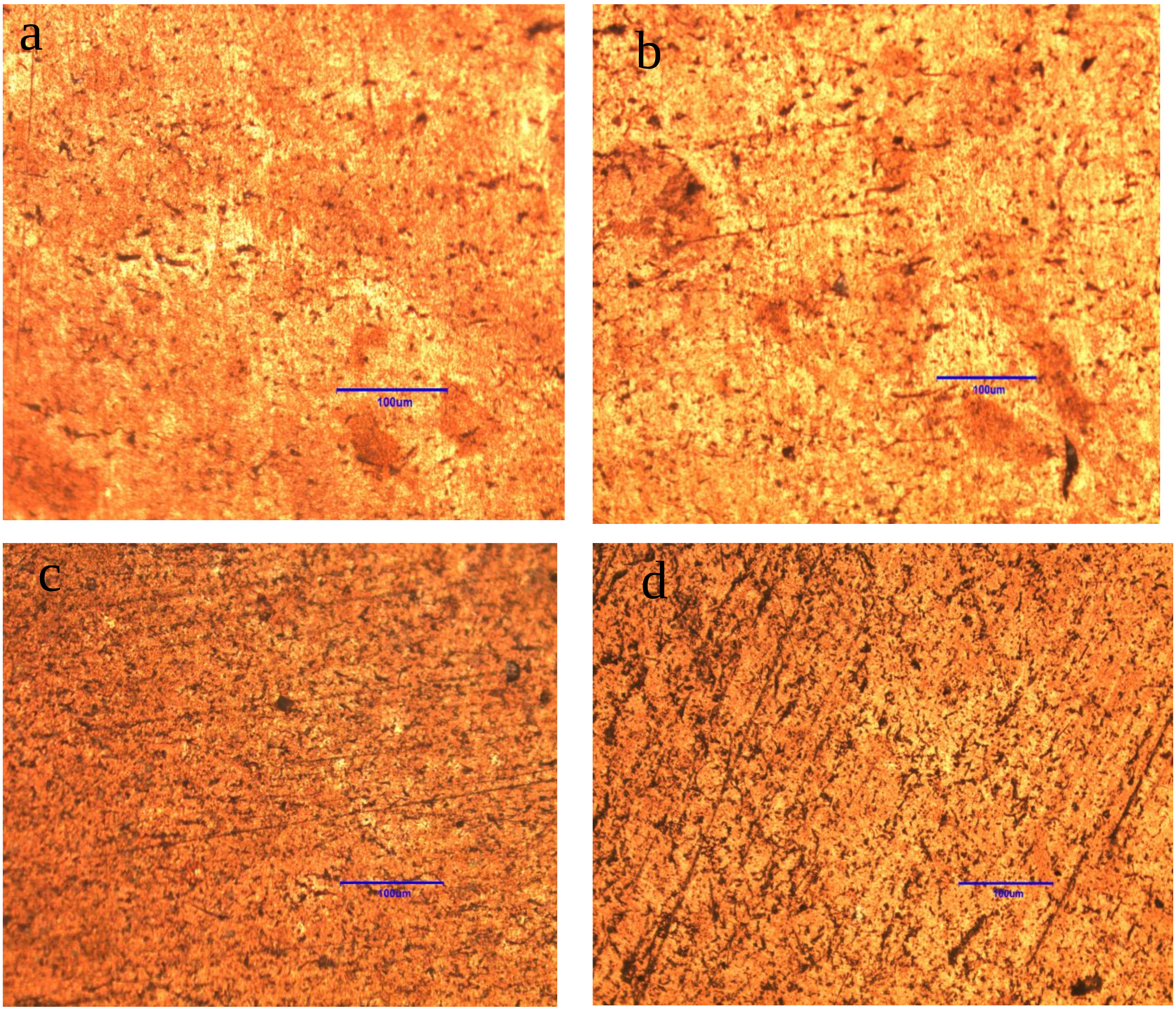

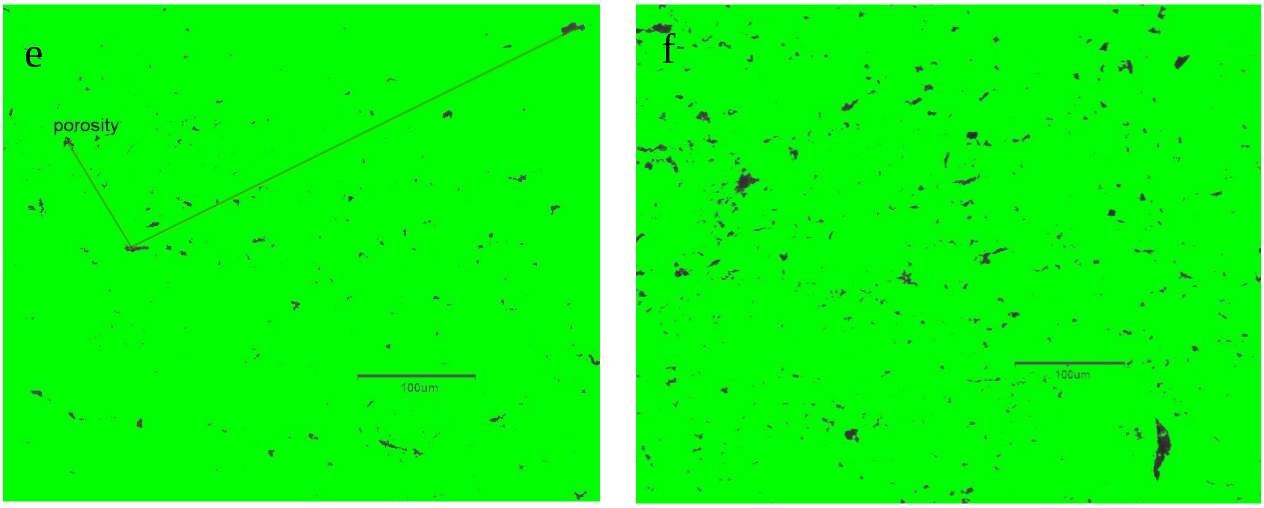

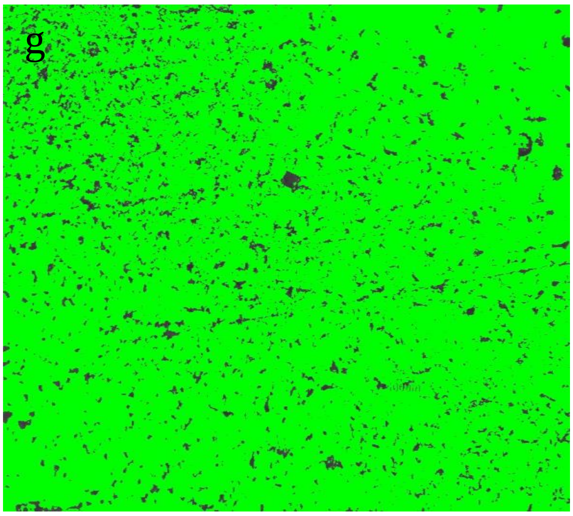

Sample code	Porosity Percentage
S1	0.92
S3	2.46
S5	5.78

Figure 4-6 Image of optical microscopy for (a) sample 1 (b) sample 3 (c) and (d) sample 5 and porosity level using ImageJ software for (e) sample 1 (f) sample 3 and (g) sample 5

4.6.2 Scanning electron microscopy

In this method, a concentrated beam of electrons was used to scan a sample's surface, causing the material to generate a variety of signals that the microscope can detect. The surface of the sample can be imaged in extremely fine detail with SEM by analyzing these signals. As illustrated in Figure 4.7 The reinforcements (SiC, Gr and Cr) are found to be homogeneously distributed in the copper matrix, without significant agglomeration. Micro holes and groove also detected on surface of scanned samples, which shows development of porosity and voids during fabrication because of poor wettability of molten copper with hard reinforcement.

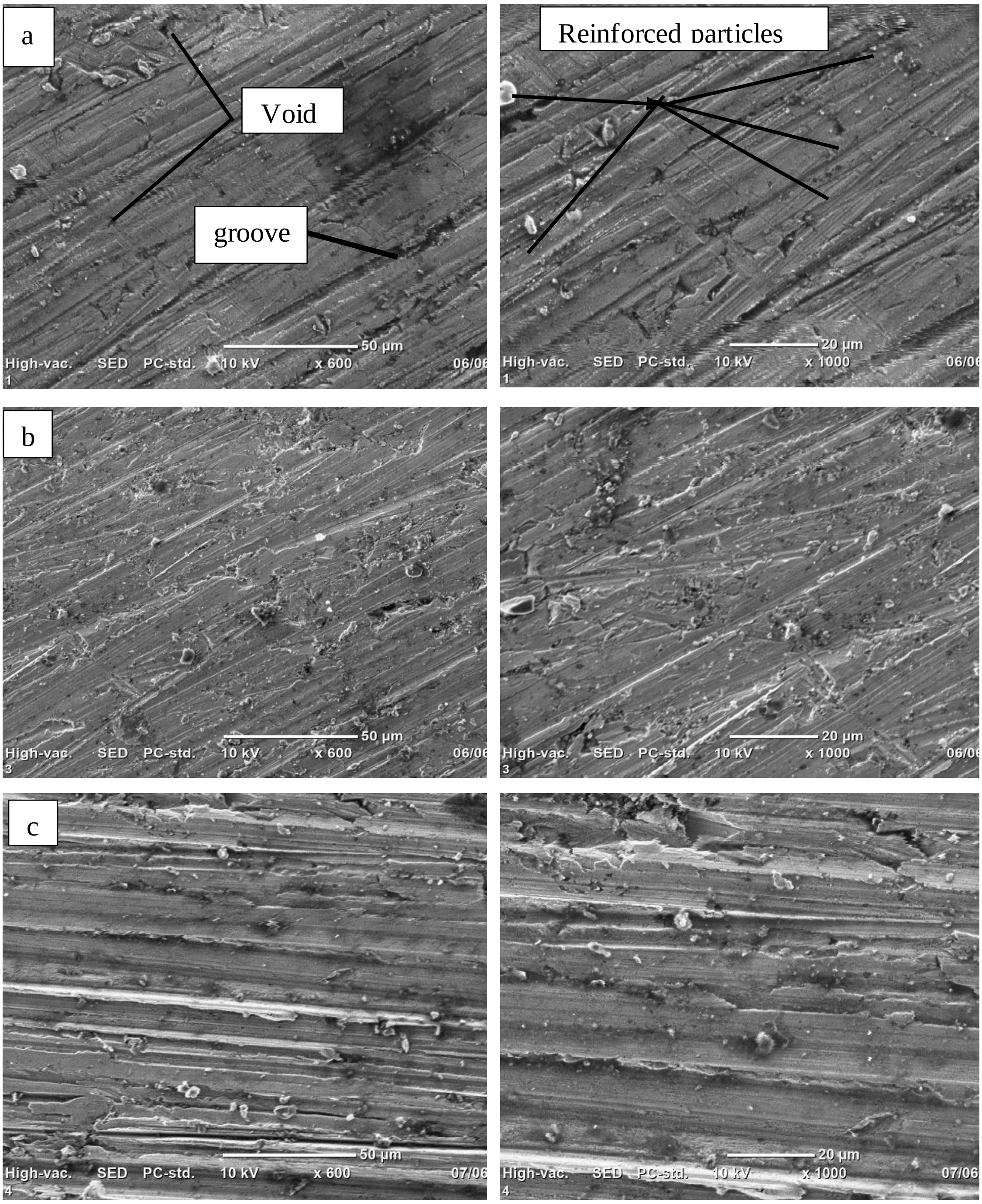

Figure 4-7 SEM image for selected samples (a) Cu-2Cr-1Gr (b) Cu-6SiC-2Cr-1Gr and (3) Cu-12SiC-2Cr-1Gr

4.7 Analysis of corrosion rate

Potentiodynamic polarization curves of unreinforced copper and copper matrix composites generated in 3.5 wt.% NaCl solution show that the composites have similar polarization and passivity properties. However, the corrosion current densities (Icorr) and corrosion potentials (Ecorr) show a considerable difference in corrosion behavior between ceramic and metal reinforced composite series and the unreinforced composite series. To ensure the material's life spam, a lower corrosion rate value is required. Several methodologies are widely used to give quantitative assessments of metal corrosion rates. Corrosion engineers consider the methods of measuring weight loss and thickness loss over time to be the "genuine" corrosion testing. However, this approach is a lengthy process that is not ideal for fast corrosion screening. Tafel plots are a quick and easy electrochemical method. The corrosion current obtained from the intersection of two slopes of cathodic and anodic Tafel plots can theoretically be used to calculate the rate of corrosion.

.

Table 4.4 Electrochemical corrosion for casted specimens in 3.5% NaCl solution

Sample code	Composition	Corrosion potential (E_{corr})(V)	Corrosion current (I_{corr})(A/cm2)	corrosion rate(mm/year)
S1	Cu -1%Gr -2%Cr	-0.2087	1.586	0.002529
S2	Cu-3%-SiC-1%Gr - 2%Cr	-0.20165	2.16	0.00344
S3	Cu-6%-SiC-1%Gr - 2%Cr	-0.2204	3.68	0.005868
S4	Cu-9%-SiC-1%Gr - 2%Cr	-0.2365	3.95	0.006299
S5	Cu-12%-SiC-1%Gr - 2%Cr	-0.1891	4.18	0.006666

Table 4.4 shows corrosion electrochemical corrosion of prepared samples and corrosion rate of samples in 3.5%Nacl solution based on corrosion potential and current density obtained from Tafel plot during test. Result shows corrosion rate is improved with addition of chromium and graphite in sample 1 when compared finding made by (Alaneme and Odoni, 2016) for unreinforced copper in same solution. Addition of chromium plays vital role in improved corrosion resistance composite because of chromium is more corrosion resistant than copper (Uzun and Usca, 2018). Corrosion rate is increased with addition of silicon carbide as reinforcement in sample 2 to sample 5 however it is better than unreinforced copper. A copper matrix composite's corrosion rate

might increase as the weight percentage of silicon carbide increases due to a number of factors. When silicon carbide is added to a copper matrix, it can cause galvanic corrosion due to the development of micro-galvanic cells between the two materials. When compared to pure copper, this can accelerate the corrosion rate of the composite material. Furthermore, as the proportion of silicon carbide in the composite increases, the composite becomes more porous and prone to corrosion. Because it enables an aqueous solution easier access to the underlying copper and silicon carbide particles, porosity is a primary driver of corrosion. As a result, the higher the weight percentage of silicon carbide, the more likely voids and other forms of porosity will emerge during processing, potentially accelerating corrosion (Azaath et al., 2022). In conclusion, micro-galvanic cells and porosity formation are two elements that can lead to an increase in the corrosion rate of a copper matrix composite with increasing weight percentage of silicon carbide.

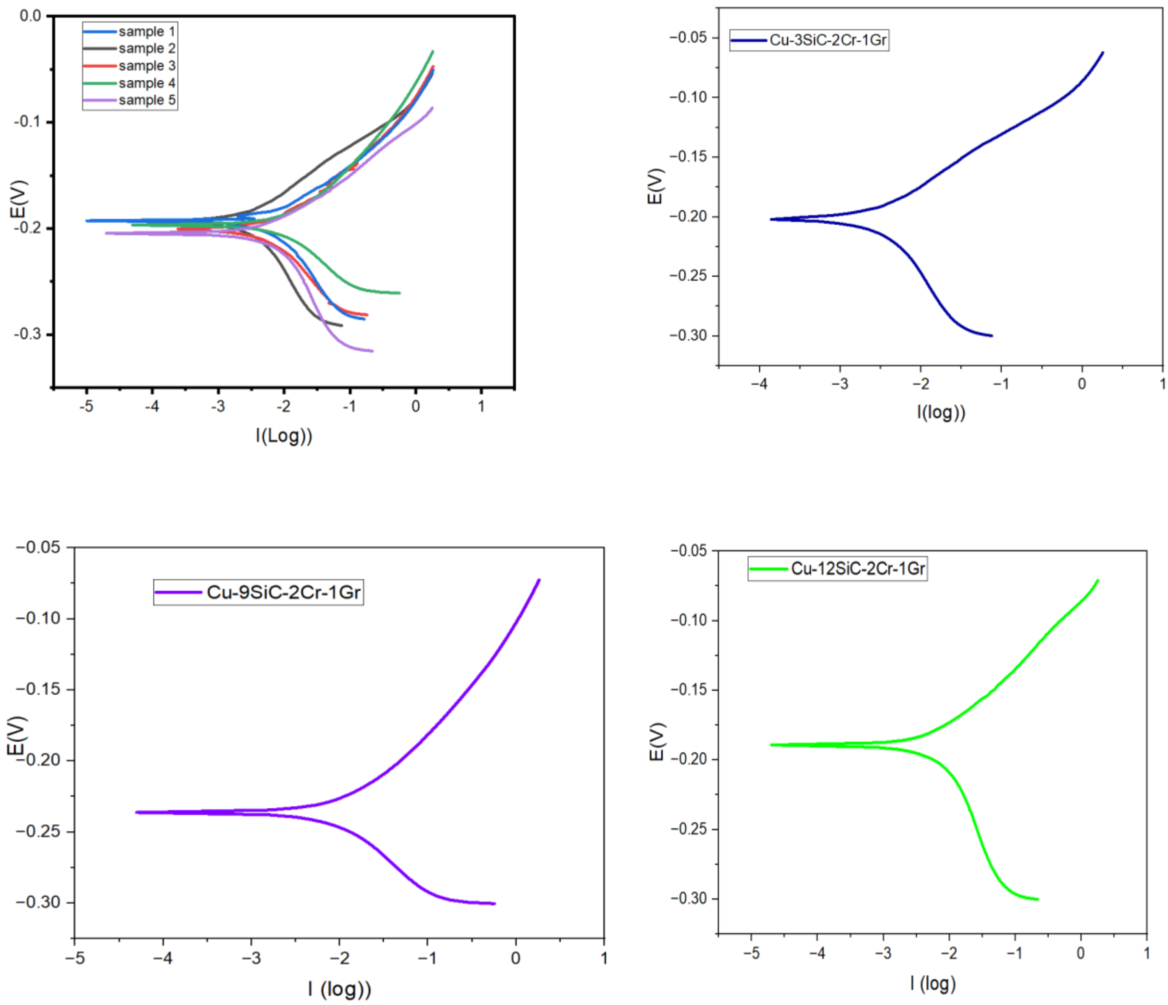

Figure 4-8Tafel plot of copper matrix hybrid composite specimens in 3.5%NaCl solution

4.8 Selection of sample for hot extrusion

Grey Relational Analysis was used to select best sample among fabricated copper matrix hybrid composites. Grey relational analysis is used to solve interrelationships between numerous responses. In this approach, a grey relational grade is developed for analyzing the relational degree of the various responses. In this study hardness, compression strength, electrical conductivity and corrosion rate is used as response to be analyzed. The experimental results are converted into a signal-to-noise (S/N) ratio. In general, three sorts of S/N ratios are used: the smaller-the-better, the higher-the-better, and the nominal the-best (Prakash et al., 2017). The S/N ratio for the current study falls under the smaller the-better category for (corrosion rate) and larger-the-better category for (hardness, conductivity, and compression strength) because the ultimate goal is to increase hardness, electrical conductivity, and compression strength while decreasing corrosion rate. The S/N ratio can be computed by performing an algorithmic change on the loss function using equation (3.21) and (3.22). The steps described in the chapter 3 were used to convert two responses into single-responses, or GRG, in order to achieve the desired outcome.

Step1: Transformation of data into S/N ratios

Data obtained from tests are converted to SN ratio using equation (3.21) and (3.22)

Table 4.5 Experimental data and S/N ratio for response of Cu-SiC-Cr-Gr composites

	Experimental result				**S/N Ratio**			
Sample code	hardness	E/Cond	Compression/st	Corr/rate	hardness	E/Cond	strength	Corr/rate
S1	102.7	47.1	241	0.002529	40.23141	33.46042	47.64034	51.9410
S2	118.63	39.3	275	0.00344	41.48389	31.88785	48.78665	49.2688
S3	125.3	31.2	314	0.005868	41.95902	29.88309	49.93859	44.6302
S4	154.37	26.9	278	0.006299	43.77126	28.59505	48.8809	44.0146
S5	184.93	18.3	207	0.006666	45.34015	25.24902	46.31941	45.5227

Step2: Normalization of S/N ratio: Normalization is a transformation done on a single input to uniformly distribute and scale the data into an acceptable range using equation (3.23) for larger the better and equation (3.24) for smaller-the-better.

Table 4.6 Normalized data of multi-responses

Sample code	**hard**	**Electrical conductivity**	**Compression strength**	**Corrosion rate**
Sample 1	0	1	0.364981	0
Sample 2	0.24516458	0.80849	0.681713	0.317425
Sample 3	0.338168129	0.564346	1	0.868441
Sample 4	0.69290084	0.407485	0.707753	0.941571
Sample 5	1	0	0	1

Step3: Determination of deviation sequence and grey relational coefficient. Grey relational coefficient (GRC) determined using equation (3.25). To meet the practical requirements, the identification coefficient (or distinguishing coefficient) is assumed to be 0.5 (Jajimoggala et al., 2019).

Table 4.7 Deviation sequence of normalized data

Sample code	hardness	Electrical conductivity	Compression strength	Corrosion rate
Sample 1	1	0	0.635019	1
Sample 2	0.754835	0.19151	0.318287	0.682575
Sample 3	0.661832	0.435654	0	0.131559
Sample 4	0.307099	0.592515	0.292247	0.058429
Sample 5	0	1	1	0

Step 4: Compute the grey relational grade (GRGi) and its order sequencing. GRGi is computed using equation (3.26). where m is number of responses.

Table 4.8 Grey relational coefficient and grey relational grade with $\boldsymbol{\delta}$ = 0.5

Sample code	Grey relation coefficient				Grey relational grade	Rank
	hardness	Electrical conductivity	Compression strength	Corrosion rate		
Sample 1	0.333333	1	0.440521	0.333333	0.526797	5
Sample 2	0.398459	0.723055	0.611033	0.422806	0.538838	4
Sample 3	**0.430355**	**0.534386**	**1**	**0.791692**	**0.689108**	**1**
Sample 4	0.619503	0.45766	0.631116	0.895369	0.650912	3
Sample 5	1	0.333333	0.333333	1	0.666667	2

Sample with the greatest GRG score is experiment 3, and the experiment with the lowest GRG score is sample 1. Sample 3, which is marked in grey, is the ranked as best sample among fabricated composite. sample 3 is copper based hybrid composite reinforced with 2% chromium, 1% graphite and 6% silicon carbide particles. Selected composite was led to secondary operation with hot extrusion for further enhancement of properties.

4.9 Simulation result for hot extrusion

Cu-6SiC-2Cr-1Gr is simulated to predict damage percentage distribution and required extrusion load for experimental process. In this study cosine die was selected and extrusion ratio, ram speed and billet temperature were used as parameter since they have significant effect on extrusion responses based on previous studies. DEFORM 3D was employed for simulation to predict load required and damage percentage distributed during extrusion.

Table 4.9 data required to define material and assumption made for simulation

S.No	Defined parameters	Data/formula	Source of data
1	Compression strength	314 MPa	Compression test
2	Density	8.211 g/cm^3	Archimedes principle and experimental result
3	Flow stress constitutive equation (power law)	$\bar{\sigma} = C\bar{\varepsilon}^n \dot{\bar{\varepsilon}}^m + y$	Selected to determine flow stress from DEFORM 3D software
4	constants defined in power law C=material constant n= strain exponent m=strain rate exponent y=initial yield vale	C=1509.65 MPa n=0.499 m=0.352 y=171 MPa	Calculated data with equation (3.13) to (3.20) based on compression strength of Cu-6SiC-2Cr-1Gr hybrid composite
5	Coefficient of friction	0.3	Assumption (as lubricated condition is assumed)

ANOVA and S/N ratio was used to analyze effect of each process parameter on hot extrusion responses. Finally, Grey Relational Analysis (GRA) was used for multi response optimization to know optimal level combination for minimum damage percentage and required extrusion load. Because selected composite is new it should be defined based on compression test. Table 4.9 shows input data obtained from compression test to define material and assumption made for hot extrusion

4.9.1 Analysis of damage percentage

Damage was predicted using DEFORM 3D V11 software. Using Taguchi's L_{16} design of experiment simulation data in table 4.10 were converted to signal ratios. In this study effect of varying control factor: extrusion ratio, ram speed and billet temperature were analyzed at different levels. As lower damage of material is required for engineering applications, smaller the better-quality characteristics was selected to investigate influence of extrusion process parameter on damage of material. Table 4.10 shows that separate signal to noise ratio of each run of experimental design. The largest S/N ratio was indicated in run 5 and lowest value of S/N ratio was indicated in run14. Perspective lowest and largest value of S/N ratio are -7.53154 and 8.683044 respectively.

Table 4.10 Simulation result for damage percentage

Run	ratio	speed	temperature	damage	S/N Ratio
1	2	1	800	1.7	-4.60898
2	2	2	850	1.69	-4.55773
3	2	3	900	1.21	-1.65571
4	2	4	950	1.08	-0.66848
5	3	1	850	0.368	8.683044
6	3	2	800	1.19	-1.51094
7	3	3	950	1.21	-1.65571
8	3	4	900	1.26	-2.00741
9	4	1	900	1.02	-0.172
10	4	2	950	1	0
11	4	3	800	1.07	-0.58768
12	4	4	850	1.11	-0.90646

13	5	1	950	2.03	-6.14992
14	5	2	900	2.38	-7.53154
15	5	3	850	1.4	-2.92256
16	5	4	800	1.49	-3.46373

4.9.1.1 Analysis of SN ratio for damage

The statistical formula of "smaller the better" has been applied to measure and characterize hardness. In the instance when smaller is better, the signal noise ratio can be calculated using equation (3.21).

According to the ranks of the parameters influencing responses based on the S/N ratios produced using the Taguchi orthogonal array, the delta statistics of the S/N ratio for the hardness are shown in table. The difference between the highest and lowest average values of each factor was used to calculate the delta statistics. The factor that most significantly affects damage percentage is represented by the largest value of delta, which was given the first rank. Analysis shows that extrusion ratio of extruded material assigned a rank 1 with delta value of 5.89 implies that it was predominant factor affecting damage percentage of Cu/SiC/Gr/Cr hybrid composite. Billet material and ram speed assigned as second (2.92) and third (2.84) respectively.

Table 4.11 Signal to Noise Ratios for the damage percentage (smaller the better)

Level	Extrusion Ratio	Ram speed	Billet temperature
1	-2.87	-0.56	-2.54
2	0.88	-3.40	0.07
3	-0.42	-1.71	-2.84
4	-5.02	-1.76	-2.12
Delta	5.89	2.84	2.92
Rank	**1**	**3**	**2**

Figure 4.9 shows that optimal combination of extrusion parameters for minimal damage percentage (smaller the better). The maximum point on each graph represents the best possible combination of the parameters in the S/N ratio, and the above graph demonstrates maximum point of SN ratio for extrusion ratio at level 2, ram speed at level 1 and billet temperature at level 2 are extrusion ratio of 3, speed of 1mm/s and billet temperature of

850°C (**A2B1C2**). most effective parameter to minimize damage percentage is extrusion ratio when compared to other factor and least effective factor is ram speed. Where **A** is stand for extrusion ratio, **B** is for ram speed and **C** is for billet temperature.

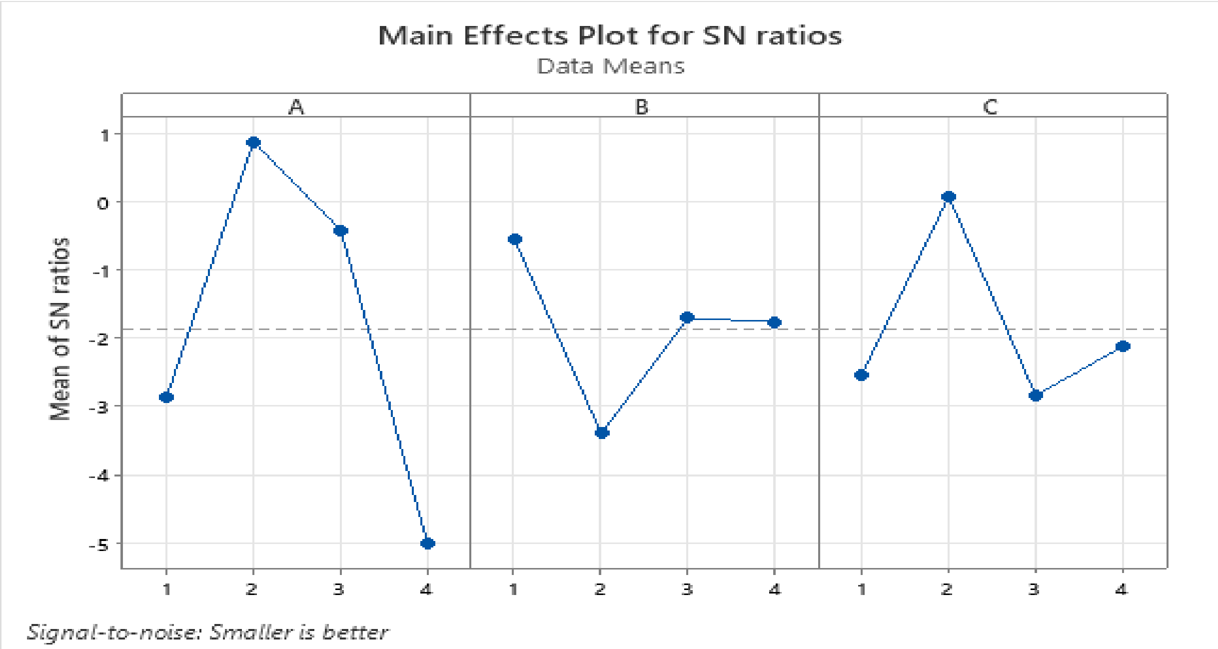

Figure 4-9 Main effect plot for SN ratio

4.9.1.2 Determining Optimum Conditions for Damage Percentage

Table 4.12 shows the ideal prediction condition for the S/NL ratio in which the composite achieves a minimum damage percentage with the parameters set. The best parameters in this investigation were at **A2B1C2** with a extrusion ratio of 3, lower ram speed, and billet temperature of 850°C.

Table 4.12 The optimum conditions for damage result prediction-settings

	Extrusion ratio	Ram speed	Billet temperature
Value of each level	3	1mm/s	850°C
rank	1	3	2

4.9.1.3 ANOVA for damage responses

For statistical reliability, Taguchi analysis results should be confirmed using analysis of variance (ANOVA). As a result, the percentage contribution of each parameter in extrusion of copper matrix hybrid composite to damage percentage was calculated. The

ANOVA results on the damage percentage of the copper-based metal matrix composite during hot extrusion in Table 4.13 show the percentage contribution of each extrusion process parameter to the response. Based on the results of the ANOVA analysis, the bigger percentage contribution was calculated to be 68.00%, which was attributed to extrusion ratio of cosine die. The percentage contribution of billet temperature was 9.016%, while ram speed had the lowest percentage contribution of 8.14%. The percent concentration of ram speed and the billet temperature are nearly same.

Table 4.13 ANOVA result on the damage percentage

Source	DF	Adj SS	Adj MS	F-Value	P-Value	Percentage contribution
Extrusion Ratio	3	3.4582	1.1527	9.16	0.012	68.00
Ram Speed	3	0.4140	0.1380	1.10	0.420	8.14
Billet Temperature	3	0.4585	0.1528	1.21	0.382	9.016
Error	6	0.7548	0.1258			
Total	15	5.0854				

S	R-sq	R-sq(adj)
0.354680	98.16%	89.89%

F0.05, 3, 6 = 4.78 from ANOVA table

The ANOVA table additionally displays the significance of factors using F-values and P-values. If the obtained F-value of a parameter is higher than the tabulated one, that parameter has a considerable influence on the response variable. According to Table 4.13 the F value of extrusion ratio is 9.16 > 4.78 thus, extrusion ratio has a considerable influence on the damage percentage of copper matrix hybrid composite. As a result of the F-value for billet temperature (1.21) which is less than 4.78 and ram speed (1.10) which is less than 4.78, ram speed and billet temperature have no significant effect on the damage of composite. The ANOVA with p values also reveals that extrusion ratio (P=0.012< 0.05) and extrusion ratio is significant factors affecting the wear rate whereas ram speed and billet temperature have little relevance (P>0.05). When the R-square value is 98.16%, the model fits the data which is more than 70%.

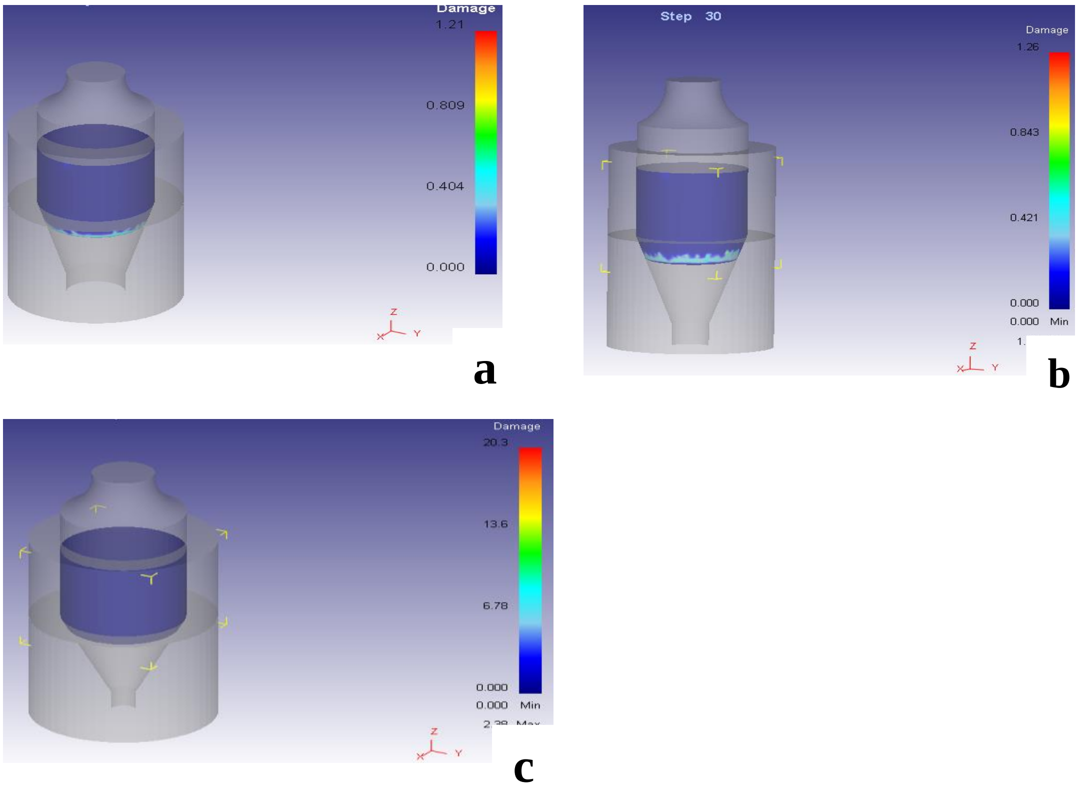

Figure 4-10 Damage distribution over the surface of composite at billet temperature of 900°C. (a) extrusion ratio of 2 (b) extrusion ratio of 3 (c) extrusion ratio of 5

From figure 4.10 shows that increasing extrusion ratio of cosine die tends to increase damage percentage of extruded composite. Kothasiri and Chalamalasetti, (2022) illustrates the damage value increases when the extrusion ratio and maximum stress are increased. Damage increases from 0.15% to 2.75% as die extrusion ratio increase from 2 to 4. The conical die functions as a stress raiser during the extrusion process.

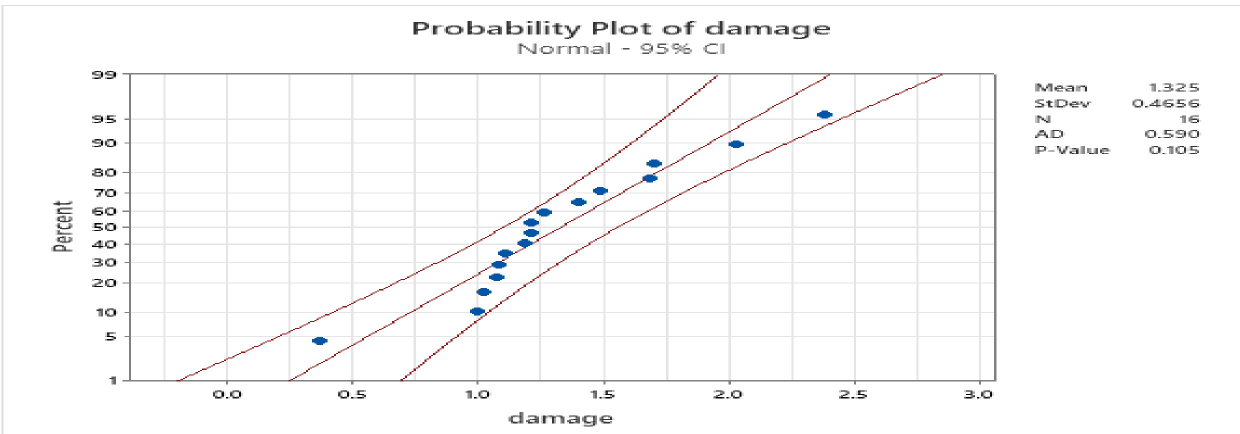

Figure 4-11 Normal probability plot of damage

A normal probability plot of effects is used to assess the significance of effects If all of the residuals fall along a straight line drawn across the plotted points, it is assumed that the residuals/errors have a normal distribution. Figure 4.11 demonstrates that the data points are pretty near to the fitted normal distribution line (the middle solid line of the graph). The normal probability plots of residuals show that the residuals are reasonably close to the normal probability lines, and the p-value is greater than the significance level of 0.05 in figure 4.11, implying that residuals are distributed normally and the terms mentioned in the regression models are significant and adequate.

4.9.2 Analysis of Extrusion Load

DEFORM 3D software was used to calculate predicted extrusion load on 16 runs based on experimental design of simulation. Table 4.14 shows extrusion force recorded a load versus time curve using simulation data. The results show that larger extrusion ratio requires marginally higher extrusion load than die with smaller extrusion ratio of the same material. In this study, the influence of altering control factors such as extrusion ratio, ram speed, and billet temperature were investigated at various levels. Because reduced extrusion force is necessary for engineering applications, the smaller the better-quality criteria were chosen to explore the influence of extrusion process parameters on extrusion load. Each run of the experimental design's signal to noise ratio is shown separately in the table. Run 1 had the highest S/N ratio, while run 16 had the lowest. The lowest and highest values of the S/N ratio are-43.2274and -66.1926, respectively.

Table 4.14 Numerical simulation result for extrusion load

S. No	extrusion ratio	extrusion speed (mm/s)	Temperature (°C)	Extrusion Load (KN)	SN ratio
1	2	1	800	145	-43.2274
2	2	2	850	180	-45.1055
3	2	3	900	201	-46.0639
4	2	4	950	208	-46.3613
5	3	1	850	319	-50.0758
6	3	2	800	600	-55.563
7	3	3	950	721	-57.1587
8	3	4	900	767	-57.6959

9	4	1	900	935	-59.4162
10	4	2	950	683	-56.6884
11	4	3	800	818	-58.2551
12	4	4	850	1300	-62.2789
13	5	1	950	1420	-63.0458
14	5	2	900	1710	-64.6599
15	5	3	850	1800	-65.1055
16	5	4	800	2040	-66.1926

4.9.2.1 Analysis of SN ratio for Extrusion Ratio

The statistical formula of the smaller the better has been employed to measure and characterize required extrusion load. In the case that smaller is better, the signal-to-noise ratio can be given by equation (3.21).

Table 4.15 Signal to Noise Ratios for the damage percentage (smaller the better)

Level	Extrusion Ratio	Ram Speed	Billet Temperature
1	-45.19	-53.94	-55.81
2	-55.12	-55.50	-55.64
3	-59.16	-56.65	-56.96
4	-64.75	-58.13	-55.81
Delta	19.56	4.19	1.32
Rank	**1**	**2**	**3**

The delta statistics for extrusion load shown in Table 4.15 rank the factors influencing the responses based on the S/N ratios acquired using the Taguchi orthogonal array. The delta statistics were calculated by subtracting the highest and lowest average value of each factor. The largest delta value was allocated first rank and indicates the most important factor influencing extrusion load. The extrusion ratio was assigned a rank of 1 with a delta value of 19.56, indicating that it is the most important factor influencing the required load of the composite during hot extrusion. The ram speed and billet temperature were ranked second (4.19) and third (1.32) respectively.

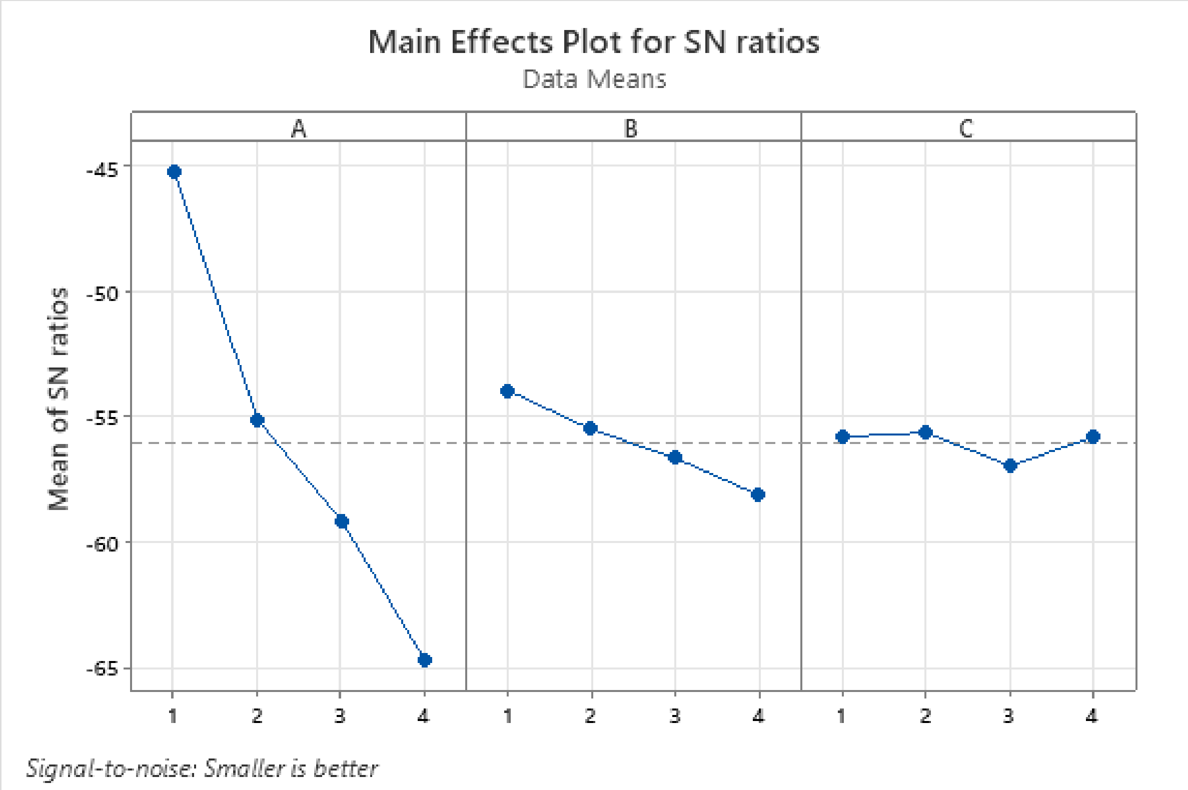

Figure 4-12 Main effect plot for SN ratios for extrusion load parameters

The best parameter combination for tensile strength control factors is shown in Figure 4.12 (smaller the better-quality characteristics for extrusion load) Due to the fact that a higher S/N ratio is preferable, it was chosen for this investigation. In the S/N ratio, the numerical value of the maximum point in each graph indicates the best optimal combination of the factors at that level. The above figure shows the optimum value for extrusion ratio at level 1, ram speed at level 1 and billet temperature at level 2 **(A1B1C2).** Where **A** is stand for extrusion ratio, **B** is for ram speed and **C** is for billet temperature.

Comparatively speaking, extrusion ratio is the most efficient factor for minimizing required extrusion load Compared to other parameters, billet temperature has the least impact on the extrusion load of composites.

4.9.2.2 Determining Optimum Conditions for extrusion load

The S/N ratio at which minimum extrusion load result of the composite is obtained with the conditions set is the optimum prediction condition, as shown in table 4.16 In this investigation, **A1B1C2** were the chosen optimum parameters.

Table 4.16 The optimum conditions for extrusion load result prediction-settings

	Extrusion ratio	Ram speed	Billet temperature
Value of each level	2	1mm/s	850℃
rank	1	2	3

4.9.2.3 ANOVA for extrusion load responses

ANOVA is used to determine the percent contribution of each element and the most important factors that influence the tensile toughness of composite. DF stands for degree of freedom, SS for squares, MSS for mean squares, and F for the F-Ratio.

Table 4.17 Analysis of Variance of tensile toughness of Composite

Source	**DF**	**Seq SS**	**Adj SS**	**Adj MS**	**F**	**P**	**Percentage contribution**
A	3	5234037	5234037	1744679	64.65	0.000	90.78
B	3	307666	307666	102555	3.80	0.077	5.33
C	3	61588	61588	20529	0.76	0.556	1.06
Residual Error	6	161915	161915	26986			
Total	15	5765206					

$F_{0.05, 3, 6} = 4.78$

S	**R-Sq**	**R-Sq(adj)**
164.2738	97.19%	92.98%

Table 4.17 shows the percentage contributions of the key parameters of extrusion ratio (90.78%), ram speed (5.33%), and billet temperature (1.06%) on the required extrusion load for copper matrix composite. This analysis was conducted with a 95% level of confidence and a level of significance of 5%. According to the aforementioned table, extrusion ratio has statistical significance and contributes the maximum percentage (i.e., 90.78%) to the extrusion load value, followed by ram speed and extrusion temperature. Using the F-values and P-values, the ANOVA table additionally displays the significance of each factor. A parameter's effect on the response variable is significant if the obtained

F-value of that parameter is higher than the tabulated one. Since extrusion ratio has a considerable impact on extrusion load, from table F value for that percentage is 64.65 > F0.05, 1, 6 = 4.78. ram speed and billet temperature show no considerable influence on the required load for extrusion of composite (3.80 and 0.76 both are less than 5.32), which means that they do not significantly affect it. The ANOVA with p values also reveals that extrusion (P=0.00 < 0.05) is a significant factor impacting extrusion load but ram speed and billet temperature are not. extrusion load of the composite will therefore rise when extrusion ratio is increased. Because the R-square value is greater than average (92.98%), the regression model fits the data well.

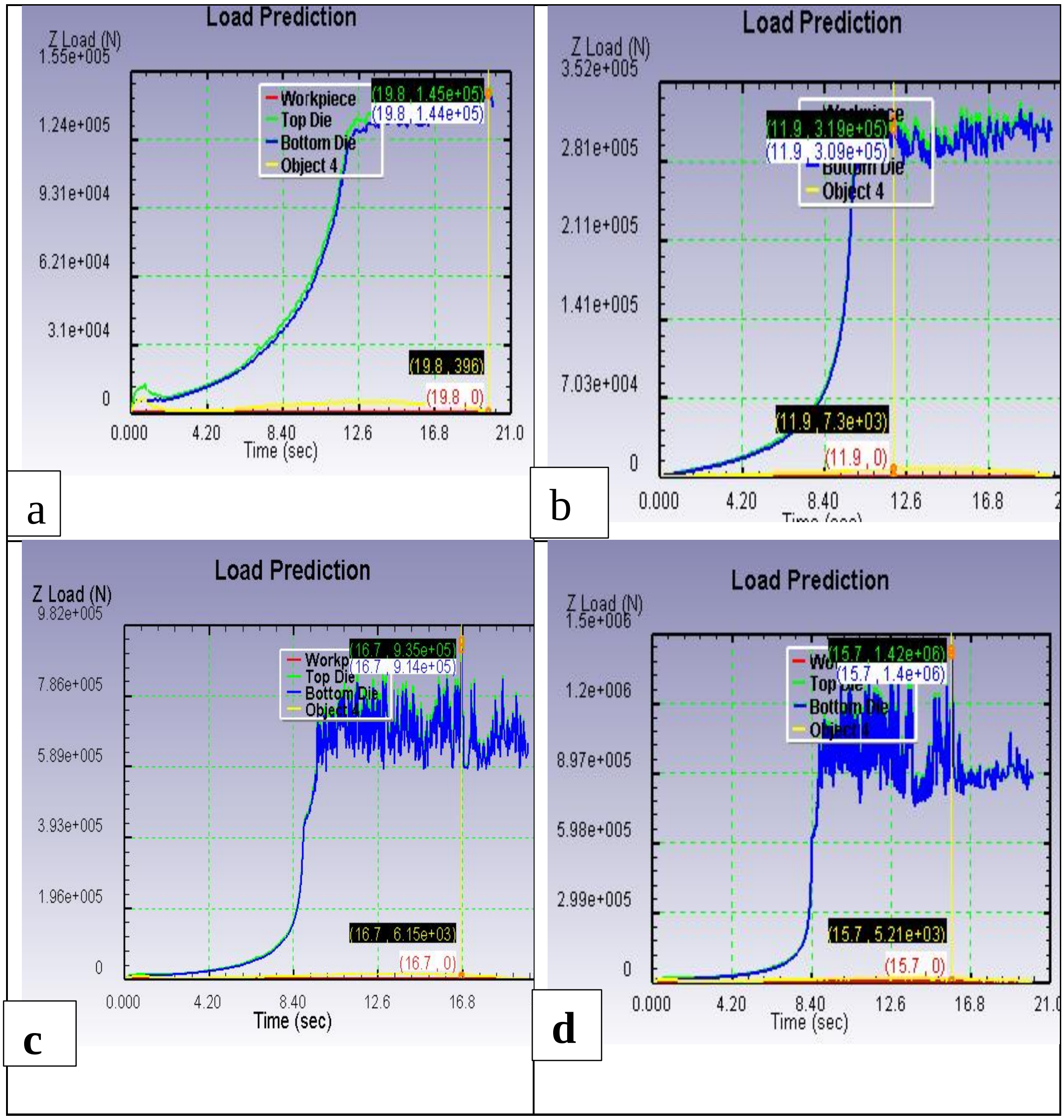

Figure 4-13 extrusion load distribution over surface of composites at speed of 1mm/s. (a) extrusion ratio of 2 (b) extrusion ratio of 3 (c) extrusion ratio of 4 (d) extrusion ratio of 5

The above figure 4.13 demonstrates that as the extrusion ratio of the cosine die is increased, the load required to extrude composite tends to increase. According to the ANOVA results, (Kothasiri and Chalamalasetti, 2022)analyzed the die angle has the highest significance (99.09%), followed by the ram speed (0.59%). ANOVA was used to determine the significance of each parameter. According to the ANOVA results, the CHA has the highest significance rating, followed by ram speed and COF. According to the ANOVA results, the cosine die extrusion ratio has the highest significance ranking at first, followed by ram speed, as indicated by (Jajimoggala et al., 2019). ANOVA was used to determine the importance of each parameter on hot extrusion of AA6061.

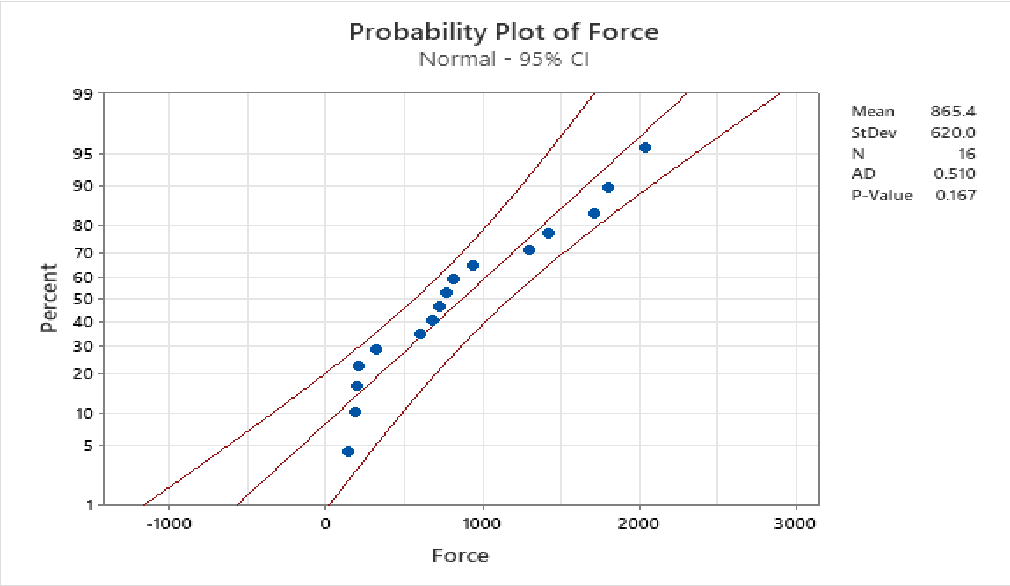

Figure 4-14 Normal probability plot of extrusion load

A normal probability plot of effects is used to assess the significance of effects If all of the residuals fall along a straight line drawn across the plotted points, it is assumed that the residuals/errors have a normal distribution. Figure 4.14 demonstrates that the data points are pretty near to the fitted normal distribution line (the middle solid line of the graph). The normal probability plots of residuals show that the residuals are reasonably close to the normal probability lines, and the p-value is greater than the significance level of 0.05 in figure 4.14 implying that residuals are distributed normally and the terms mentioned in the regression models are significant and adequate.

4.9.2.4 Multi-Response Optimization for Developed Composite

Grey relational analysis is used to solve interrelationships between numerous responses. In this approach, a grey relational grade is developed for analyzing the relational degree of the various responses. The GRA approach was utilized to optimize process parameters in current research work. In this method, the key input process parameters are extrusion ratio, ram speed and billet temperature and the experiment are performed using a L_{16} orthogonal array, in order to obtain more trustworthy results, simulation were performed on each run according to experimental design. Table 4.18 revealed Taguchi based experimental design responses obtained from simulation as per experimental design.

Table 4.18 Simulation responses at different levels of extrusion process parameter

S. No	Extrusion ratio	Ram speed	Billet temperature	Simulation Responses	
				damage	Load (KN)
1	2	1	800	1.7	139
2	2	2	850	1.69	174
3	2	3	900	1.21	194
4	2	4	950	1.08	202
5	3	1	850	0.368	315
6	3	2	800	1.19	553
7	3	3	950	1.21	604
8	3	4	900	1.26	727
9	4	1	900	1.02	743
10	4	2	950	1.0	683
11	4	3	800	1.07	818
12	4	4	850	1.11	937
13	5	1	950	2.03	1100
14	5	2	900	2.38	1340
15	5	3	850	1.4	1790
16	5	4	800	1.49	2040

4.9.2.5 Performance evaluation using Taguchi's S/N ratio

Taguchi's method, one of the most used and efficient optimization techniques today, creates a high-quality system based on orthogonal array (OA) trials that deliver numerous reduced experiments with an optimal configuration for process control parameters. The experimental results are converted into a signal-to-noise (S/N) ratio. In general, three sorts of S/N ratios are used: the smaller-the-better, the higher-the-better, and the nominal-the-best (PRAKASH et al., 2017). Because the ultimate goal is to reduce damage percentage and required extrusion load, the S/N ratio for the current study falls under the smaller-the-better category. The S/N ratio can be computed by performing an algorithmic change on the loss function using equation (3.21). The obtained S/N values were employed in the next calculations, which were the grey relation coefficients (GRC). The Taguchi technique was used to optimize a single independent-objective function, not many responses. The GRA was the more desired strategy for optimizing numerous responses in many sectors (Jajimoggala et al., 2019). In order to minimizing extrusion load and damage value, the optimal combination of parameters needed to be determined. The steps described in the next section were used to convert two responses into single-responses, or GRG, in order to achieve the desired outcome.

Step 1: Transformation of data into S/N ratios

Table 4.19 Experimental results and S/N ratio of response values

Run	Simulation Responses		S/N ratio	
	Damage	Load (KN)	damage	load
1	1.7	145	-4.60898	-43.2274
2	1.69	180	-4.55773	-45.1055
3	1.21	201	-1.65571	-46.0639
4	1.08	208	-0.66848	-46.3613
5	0.368	319	8.683044	-50.0758
6	1.19	600	-1.51094	-55.563
7	1.21	721	-1.65571	-57.1587
8	1.26	767	-2.00741	-57.6959
9	1.02	935	-0.172	-59.4162
10	1	683	0	-56.6884
11	1.07	818	-0.58768	-58.2551
12	1.11	1300	-0.90646	-62.2789
13	2.03	1420	-6.14992	-63.0458
14	2.38	1710	-7.53154	-64.6599
15	1.4	1800	-2.92256	-65.1055
16	1.49	2040	-3.46373	-66.1926

Step 2: Normalization of S/N values: Normalization is a transformation done on a single input to uniformly distribute and scale the data into an acceptable range using equation (3.24) as smaller-the-better characteristic is considered.

Table 4.20 Normalized data of the experimental results

Designation (Run)	Damage	Extrusion load
1	0.819757	0

2	0.816597	0.08178
3	0.637621	0.123513
4	0.576735	0.136463
5	0	0.298208
6	0.628692	0.537143
7	0.637621	0.606627
8	0.659311	0.630018
9	0.546116	0.704927
10	0.535508	0.586148
11	0.571752	0.654368
12	0.591412	0.829581
13	0.914792	0.862975
14	1	0.93326
15	0.715751	0.952663
16	0.749126	1

Step3: Determination of deviation sequence and grey relational coefficient. Grey relational coefficient (GRC) determined using equation (3.24). To meet the practical requirements, the identification coefficient (or distinguishing coefficient) is assumed to be 0.5 (Jajimoggala et al., 2019).

Step 4: Compute the grey relational grade (GRGi) and its order sequencing. GRGi is computed using equation (3.26). where m is number of responses.

Table 4.21 Deviation sequence and Grey relational coefficient with $\boldsymbol{\delta}$ = 0.5

Designation	Normalized data		grey relational coefficient		Grey relational grade	Rank
	Damage	Load	Damage	Load		
1	0.81976	0	0.37886	1	0.68943	2
2	0.8166	0.08178	0.37977	0.85943	0.6196	5
3	0.63762	0.12351	0.43951	0.80191	0.62071	4
4	0.57674	0.13646	0.46437	0.78559	0.62498	3

5	0	0.29821	1	0.6264	0.8132	1
6	0.62869	0.53714	0.44299	0.48209	0.46254	7
7	0.63762	0.60663	0.43951	0.45182	0.44567	10
8	0.65931	0.63002	0.43129	0.44247	0.43688	11
9	0.54612	0.70493	0.47796	0.41496	0.44646	9
10	0.53551	0.58615	0.48285	0.46034	0.4716	6
11	0.57175	0.65437	0.46653	0.43314	0.44983	8
12	0.59141	0.82958	0.45812	0.37606	0.41709	12
13	0.91479	0.86298	0.35341	0.36684	0.360125	15
14	1	0.93326	0.33333	0.34886	0.341095	16
15	0.71575	0.95266	0.41127	0.3442	0.37773	13
16	0.74913	1	0.40028	0.33333	0.366805	14

The experiment with the greatest GRG score is experiment 5, and the experiment with the lowest GRG score is experiment 14. The experiment number 5, which is marked in grey, is the aligned best controllable parameter combination. Its components are reinforcement extrusion ratio of 3 (level 2), ram speed of 60 1mm/s (level 1), and billet temperature (level)

4.9.2.6 Optimization of hot extrusion process parameter for Grey Relational Grades

The larger, the better statistic has been applied to quantify and define the GRG, and the data have been translated into SNs-ratio.

Table 4.22 Signal to Noise Ratios for GRG for larger is better

Level	**A**	**B**	**C**
1	2.1174	0.7952	-0.3738
2	0.3442	-0.6609	0.5192
3	-0.9962	-0.6187	-0.8999
4	-2.8246	-0.8749	-0.6049
Delta	4.9420	1.6702	1.4191
Rank	1	2	3

The delta statistics for extrusion load and damage shown in Table 4. 22 rank the factors influencing the responses based on the S/N ratios acquired using the Taguchi orthogonal array. The delta statistics were calculated by subtracting the highest and lowest average value of each factor. The largest delta value was allocated first rank and indicates the most important factor influencing extrusion responses. The extrusion ratio was assigned a rank of 1 with a delta value of 4.9420, indicating that it is the most important factor influencing the required load and damage occurred in composite during hot extrusion. The ram speed and billet temperature were ranked second (1.6702) and third (1.4191) respectively.

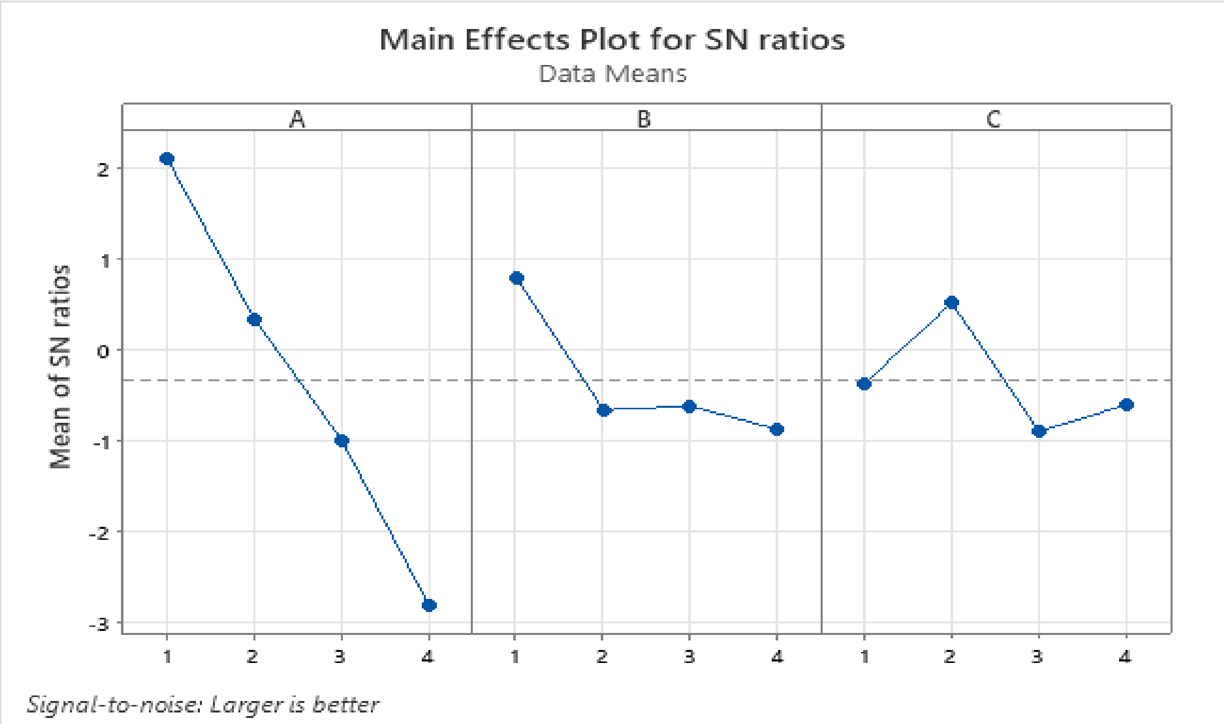

Figure 4-15 Main effect plot for SN ratios for multi-response parameters

The optimum parameter combination on the grey relational grade is shown in Figure 4.15 together with the control factor's main effect plot for the grey relational grade (the higher the better). Since the S/N ratio used for this study is larger is better, the highest S/N ratio was chosen, and the numerical value of the maximum point in each graph indicates the best value of that particular parameter at that level for the best combination of the factors of extrusion ratio level, ram speed at level 1, and billet temperature at level 2 are, respectively, 2, 1 mm/s, and 850°C (i.e.**A1B1C2**) was chosen. Where **A** is stand for extrusion ratio, **B** is for ram speed and **C** is for billet temperature.

When compared to other variables, the extrusion ratio has the greatest impact on the grey relational grade, while billet temperature has the minimal impact. The terms setting composite's higher GRG result has the following optimal prediction condition: (i.e., **A1B1C2**).

4.9.2.7 Predicting optimal value and confirmation test

At the optimal setup of controllable factors, the optimal grey relational grade is predicted. A1 (extrusion ratio) was already chosen as the most significant characteristic with the best level, followed by B1 (ram speed) and C2 (billet temperature). The **A1B1C2** is a confirmation test for an optimal parameter combination of the hot extrusion process developed using GRA. Confirmation tests are required in this article because the optimum parameter level combination, A1B1C2, not accessible in the current study.

The simulated damage percentage and predicted load values for optimal parameter level combinations are 0.593 and 148KN, respectively which has overall improvement when compared to run ranked first (which has 0.368 damage percentage and 319KN extrusion load). As a result, by combining the Taguchi technique with GRA, the attributes damage and extrusion load value of Cu-Gr-SiC-Cr hybrid composite are improved.

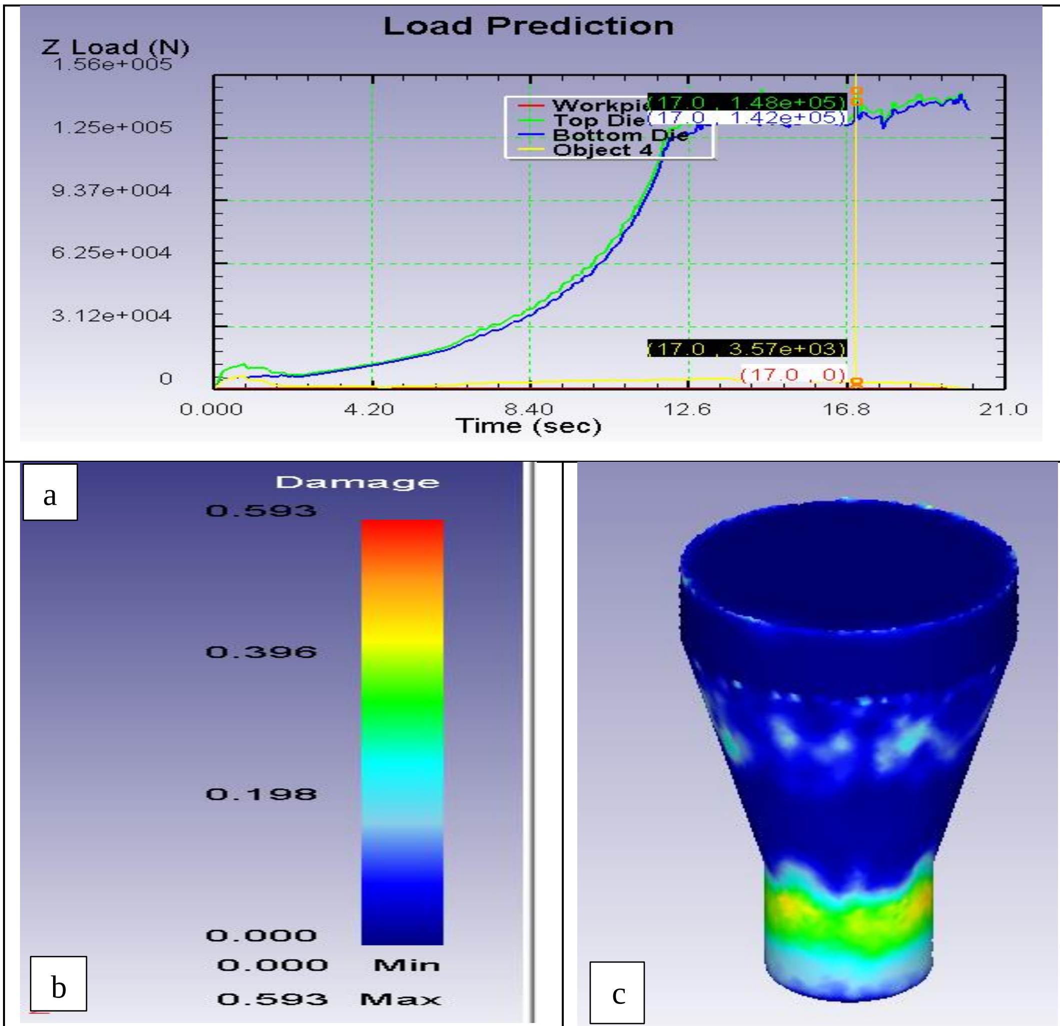

Figure 4-16 Simulation result for confirmation result (a) extrusion load (b) damage (c) billet

4.10 Analysis of results after extrusion process

Density, hardness, electrical conductivity and compression hardness tests were used to determine how the qualities of the composite samples improved during hot extrusion. Extrusion was performed with optimal parameter combination obtained for damage percentage and extrusion ratio responses obtained using numerical simulation with DEFORM 3D for selected sample (Cu-6SiC-1Gr-2Cr). Selected Cu-6SiC-1Gr-2Cr hybrid composite was extruded with cosine die of 2 extrusion ratios, 1mm/s ram speed and at 850 °C billet temperature. Composite was lubricated with semi-solid grease and solid lubricant graphite as lubricated hot forming is assumed for simulation.

4.10.1.1 Density and hardness test after Extrusion

Density and porosity of Cu-6SiC-1Gr-2Cr hybrid composite was investigated after extrusion. Results of actual density of synthesized composite and extruded composite as shown in table 4.23 Increased from 8.211g/cm^3 to 8.307g/cm^3 which shows Significant improvement in porosity percentage. Porosity percentage is decreased from 2.71% to 1.57% with aid of hot extrusion. Decreasing value of porosity percentage helps to improve mechanical and physical property of composite. During the hot extrusion process, the composite material is heated to a temperature above its recrystallization temperature and then forced through a die with a specified shape, under high pressure. The extrusion process causes plastic deformation and reduce the size and spacing of pores inside the material. Several factors contribute to the lowering of porosity during hot extrusion. One important method is the application of compressive stresses, which happens as the material is driven through the die. These compressive pressures might cause some pores to collapse or close up, lowering their size and quantity. Furthermore, while the material runs through the die, shear stresses are applied, which can aid to break up and eliminate pores. Dynamic recrystallization is another method that helps to reduce porosity during hot extrusion. This happens when heated deformation induces new grains to develop, which can assist close pores by filling up gaps between existing grains.

Overall, hot extrusion is an efficient way for minimizing porosity in stir casted copper matrix composites. Hot extrusion can improve the mechanical characteristics of a material by lowering its porosity. The bond strength between matrix and reinforcing material improved after extrusion, which improves porosity. Secondary processes can be used to achieve a homogenous density distribution in the composite(Mohapatra et al., 2019).

Table 4.23 density and hardness of extruded sample

sample	Stir casted density	Extrudate density	Stir casted hardness (HV)	Extrudate hardness (HV)
Cu-6SiC-1Gr-2Cr	8.211	8.44	125.3	147.1 (145.0, 158.1, 138.2)

The results show that there is also a 17.4% increase in hardness compared to the hardness of the sample before hot extrusion, which may be due to changes occurred in the material's microstructure by high temperature and pressure, particularly the grain structure. During hot deformation, dislocation density increases, resulting in a reduction in grain size via dynamic recrystallization. Smaller grain size and higher dislocation density can boost the material's strength, hardness, and yield strength. The presence of reinforcing particles in copper matrix hybrid composites can also contribute to an increase in hardness with heat deformation. The reinforcing particles may be distorted and dispersed more uniformly throughout the material as the material is subjected to pressure during extrusion, resulting in a strengthening effect. The combined effect of these factors may result in a rise in overall composite harness.

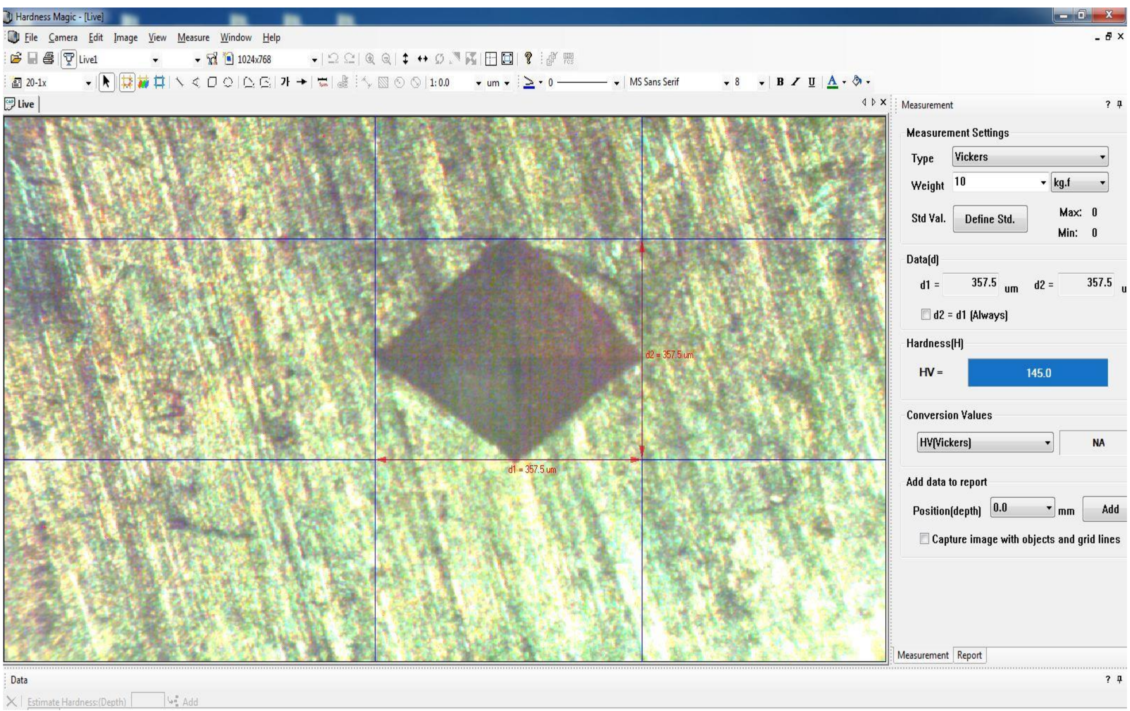

Figure 4-17 Hardness of extruded sample trial 1.

4.10.1.2 Compression strength of extruded sample

Following Cu-6SiC-1Gr-2Cr hybrid composite hot extrusion there was a significant decrement in porosity and rise in hardness in composite which implies that reduction in porosity improves strength of material. Result obtained from test after hot extrusion shows there is 21.4% improvement in compressive strength when compared to sample before extrusion which is increased from 314 MPa to 381 MPa. The composite material was subjected to high pressure and temperature during the hot extrusion process, resulting in plastic deformation and better interfacial bonding between matrix and reinforcement phases. This enhanced bonding results in a more uniform in material with fewer defects, which improves mechanical strength. The hot extrusion process can also result in grain refinement, in which the size of the grains in the material is reduced due to recrystallization. This finer grain structure may result in greater mechanical strength(T. Li et al., 2021). Alignment of reinforced particles: During the heated extrusion process, the reinforced particles in the copper matrix hybrid composite can also get orientated and aligned in the direction of extrusion, resulting in improved compressive strength in that direction.

4.10.1.3 Electrical conductivity of extruded sample

After hot extrusion of Cu-6SiC-1Gr-2Cr hybrid composite there was slight decrement in electrical conductivity which was decreased by 1.6% which has good alignment with investigation made by(Ren et al., 2015). The presence of intermetallic compounds in the composite material is one key factor that can contribute to a decrease in electrical conductivity during hot deformation. When the composite material is subjected to high temperatures and pressures during hot deformation, these intermetallic compounds can vary in shape and distribution within the material. This might result in the production of microscopic holes or pores inside the composite material, which can obstruct the flow of electrons through the material and impair its electrical conductivity. An increase in dislocation density is another factor that might lead to a decrease in electrical conductivity during heat deformation. When the composite material is subjected to plastic deformation during hot deformation, dislocations can occur and multiply within the material. These dislocations obstruct the flow of electrons through the material, lowering its electrical conductivity. The copper granules were refined further during the hot extrusion process via dynamic recrystallization, resulting in a decrease in electrical conductivity. As a result, electrons must cross more grain boundaries while flowing in the axial direction, and greater electron scatter at grain borders causes conductivity to drop(T. Li et al., 2021).

CONCLUSION AND RECOMMENDATION

In this experimental study Five samples were synthesized using stir casting with varying weight percentage of silicon carbide (0,3, 6, 9 and 12 wt.%) mixed with 2wt% of Cr and 1%wt.% of Gr at 500rpm stirring speed, 30-minute stirring time and 1200℃ stirring temperatures. To investigate the effect of reinforcement weight percentage on microstructure, corrosion behavior, electrical and mechanical characteristics copper matrix composites have been developed and studied. Based on the experimental results, the best composite was selected and its deformation behavior were investigated using numerical simulation with DEFORM 3D software to determine the effect of extrusion parameters such as ram speed (1, 2, 3, 4 mm/s), extrusion ratio (2, 3, 4, 5), and billet temperature (800, 850 ,900 and 950℃) on damage distribution and extrusion load in hot extrusion condition of copper matrix composite. Grey relational analysis multi-optimization technique was used to predict optimum extrusion parameter combination for minimum damage percentage and extrusion load. With optimum process parameter obtained following numerical simulation selected Cu-6SiC-2Cr-1Gr composite material was deformed using an experimental hot extrusion technique to investigate the deformational behavior of a copper-based metal matrix composite. The grain refinement following the extrusion process exhibits good agreement with theoretical facts regarding the impact of the extrusion technique on the materials. The findings are as follows:

5.1 Conclusion

- Scanning electron microscope showed homogenous dispersion of particle were found while optical microscope image indicated maximum porosity percentage obtained was 5.78% in composite reinforced with 15wt.%
- Hardness tests and density measurements showed that adding silicon carbide, chromium, and graphite to the copper matrix enhanced the metal's mechanical qualities but decreased its electrical conductivity.
- Even though corrosion rate of fabricated sample was increased with increasing weight percentage of reinforcement, corrosion resistant of composites were improved with addition of reinforcement up to 15wt.% when compared to pure copper.

- The addition of SiC-Gr-Cr up to 12%wt enhanced compression strength, although when the amount of reinforcement approaches 15% wt., the compressive strength of the composite decreased due to an increased in brittleness.
- Based on experimental result, Cu-6SiC-2Cr-1Gr hybrid composite was selected for secondary process (hot extrusion) to predict damage distribution and extrusion load via DEFORM 3D.
- ANOVA and S/N ratio results revealed that extrusion ratio is most significant extrusion parameter on both responses. both damage and extrusion load were increased with increasing extrusion ratio of cosine die. The optimum prediction condition for multi-response features has been obtained using HTGRA at extrusion ratio of 2, ram speed of 1mm/s and billet temperature of 850℃. Cu-6SiC-2Cr-1Gr composite was finally extruded with optimum combination of parameter using extruder machine.
- Results after extrusion showed that that porosity percentage was decreased from 2.71% to 1.57% when compared to sample before extrusion.
- Compression strength and hardness of Cu-6SiC-2Cr-1Gr were improved by 21.4% and 17.4% following extrusion although electrical conductivity showed slight decrement.

5.2 Recommendation

Based on the results and conclusions found from this study, the following recommendations were made:

- It can be suggested that Cu-SiC-Gr-Cr hybrid composite be employed as a good substitute for materials used in the resistant welding electrode, rail brake disk and heat exchanger because it exhibits larger improvements in hardness, compression strength and corrosion rate than commercial copper.
- Thermal conductivity test could be employed for similar studies
- Machining of developed hybrid composite material can be done.
- In this study, a few mechanical properties were studied and characterized. Other tests, like as wear, tensile and impact tests, can be employed in similar studies.

SPECIAL AKCKOWLEDGEMENT

This research work is funded by Adama Science and Technology University under the grant number ASTU/SM-R/912/23, Adama, Ethiopia.

REFERENCES

Akbarpour, M. R., Mousa Mirabad, H., & Alipour, S. (2019). Microstructural and mechanical characteristics of hybrid SiC/Cu composites with nano- and micro-sized SiC particles. *Ceramics International*, *45*(3), 3276–3283. https://doi.org/10.1016/j.ceramint.2018.10.235

Akbarpour, M. R., Mousa Mirabad, H., Khalili Azar, M., Kakaei, K., & Kim, H. S. (2020). Synergistic role of carbon nanotube and SiCn reinforcements on mechanical properties and corrosion behavior of Cu-based nanocomposite developed by flake powder metallurgy and spark plasma sintering process. *Materials Science and Engineering A*, *786*, 139395. https://doi.org/10.1016/j.msea.2020.139395

Akhtar, F., Askari, S. J., Shah, K. A., Du, X., & Guo, S. (2009). Microstructure, mechanical properties, electrical conductivity and wear behavior of high volume TiC reinforced Cu-matrix composites. *Materials Characterization*, *60*(4), 327–336. https://doi.org/10.1016/j.matchar.2008.09.014

Aktar Zahid Sohag, M., Gupta, P., Kondal, N., Kumar, D., Singh, N., & Jamwal, A. (2020). Effect of ceramic reinforcement on the microstructural, mechanical and tribological behavior of Al-Cu alloy metal matrix composite. *Materials Today: Proceedings*, *21*(xxxx), 1407–1411. https://doi.org/10.1016/j.matpr.2019.08.179

Alaneme, K. K., & Odoni, B. U. (2016). Mechanical properties, wear and corrosion behavior of copper matrix composites reinforced with steel machining chips. *Engineering Science and Technology, an International Journal*, *19*(3), 1593–1599. https://doi.org/10.1016/j.jestch.2016.04.006

Alaneme, K. K., Okotete, E. A., Fajemisin, A. V., & Bodunrin, M. O. (2019). Applicability of metallic reinforcements for mechanical performance enhancement in metal matrix composites: a review. *Arab Journal of Basic and Applied Sciences*, *26*(1), 311–330. https://doi.org/10.1080/25765299.2019.1628689

Ali, Z., Muthuraman, V., Rathnakumar, P., Gurusamy, P., & Nagaral, M. (2020). Investigation on the tribological properties of copper alloy reinforced with Gr/Zro2 particulates by stir casting route. *Materials Today: Proceedings*, *33*(xxxx), 3449–3453. https://doi.org/10.1016/j.matpr.2020.05.351

Anandaraj, T., Sethusundaram, P. P., Chanakyan, C., Sakthivelu, S., & Meignanamoorthy, M. (2020). Influence of different reinforcements on properties of metal matrix composites: A review. *Materials Today: Proceedings*, *37*(Part 2), 3480–3484. https://doi.org/10.1016/j.matpr.2020.09.386

Anil Kumar, B. K., Ananthaprasad, M. G., & GopalaKrishna, K. (2016). A review on mechanical and tribological behaviors of nickel matrix composites. *Indian Journal of Science and Technology*, *9*(2), 2658–2664. https://doi.org/10.17485/ijst/2016/v9i2/82868

Argon, A. S. (2007). Strain Hardening. *Strengthening Mechanisms in Crystal Plasticity*, *50*, 283–343. https://doi.org/10.1093/acprof:oso/9780198516002.003.0007

Astm, B., Brass-headquarters, O., & Mill, O. B. (2013). *C15100*. *107*.

Atuanya, C. U., & Aigbodion, V. S. (2014). Evaluation of Al-Cu-Mg alloy/bean pod ash nanoparticles synthesis by double layer feeding-stir casting method. *Journal of Alloys and Compounds*, *601*, 251–259. https://doi.org/10.1016/j.jallcom.2014.02.086

Ayyappadas, C., Muthuchamy, A., Raja Annamalai, A., & Agrawal, D. K. (2017). An investigation on the effect of sintering mode on various properties of copper-graphene metal matrix composite. *Advanced Powder Technology*, *28*(7), 1760–1768. https://doi.org/10.1016/j.apt.2017.04.013

Azaath, L. M., Natarajan, U., Veerappan, G., Ravichandran, M., & Marichamy, S. (2022). Experimental Investigations on the Mechanical Properties, Microstructure and Corrosion Effect of Cu-20Al-4Ni/SiC Composites Synthesized Using Powder metallurgy Route. *Silicon*, *14*(11), 5993–6002. https://doi.org/10.1007/s12633-021-01363-2

Bagheri, G. A. (2016). The effect of reinforcement percentages on properties of copper matrix composites reinforced with TiC particles. *Journal of Alloys and Compounds*, *676*, 120–126. https://doi.org/10.1016/j.jallcom.2016.03.085

Bakhtiari, H., Karimi, M., & Rezazadeh, S. (2016). Modeling, analysis and multi-objective optimization of twist extrusion process using predictive models and meta-heuristic approaches, based on finite element results. *Journal of Intelligent Manufacturing*, *27*(2), 463–473. https://doi.org/10.1007/s10845-014-0879-6

Balamurugan, P., & Uthayakumar, M. (2015). Influence of process parameters on Cu-fly ash composite by powder metallurgy technique. *Materials and Manufacturing Processes*, *30*(3), 313–319. https://doi.org/10.1080/10426914.2014.984220

Barnhart, J. (1997). Occurrences, Uses, and Properties of Chromium. *Regulatory Toxicology and Pharmacology*, *26*(1 I), 3–7. https://doi.org/10.1006/rtph.1997.1132

Boulger, F. W. (2016). *Flow Stress of Metals and Its Application in Metal Forming Analyses*. *November 1973*.

Brabazon, D., Browne, D. J., & Carr, A. J. (2002). Mechanical stir casting of aluminium alloys from the mushy state: Process, microstructure and mechanical properties. *Materials Science and Engineering A*, *326*(2), 370–381. https://doi.org/10.1016/S0921-5093(01)01832-9

Chawla, K. K. (2012). Composite materials: Science and engineering, third edition. In *Composite Materials: Science and Engineering, Third Edition* (Issue 1994). https://doi.org/10.1007/978-0-387-74365-3

Dasgupta, R. (2012). Aluminium Alloy-Based Metal Matrix Composites: A Potential Material for Wear Resistant Applications. *ISRN Metallurgy*, *2012*, 1–14. https://doi.org/10.5402/2012/594573

Dehghan Hamedan, A., & Shahmiri, M. (2012). Production of A356-1wt% SiC nanocomposite by the modified stir casting method. *Materials Science and Engineering A*, *556*, 921–926. https://doi.org/10.1016/j.msea.2012.07.093

Dong, S. R., Tu, J. P., & Zhang, X. B. (2001). An investigation of the sliding wear behavior of Cu-matrix composite reinforced by carbon nanotubes. *Materials Science and Engineering A*, *313*(1–2), 83–87. https://doi.org/10.1016/S0921-5093(01)00963-7

Duong, X. T., Mayer, J. R. R., & Balazinski, M. (2016). Initial tool wear behavior during machining of titanium metal matrix composite (TiMMCs). *International Journal of Refractory Metals and Hard Materials*, *60*, 169–176. https://doi.org/10.1016/j.ijrmhm.2016.07.021

Feijoo, I., Merino, P., Pena, G., Rey, P., & Cabeza, M. (2020). Microstructure and mechanical properties of an extruded 6005a al alloy composite reinforced with tic nanosized particles and strengthened by precipitation hardening. *Metals*, *10*(8), 1–15. https://doi.org/10.3390/met10081050

Gao, X., Yue, H., Guo, E., Zhang, H., Lin, X., Yao, L., & Wang, B. (2016). Mechanical properties and thermal conductivity of graphene reinforced copper matrix composites. *Powder Technology*, *301*, 601–607. https://doi.org/10.1016/j.powtec.2016.06.045

Gautam, Y. K., Somani, N., Kumar, M., & Sharma, S. K. (2018). A review on fabrication and characterization of copper metal matrix composite (CMMC). *AIP Conference Proceedings*, *2018*(Cmmc). https://doi.org/10.1063/1.5058254

Ghosh, P. K., Ray, S., & Rohatgi, P. K. (1984). Incorporation of Alumina Particles in Aluminium-Magnesium Alloy By Stirring in Melt. *Transactions of the Japan Institute of Metals*, *25*(6), 440–444. https://doi.org/10.2320/matertrans1960.25.440

Gupta, P., Kumar, D., Parkash, O., & Jha, A. K. (2013). Structural and mechanical behaviour of 5% Al2O3-reinforced Fe metal matrix composites (MMCs) produced by powder metallurgy (P/M) route. *Bulletin of Materials Science*, *36*(5), 859–868. https://doi.org/10.1007/s12034-013-0545-1

Hannula, P. M., Masquelier, N., Lassila, S., Aromaa, J., Janas, D., Forsén, O., & Lundström, M. (2018). Corrosion behaviour of cast and deformed copper-carbon nanotube composite wires in chloride media. *Journal of Alloys and Compounds*, *746*, 218–226. https://doi.org/10.1016/j.jallcom.2018.02.289

Hashim, J., Looney, L., & Hashmi, M. S. J. (2002). Particle distribution in cast metal matrix composites - Part I. *Journal of Materials Processing Technology*, *123*(2), 251–257. https://doi.org/10.1016/S0924-0136(02)00098-5

Hsia, S. Y. (2013). Optimization of microextrusion preforming using taguchi method. *Mathematical Problems in Engineering*, *2013*. https://doi.org/10.1155/2013/305797

Idusuyi, N., & Olayinka, J. I. (2019). Dry sliding wear characteristics of aluminium metal matrix composites: A brief overview. *Journal of Materials Research and Technology*, *8*(3), 3338–3346. https://doi.org/10.1016/j.jmrt.2019.04.017

Jabinth, J., & Selvakumar, N. (2021). Enhancing the mechanical, wear behaviour of copper matrix composite with 2V-Gr as reinforcement. *Proceedings of the*

Institution of Mechanical Engineers, Part J: Journal of Engineering Tribology, *235*(7), 1405–1419. https://doi.org/10.1177/1350650120960573

Jajimoggala, S., Dhananjay, R., Lakshmi, V. V. K., & Shabana. (2019). Multi-response optimization of hot extrusion process parameters using FEM and Grey relation based Taguchi method. *Materials Today: Proceedings*, *18*, 389–401. https://doi.org/10.1016/j.matpr.2019.06.316

Jamaati, R., & Toroghinejad, M. R. (2010). Application of ARB process for manufacturing high-strength, finely dispersed and highly uniform Cu/Al2O3 composite. *Materials Science and Engineering A*, *527*(27–28), 7430–7435. https://doi.org/10.1016/j.msea.2010.08.038

Jamwal, A., Mittal, P., Agrawal, R., Gupta, S., Kumar, D., Sadasivuni, K. K., & Gupta, P. (2020). Towards sustainable copper matrix composites: Manufacturing routes with structural, mechanical, electrical and corrosion behaviour. *Journal of Composite Materials*, *54*(19), 2635–2649. https://doi.org/10.1177/0021998319900655

Jamwal, A., Prakash, P., Kumar, D., Singh, N., Sadasivuni, K. K., Harshit, K., Gupta, S., & Gupta, P. (2019). Microstructure, wear and corrosion characteristics of Cu matrix reinforced SiC–graphite hybrid composites. *Journal of Composite Materials*, *53*(18), 2545–2553. https://doi.org/10.1177/0021998319832961

Jamwal, A., Seth, P. P., Kumar, D., Agrawal, R., Sadasivuni, K. K., & Gupta, P. (2020). Microstructural, tribological and compression behaviour of Copper matrix reinforced with Graphite-SiC hybrid composites. *Materials Chemistry and Physics*, *251*, 123090. https://doi.org/10.1016/j.matchemphys.2020.123090

Jojith, R., & Radhika, N. (2019). Mechanical and tribological properties of LM13/TiO2/MoS2 hybrid metal matrix composite synthesized by stir casting. *Particulate Science and Technology*, *37*(5), 566–578. https://doi.org/10.1080/02726351.2017.1407381

Kennedy, A. R., Wood, J. D., & Weager, B. M. (2000). Wetting and spontaneous infiltration of ceramics by molten copper. *Journal of Materials Science*, *35*(12), 2909–2912. https://doi.org/10.1023/A:1004714407371

Kothasiri, A. F., & Chalamalasetti, S. R. (2022). Investigation of Cold Extrusion of

Aluminum AA 2024 Alloy using Finite Element Analysis. *INCAS Bulletin*, *14*(3), 157–171. https://doi.org/10.13111/2066-8201.2022.14.3.14

Kumar Singh, M., Kumar Gautam, R., Prakash, R., & Ji, G. (2018). Mechanical and corrosion behaviors of developed copper-based metal matrix composites. *IOP Conference Series: Materials Science and Engineering*, *330*(1). https://doi.org/10.1088/1757-899X/330/1/012021

Li, T., Wang, Y., Yang, M., Hou, H., & Wu, S. (2021). High strength and conductivity copper matrix composites reinforced by in-situ graphene through severe plastic deformation processes. *Journal of Alloys and Compounds*, *851*, 156703. https://doi.org/10.1016/j.jallcom.2020.156703

Li, X., Zhou, C., Overman, N., Ma, X., Canfield, N., Kappagantula, K., Schroth, J., & Grant, G. (2021). Copper carbon composite wire with a uniform carbon dispersion made by friction extrusion. *Journal of Manufacturing Processes*, *65*(March), 397–406. https://doi.org/10.1016/j.jmapro.2021.03.055

Liu, Y., Chen, J., Li, Z., Wang, X., Zhang, P., & Liu, J. (2021). AlCoCrFeNi high entropy alloy reinforced Cu-based composite with high strength and ductility after hot extrusion. *Vacuum*, *184*(July 2020), 109882. https://doi.org/10.1016/j.vacuum.2020.109882

Lunk, H. J. (2015). Discovery, properties and applications of chromium and its compounds. *ChemTexts*, *1*(1). https://doi.org/10.1007/s40828-015-0007-z

Ma, Y., Du, Z., Cui, X., Cheng, J., Liu, G., Gong, T., Liu, H., Wang, X., Chen, Y. Y., Rusnák, J., Malega, P., Svetlík, J., Rudy, V., Šmajda, N., Processes, F., Sethi, G., Myers, N. S., German, R. M., Working, C., … Thouas, G. A. (2016). University of Basrah College of Engineering Mechanical Engineering Department Lecture Notes of MANUFACTURING PROCESSES (ME337), 3. *Progress in Natural Science: Materials International*, *28*(6), 1–57. http://dx.doi.org/10.1016/j.mser.2014.10.001%0Ahttps://doi.org/10.1016/j.pnsc.2018.10.004

Malaki, M., Tehrani, A. F., Niroumand, B., & Gupta, M. (2021). Wettability in metal matrix composites. *Metals*, *11*(7), 1–24. https://doi.org/10.3390/met11071034

Markforged. (2018). H13 Tool Steel. *Material Datasheet*, 1.

http://www.astmsteel.com/product/h13-tool-steel-x40crmov5-1-skd61-hot-work-steel/

Mazaheri, Y., Bahiraei, M., Jalilvand, M. M., Ghasemi, S., & Heidarpour, A. (2021). Improving mechanical and tribological performances of pure copper matrix surface composites reinforced by Ti2AlC MAX phase and MoS2 nanoparticles. *Materials Chemistry and Physics*, *270*(April), 124790. https://doi.org/10.1016/j.matchemphys.2021.124790

Meher, A., & Chaira, D. (2017). Effect of Graphite and SiC Addition into Cu and SiC Particle Size Effect on Fabrication of Cu–Graphite–SiC MMC by Powder Metallurgy. *Transactions of the Indian Institute of Metals*, *70*(8), 2047–2057. https://doi.org/10.1007/s12666-016-1026-1

Miller, P. A., & Vecchio, F. J. (2004). *VecTor-Blast User ' s Manual Table of Contents*. *1*(August), 1–368.

Mishra, B., Mohapatra, S. K., Ranjan, V., & Maity, K. (2019). Equal channel angular pressing of the aluminium alloy: A numerical investigation. *Materials Today: Proceedings*, *26*(xxxx), 2173–2178. https://doi.org/10.1016/j.matpr.2020.02.474

MOAZAMI-GOUDARZI, M., & NEMATI, A. (2018). Tribological behavior of self lubricating Cu/MoS2 composites fabricated by powder metallurgy. *Transactions of Nonferrous Metals Society of China (English Edition)*, *28*(5), 946–956. https://doi.org/10.1016/S1003-6326(18)64729-6

Mohapatra, S. K. (2016). *Aluminium Based Material Extrusion through Mathematical Contoured Die : Numerical & Experimental Investigation Certificate of Examination*. *512*.

Mohapatra, S. K., & Maity, K. P. (2016). Parametric Optimization of Simulated Extrusion of Square to Square Section Through Linear Converging Die. *IOP Conference Series: Materials Science and Engineering*, *115*(1). https://doi.org/10.1088/1757-899X/115/1/012031

Mohapatra, S. K., Mishra, S. B., Joshi, K. K., & Pradhan, S. (2019). Effect of the hot deformation on mechanical and wear characteristics of the P/M AMC. *Materials Today: Proceedings*, *18*, 5040–5047. https://doi.org/10.1016/j.matpr.2019.07.498

Moustafa, S. F., Abdel-Hamid, Z., & Abd-Elhay, A. M. (2002). Copper matrix SiC and

Al2O3 particulate composites by powder metallurgy technique. *Materials Letters*, *53*(4–5), 244–249. https://doi.org/10.1016/S0167-577X(01)00485-2

Nageswaran, G., Natarajan, S., & Ramkumar, K. R. (2018). Synthesis, structural characterization, mechanical and wear behaviour of Cu-TiO2-Gr hybrid composite through stir casting technique. *Journal of Alloys and Compounds*, *768*, 733–741. https://doi.org/10.1016/j.jallcom.2018.07.288

Nizam, S., Ab, B., Zaniel, M., Mahadzir, B., Amri, M., & Lajis, B. (2020). *Fracture Mode Effect Using Finite Element Analysis on Recycling Aluminium Chips*. *1*(1), 26–33.

Poddar, P., Srivastava, V. C., De, P. K., & Sahoo, K. L. (2007). Processing and mechanical properties of SiC reinforced cast magnesium matrix composites by stir casting process. *Materials Science and Engineering A*, *460–461*, 357–364. https://doi.org/10.1016/j.msea.2007.01.052

Pradhan, P., Nanda, B. P., & Satapathy, A. (2020). Polyester composites filled with walnut shell powder: Preparation and thermal characterization. *Polymer Composites*, *41*(8), 3294–3308. https://doi.org/10.1002/pc.25620

Prajapati, P. K., & Chaira, D. (2019). Fabrication and Characterization of Cu–B 4 C Metal Matrix Composite by Powder Metallurgy: Effect of B 4 C on Microstructure, Mechanical Properties and Electrical Conductivity. *Transactions of the Indian Institute of Metals*, *72*(3), 673–684. https://doi.org/10.1007/s12666-018-1518-2

PRAKASH, K. S., THANKACHAN, T., & RADHAKRISHNAN, R. (2017). Parametric optimization of dry sliding wear loss of copper–MWCNT composites. *Transactions of Nonferrous Metals Society of China (English Edition)*, *27*(3), 627–637. https://doi.org/10.1016/S1003-6326(17)60070-0

Qin, Y. –Q, Tian, Y., Peng, Y. –Q, Luo, L. –M, Zan, X., Xu, Q., & Wu, Y. –C. (2020). Research status and development trend of preparation technology of ceramic particle dispersion strengthened copper-matrix composites. *Journal of Alloys and Compounds*, *848*, 156475. https://doi.org/10.1016/j.jallcom.2020.156475

Rajan, S. T. K., Balaji, A. N., Raghav, G. R., & Vettivel, S. C. (2019). Compression and corrosion behaviour of sintered copper-fly ash composite material. *Materials*

Research Express, *6*(4). https://doi.org/10.1088/2053-1591/aafaec

Ramanathan, A., Krishnan, P. K., & Muraliraja, R. (2019). A review on the production of metal matrix composites through stir casting – Furnace design, properties, challenges, and research opportunities. *Journal of Manufacturing Processes*, *42*(December 2018), 213–245. https://doi.org/10.1016/j.jmapro.2019.04.017

Ren, F., Zhi, A., Zhang, D., Tian, B., Volinsky, A. A., & Shen, X. (2015). Preparation of Cu-Al2O3 bulk nano-composites by combining Cu-Al alloy sheets internal oxidation with hot extrusion. *Journal of Alloys and Compounds*, *633*, 323–328. https://doi.org/10.1016/j.jallcom.2015.02.057

Rhee, K. Y., Han, W. Y., Park, H. J., & Kim, S. S. (2004). Fabrication of aluminum/copper clad composite using hot hydrostatic extrusion process and its material characteristics. *Materials Science and Engineering A*, *384*(1–2), 70–76. https://doi.org/10.1016/j.msea.2004.05.051

Rizi, vahid salimian. (2019). Ce Pte Us Pt. *Materials Research Express*, 0–12.

Salvo, C., Mangalaraja, R. V., Udayabashkar, R., Lopez, M., & Aguilar, C. (2019). Enhanced mechanical and electrical properties of novel graphene reinforced copper matrix composites. *Journal of Alloys and Compounds*, *777*, 309–316. https://doi.org/10.1016/j.jallcom.2018.10.357

Sankhla, A., & Patel, K. M. (2021). Metal Matrix Composites Fabricated by Stir Casting Process–A Review. *Advances in Materials and Processing Technologies*, *00*(00), 1–22. https://doi.org/10.1080/2374068X.2020.1855404

Shabani, M., Paydar, M. H., Zamiri, R., Goodarzi, M., & Moshksar, M. M. (2016). Microstructural and sliding wear behavior of SiC-particle reinforced copper matrix composites fabricated by sintering and sinter-forging processes. *Journal of Materials Research and Technology*, *5*(1), 5–12. https://doi.org/10.1016/j.jmrt.2015.03.002

Shehata, F., Fathy, A., Abdelhameed, M., & Moustafa, S. F. (2009). Preparation and properties of Al2O3 nanoparticle reinforced copper matrix composites by in situ processing. *Materials and Design*, *30*(7), 2756–2762. https://doi.org/10.1016/j.matdes.2008.10.005

Singh, J., & Sharma, R. K. (2016). Assessing the effects of different dielectrics on environmentally conscious powder-mixed EDM of difficult-to-machine material (WC-Co). *Frontiers of Mechanical Engineering*, *11*(4), 374–387. https://doi.org/10.1007/s11465-016-0388-8

Singh, M. K., & Gautam, R. K. (2017). Synthesis of Copper Metal Matrix Hybrid Composites Using Stir Casting Technique and Its Mechanical, Optical and Electrical Behaviours. *Transactions of the Indian Institute of Metals*, *70*(9), 2415–2428. https://doi.org/10.1007/s12666-017-1103-0

Singh, M. K., Gautam, R. K., & Ji, G. (2019). Mechanical properties and corrosion behavior of copper based hybrid composites synthesized by stir casting. *Results in Physics*, *13*, 102319. https://doi.org/10.1016/j.rinp.2019.102319

Street, H. (2016). Silicon Carbide Material Properties. *Accuratus Tech Sheet*, 8865. https://accuratus.com/silicar.html

Suman, P., Kumar Bannaravuri, P., Baburao, G., Ratna Kandavalli, S., Alam, S., Shanthiraju, M., & Swamy Pulisheru, K. (2021). Integrity on properties of Cu-based composites with the addition of reinforcement: A review. *Materials Today: Proceedings*, *47*(xxxx), 6609–6613. https://doi.org/10.1016/j.matpr.2021.05.096

Taha, M. A., & Zawrah, M. F. (2017). Effect of nano ZrO2 on strengthening and electrical properties of Cu-matrix nanocomposits prepared by mechanical alloying. *Ceramics International*, *43*(15), 12698–12704. https://doi.org/10.1016/j.ceramint.2017.06.153

Thomas, A. T., Parameshwaran, R., Muthukrishnan, A., & Kumaran, M. A. (2014). Development of Feeding & Stirring Mechanisms for Stir Casting of Aluminium Matrix Composites. *Procedia Materials Science*, *5*, 1182–1191. https://doi.org/10.1016/j.mspro.2014.07.415

Tiernan, P., Hillery, M. T., Draganescu, B., & Gheorghe, M. (2005). Modelling of cold extrusion with experimental verification. *Journal of Materials Processing Technology*, *168*(2), 360–366. https://doi.org/10.1016/j.jmatprotec.2005.02.249

Uzun, M., & Usca, U. A. (2018). Effect of Cr particulate reinforcements in different ratios on wear performance and mechanical properties of Cu matrix composites. *Journal of the Brazilian Society of Mechanical Sciences and Engineering*, *40*(4). https://doi.org/10.1007/s40430-018-1130-8

Varo, T., & Canakci, A. (2015). Effect of the CNT Content on Microstructure, Physical and Mechanical Properties of Cu-Based Electrical Contact Materials Produced by Flake Powder Metallurgy. *Arabian Journal for Science and Engineering*, *40*(9), 2711–2720. https://doi.org/10.1007/s13369-015-1734-6

Viswanath, A., Dieringa, H., Ajith Kumar, K. K., Pillai, U. T. S., & Pai, B. C. (2015). Investigation on mechanical properties and creep behavior of stir cast AZ91-SiCp composites. *Journal of Magnesium and Alloys*, *3*(1), 16–22. https://doi.org/10.1016/j.jma.2015.01.001

Wagih, A., Abu-Oqail, A., & Fathy, A. (2019). Effect of GNPs content on thermal and mechanical properties of a novel hybrid Cu-Al2O3/GNPs coated Ag nanocomposite. *Ceramics International*, *45*(1), 1115–1124. https://doi.org/10.1016/j.ceramint.2018.10.001

Wang, X., Wang, X., Hu, X., & Wu, K. (2020). Effects of hot extrusion on microstructure and mechanical properties of Mg matrix composite reinforced with deformable TC4 particles. *Journal of Magnesium and Alloys*, *8*(2), 421–430. https://doi.org/10.1016/j.jma.2019.05.015

Work, H., & Steel, T. (n.d.). *EXELL H-13*.

Yang, T. S. (2008). Finite element analysis of elliptic cup deep drawing of magnesium alloy sheet. *Jornal of Achievements in Materials and Manufacturing Engineering*, *27*(2), 139–142.

Zhan, Y., & Zhang, G. (2003). The effect of interfacial modifying on the mechanical and wear properties of SiCp/Cu composites. *Materials Letters*, *57*(29), 4583–4591. https://doi.org/10.1016/S0167-577X(03)00365-3

Zou, C., Chen, Z., Kang, H., Wang, W., Li, R., Li, T., & Wang, T. (2017). Study of enhanced dry sliding wear behavior and mechanical properties of Cu-TiB2 composites fabricated by in situ casting process. *Wear*, *392–393*, 118–125. https://doi.org/10.1016/j.wear.2017.09.016

Zuo, T., Li, J., Gao, Z., Wu, Y., Zhang, L., Da, B., & Zhao, X. (2020). *Simultaneous improvement of electrical conductivity and mechanical property of Cr doped Cu / CNTs composites*. *23*(December 2019). https://doi.org/10.1016/j.mtcomm.2020.100907

Appendix I: Micro-Hardness Result for S-1 and S-2 (From Vickers Hardness)

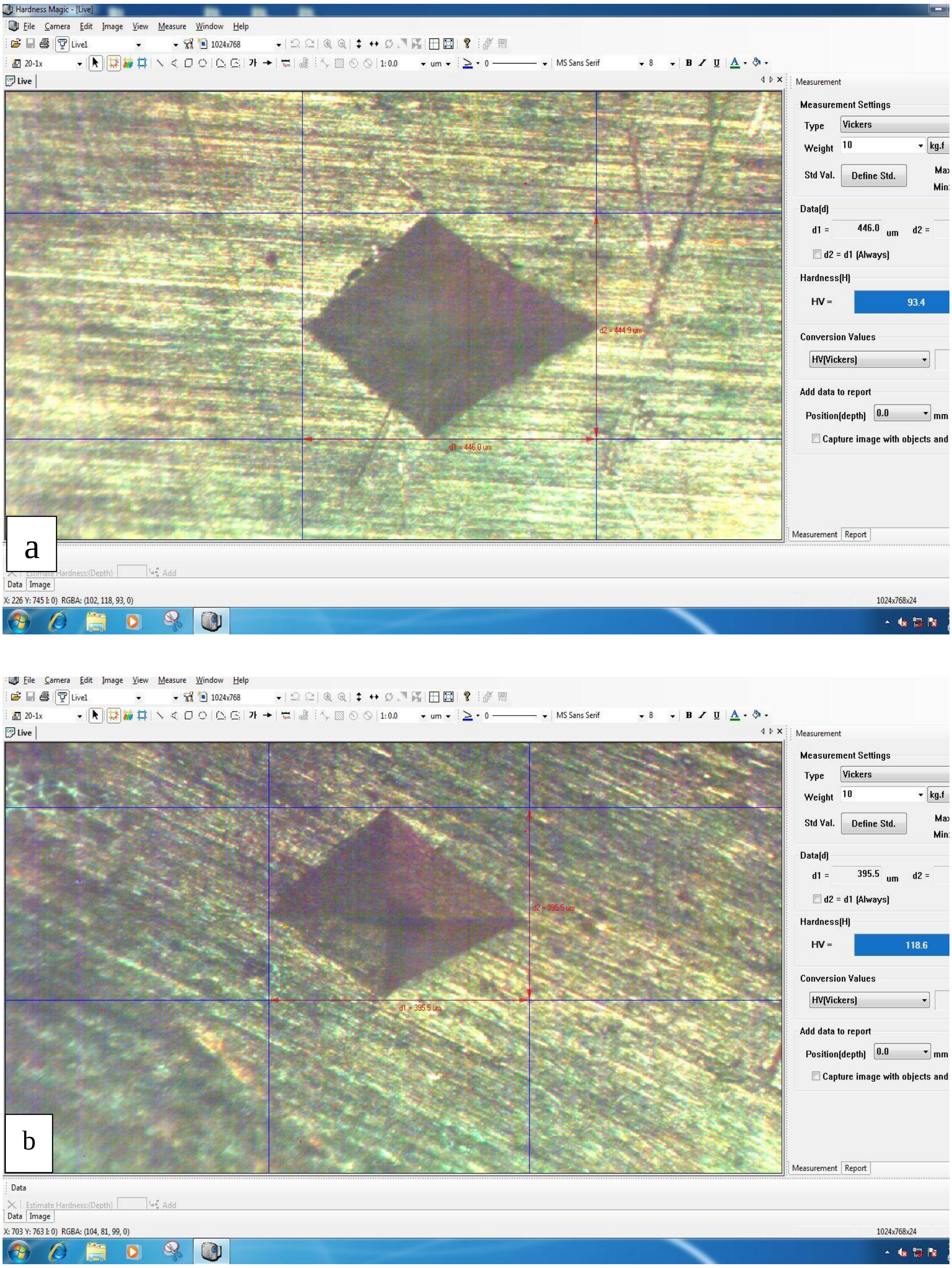

Figure A.1 Microhardness Vickers value of (a) sample 1 and (b) sample 2

Appendix II: Microstructural image of composite from SEM for sample (S1, S2 and S3)

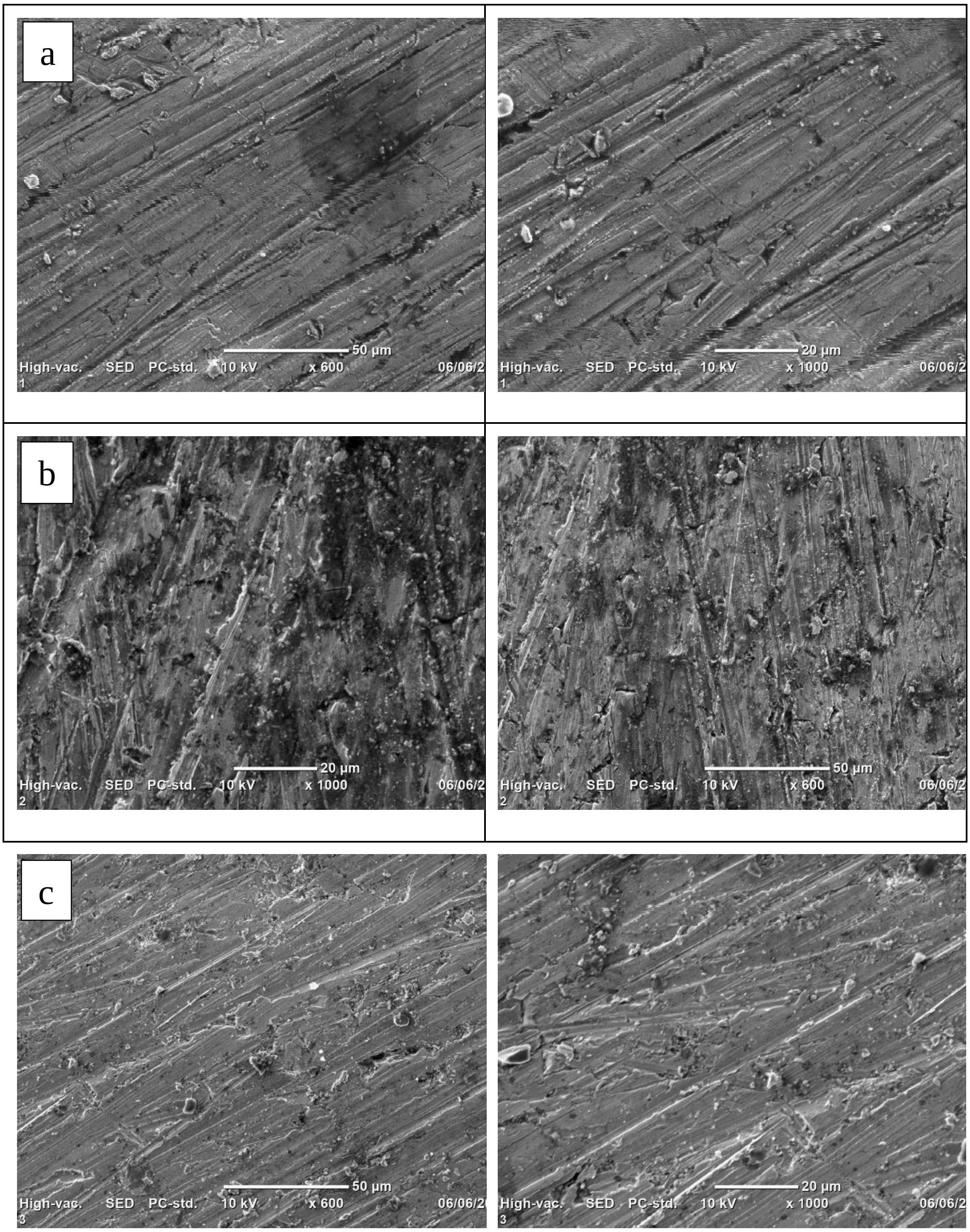

Figure A.2 Microstructural images of composite from SEM for (a) sample 1 (b) sample 2 and (c) sample 3

Appendix III: Microstructural image of composite from optical microscope for sample (S1, S3 and S5)

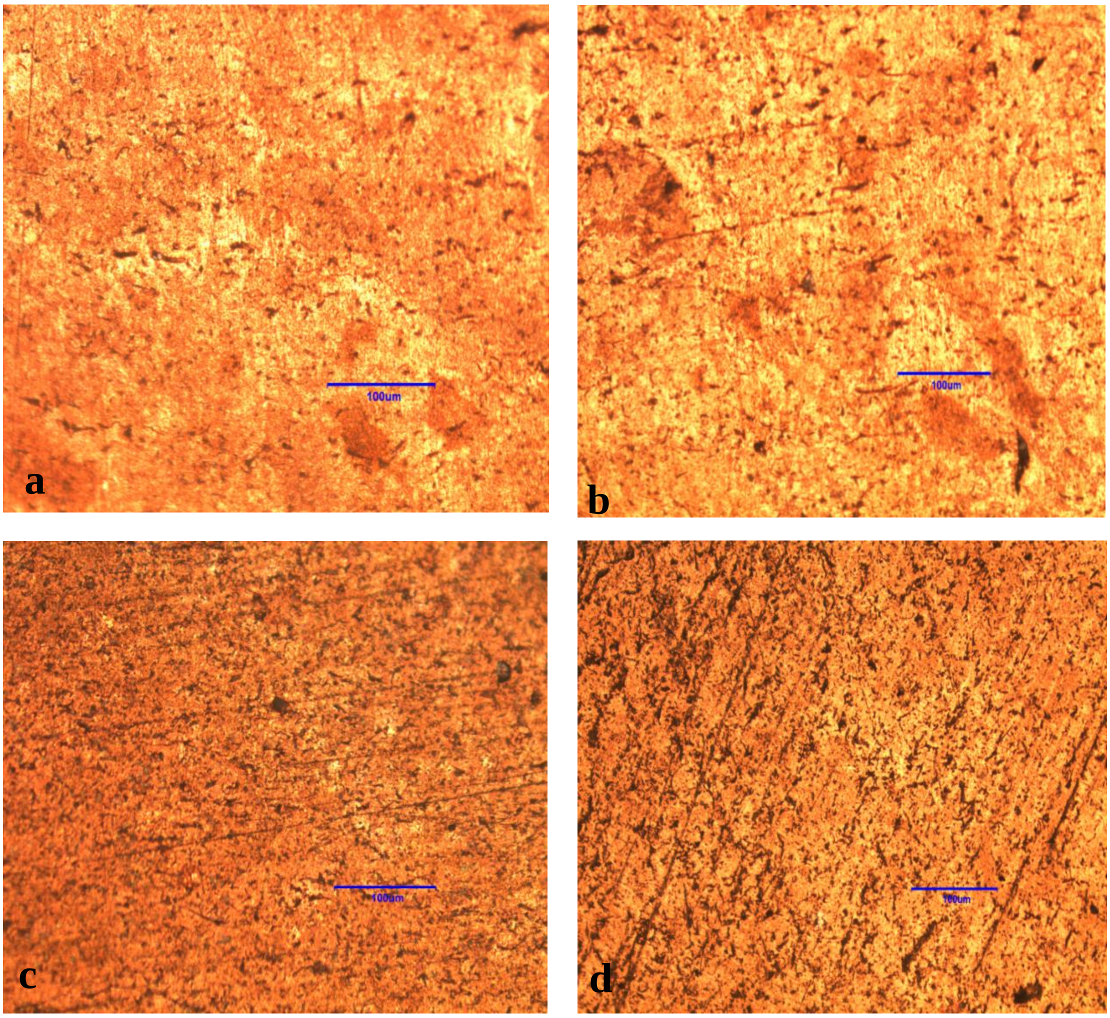

Figure A.3 Microstructural images of composite from optical microscope for (a) sample 1 (b) sample (c) and (d) sample 5

Appendix IV: calculation of current density from Tafel plot

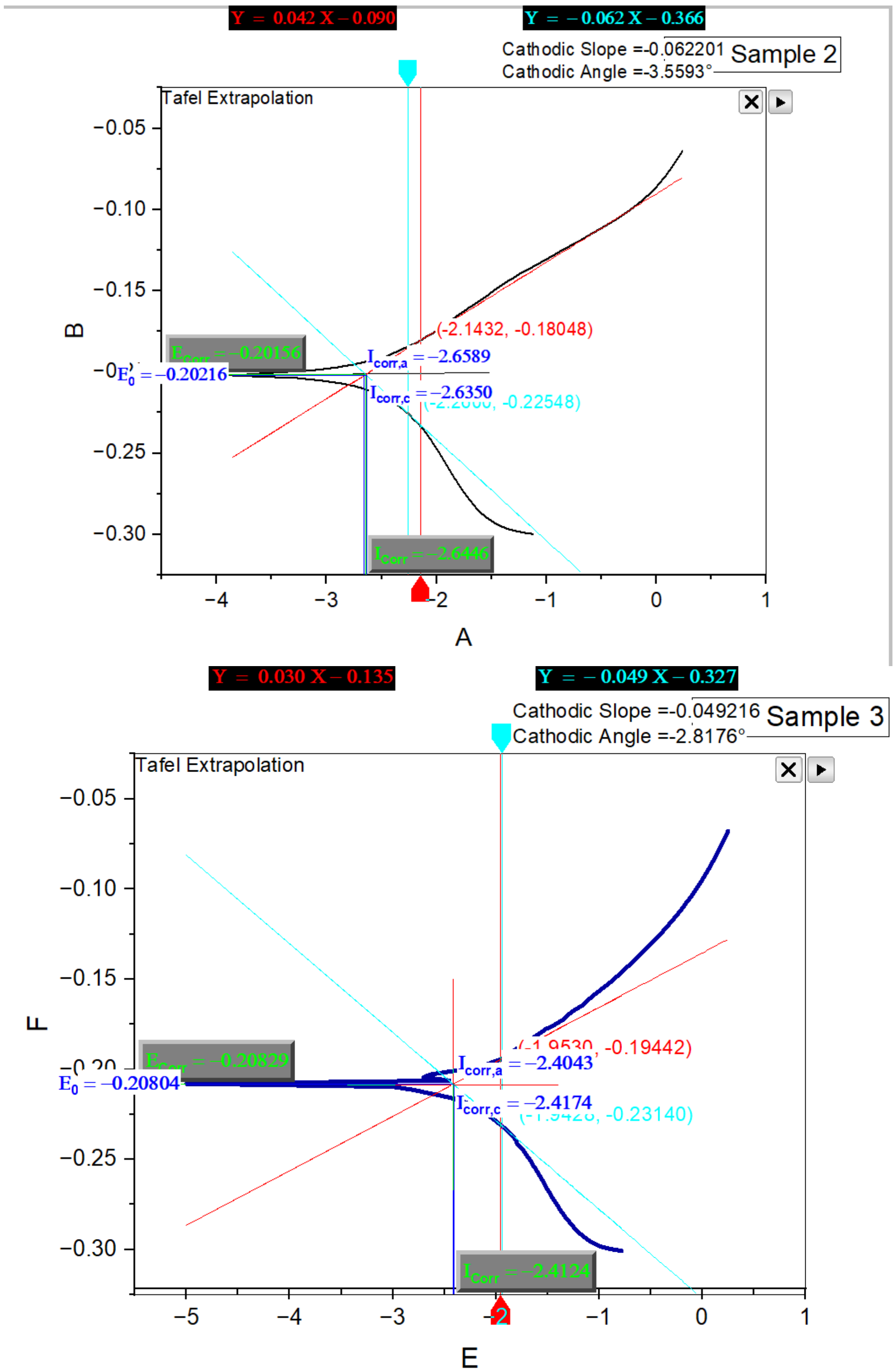

Figure A.4 corrosion current density calculation from Tafel plot

Appendix V: damage distribution of Cu-6SiC-1Gr-2Cr via numerical simulation of hot extrusion

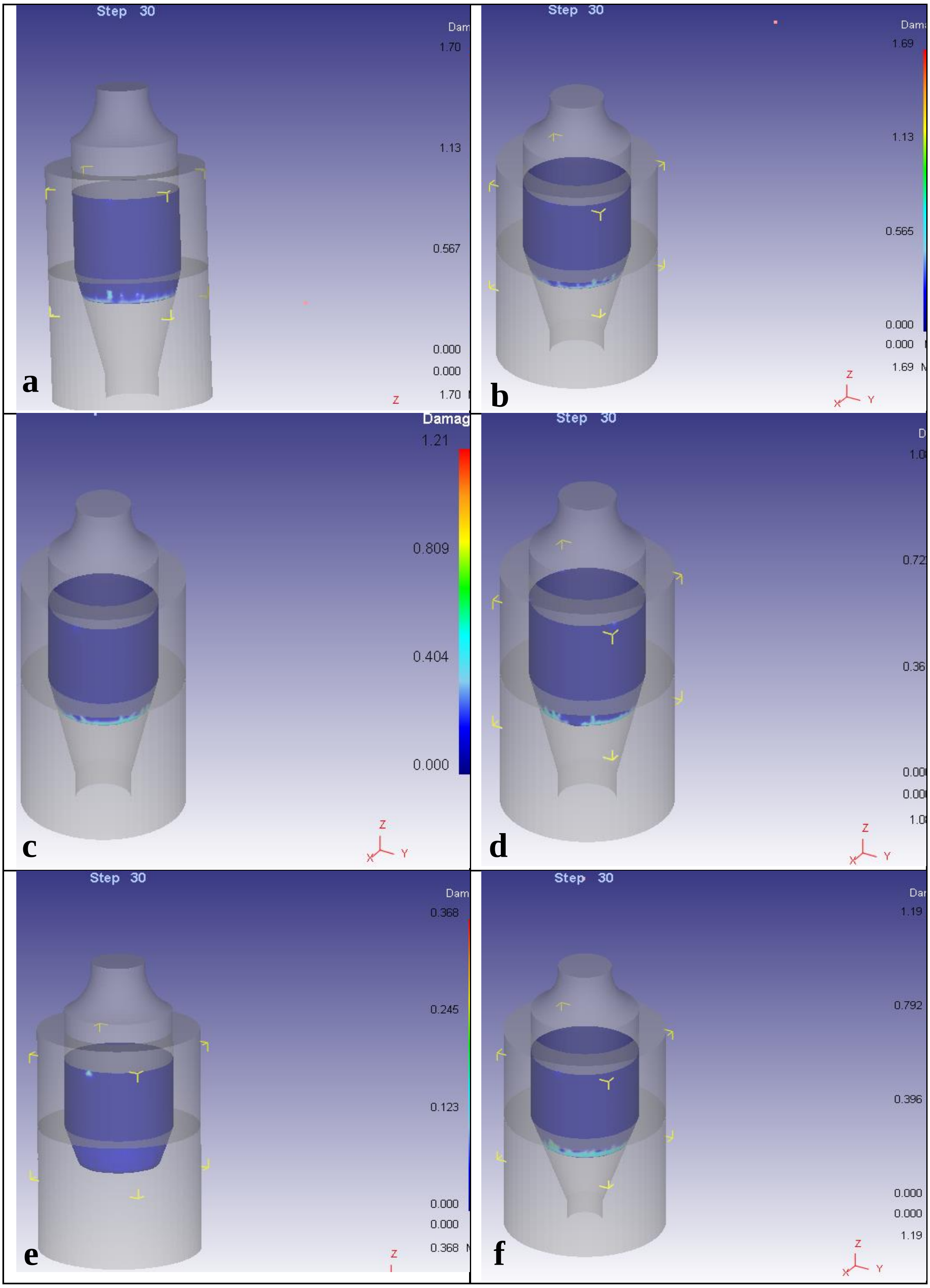

Figure A.6 damage percentage of (a) sample 1 (b) sample 2 (c) sample 3 (d) sample 4) (e) sample 5 and (f) sample 6

Appendix VI: predicted extrusion load of Cu-6SiC-1Gr-2Cr via numerical simulation of hot extrusion

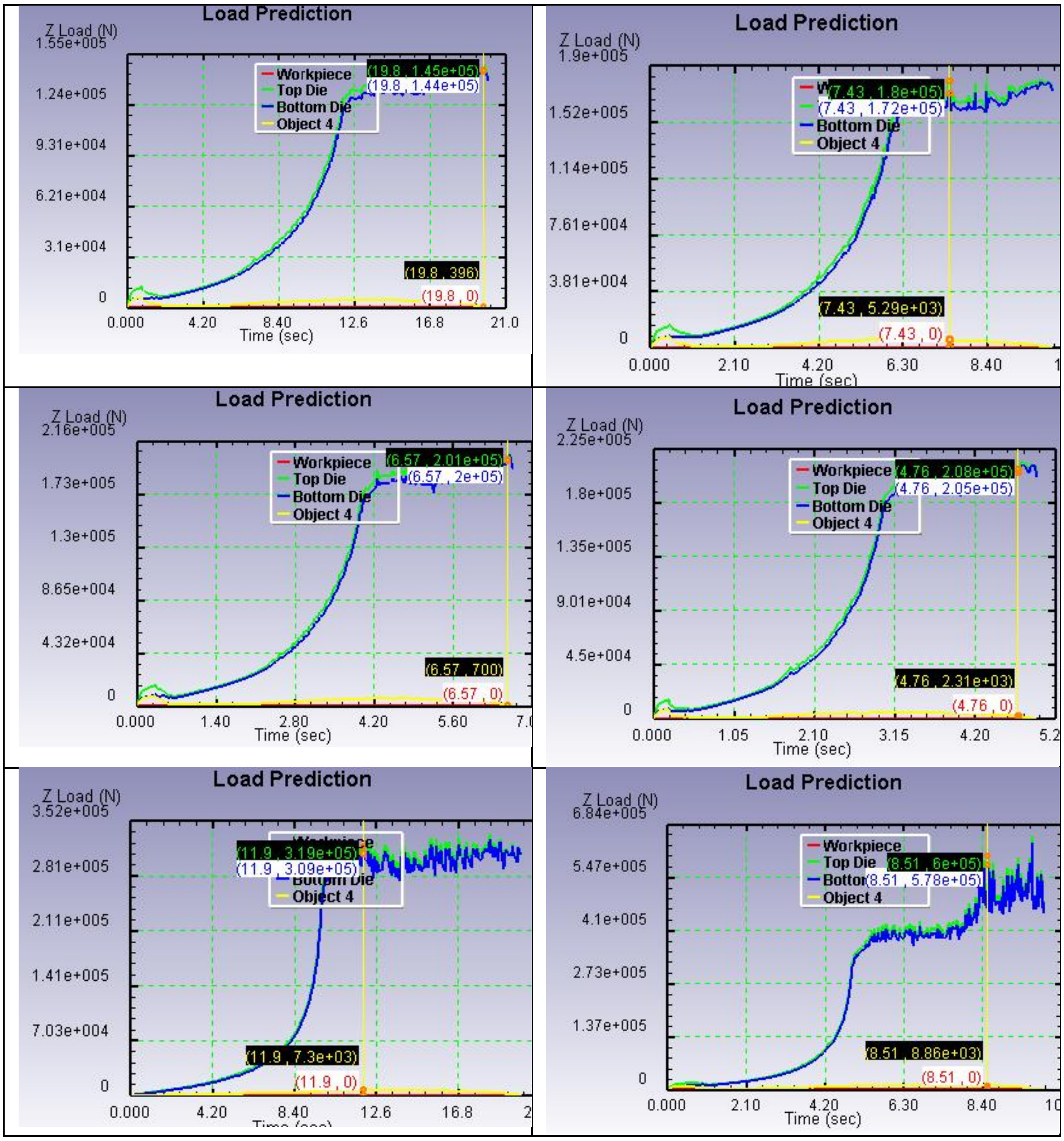

Figure A.7 predicted extrusion load of punch for (a) sample 1 (b) sample 2 (c) sample 3 (d) sample 4) (e) sample 5 and (f) sample 6

Appendix VII: IV curve characteristics for electrical conductivity test

Intercept	Intercept	Slope	Slope	Statistics	
	Value	Standard Error	Value	Standard Error	Adj. R-Square
SAMPLE 1	0.01817	7.41762E-4	0.7212	0.00441	0.99995

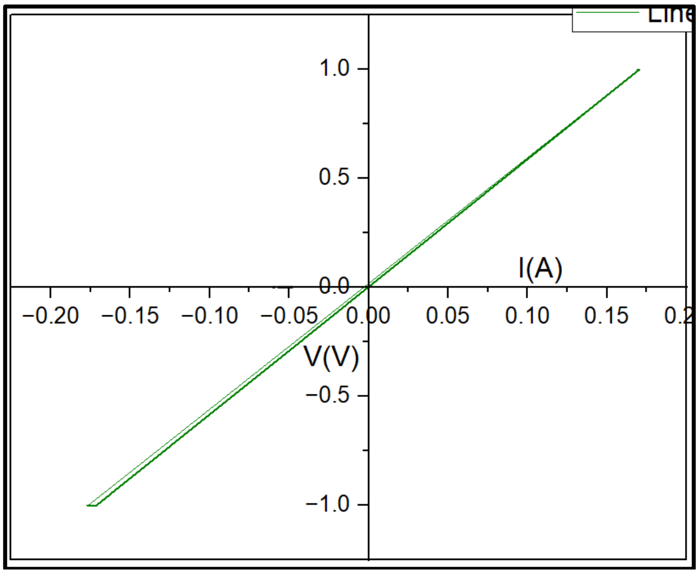

	Intercept	Intercept	Slope	Slope	Statistics
	Value	Standard Error	Value	Standard Error	Adj. R-Square
EXRUDED SAMPLE	0.01722	7.00429E-4	1.1065	0.00448	0.99996

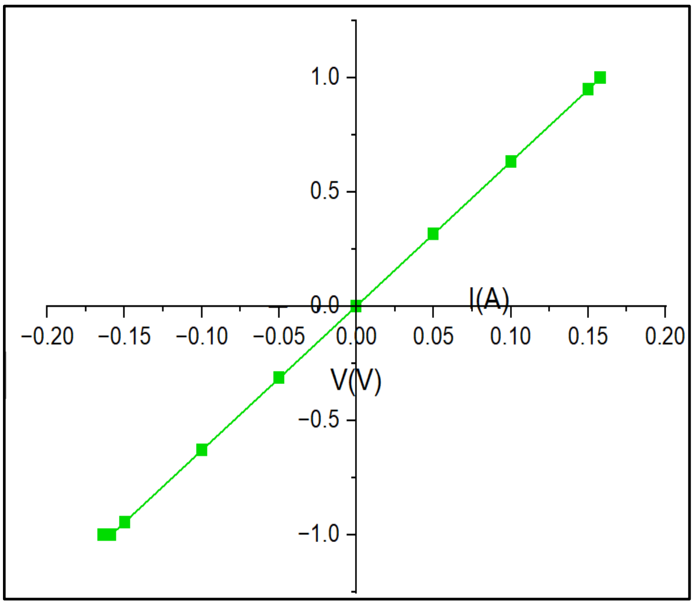

Appendix VIII: Percentage value of f distribution

$f_{0.05,\nu_1,\nu_2}$

ν_2 \ ν_1 (Degrees of Freedom for the Numerator (ν_1))	1	2	3	4	5	6	7	8	9	10	12	15	20	24	30	40	60	120	∞
	161.4	199.5	215.7	224.6	230.2	234.0	236.8	238.9	240.5	241.9	243.9	245.9	248.0	249.1	250.1	251.1	252.2	253.3	254.3
2	18.51	19.00	19.16	19.25	19.30	19.33	19.35	19.37	19.38	19.40	19.41	19.43	19.45	19.45	19.46	19.47	19.48	19.49	19.50
3	10.13	9.55	9.28	9.12	9.01	8.94	8.89	8.85	8.81	8.79	8.74	8.70	8.66	8.64	8.62	8.59	8.57	8.55	8.53
4	7.71	6.94	6.59	6.39	6.26	6.16	6.09	6.04	6.00	5.96	5.91	5.86	5.80	5.77	5.75	5.72	5.69	5.66	5.63
5	6.61	5.79	5.41	5.19	5.05	4.95	4.88	4.82	4.77	4.74	4.68	4.62	4.56	4.53	4.50	4.46	4.43	4.40	4.36
6	5.99	5.14	4.76	4.53	4.39	4.28	4.21	4.15	4.10	4.06	4.00	3.94	3.87	3.84	3.81	3.77	3.74	3.70	3.67
7	5.59	4.74	4.35	4.12	3.97	3.87	3.79	3.73	3.68	3.64	3.57	3.51	3.44	3.41	3.38	3.34	3.30	3.27	3.23
8	5.32	4.46	4.07	3.84	3.69	3.58	3.50	3.44	3.39	3.35	3.28	3.22	3.15	3.12	3.08	3.04	3.01	2.97	2.93
9	5.12	4.26	3.86	3.63	3.48	3.37	3.29	3.23	3.18	3.14	3.07	3.01	2.94	2.90	2.86	2.83	2.79	2.75	2.71
10	4.96	4.10	3.71	3.48	3.33	3.22	3.14	3.07	3.02	2.98	2.91	2.85	2.77	2.74	2.70	2.66	2.62	2.58	2.54
11	4.84	3.98	3.59	3.36	3.20	3.09	3.01	2.95	2.90	2.85	2.79	2.72	2.65	2.61	2.57	2.53	2.49	2.45	2.40
12	4.75	3.89	3.49	3.26	3.11	3.00	2.91	2.85	2.80	2.75	2.69	2.62	2.54	2.51	2.47	2.43	2.38	2.34	2.30
13	4.67	3.81	3.41	3.18	3.03	2.92	2.83	2.77	2.71	2.67	2.60	2.53	2.46	2.42	2.38	2.34	2.30	2.25	2.21
14	4.60	3.74	3.34	3.11	2.96	2.85	2.76	2.70	2.65	2.60	2.53	2.46	2.39	2.35	2.31	2.27	2.22	2.18	2.13
15	4.54	3.68	3.29	3.06	2.90	2.79	2.71	2.64	2.59	2.54	2.48	2.40	2.33	2.29	2.25	2.20	2.16	2.11	2.07
16	4.49	3.63	3.24	3.01	2.85	2.74	2.66	2.59	2.54	2.49	2.42	2.35	2.28	2.24	2.19	2.15	2.11	2.06	2.01
17	4.45	3.59	3.20	2.96	2.81	2.70	2.61	2.55	2.49	2.45	2.38	2.31	2.23	2.19	2.15	2.10	2.06	2.01	1.96
18	4.41	3.55	3.16	2.93	2.77	2.66	2.58	2.51	2.46	2.41	2.34	2.27	2.19	2.15	2.11	2.06	2.02	1.97	1.92
19	4.38	3.52	3.13	2.90	2.74	2.63	2.54	2.48	2.42	2.38	2.31	2.23	2.16	2.11	2.07	2.03	1.98	1.93	1.88
20	4.35	3.49	3.10	2.87	2.71	2.60	2.51	2.45	2.39	2.35	2.28	2.20	2.12	2.08	2.04	1.99	1.95	1.90	1.84
21	4.32	3.47	3.07	2.84	2.68	2.57	2.49	2.42	2.37	2.32	2.25	2.18	2.10	2.05	2.01	1.96	1.92	1.87	1.81
22	4.30	3.44	3.05	2.82	2.66	2.55	2.46	2.40	2.34	2.30	2.23	2.15	2.07	2.03	1.98	1.94	1.89	1.84	1.78
23	4.28	3.42	3.03	2.80	2.64	2.53	2.44	2.37	2.32	2.27	2.20	2.13	2.05	2.01	1.96	1.91	1.86	1.81	1.76
24	4.26	3.40	3.01	2.78	2.62	2.51	2.42	2.36	2.30	2.25	2.18	2.11	2.03	1.98	1.94	1.89	1.84	1.79	1.73
25	4.24	3.39	2.99	2.76	2.60	2.49	2.40	2.34	2.28	2.24	2.16	2.09	2.01	1.96	1.92	1.87	1.82	1.77	1.71
26	4.23	3.37	2.98	2.74	2.59	2.47	2.39	2.32	2.27	2.22	2.15	2.07	1.99	1.95	1.90	1.85	1.80	1.75	1.69
27	4.21	3.35	2.96	2.73	2.57	2.46	2.37	2.31	2.25	2.20	2.13	2.06	1.97	1.93	1.88	1.84	1.79	1.73	1.67
28	4.20	3.34	2.95	2.71	2.56	2.45	2.36	2.29	2.24	2.19	2.12	2.04	1.96	1.91	1.87	1.82	1.77	1.71	1.65
29	4.18	3.33	2.93	2.70	2.55	2.43	2.35	2.28	2.22	2.18	2.10	2.03	1.94	1.90	1.85	1.81	1.75	1.70	1.64
30	4.17	3.32	2.92	2.69	2.53	2.42	2.33	2.27	2.21	2.16	2.09	2.01	1.93	1.89	1.84	1.79	1.74	1.68	1.62
40	4.08	3.23	2.84	2.61	2.45	2.34	2.25	2.18	2.12	2.08	2.00	1.92	1.84	1.79	1.74	1.69	1.64	1.58	1.51
60	4.00	3.15	2.76	2.53	2.37	2.25	2.17	2.10	2.04	1.99	1.92	1.84	1.75	1.70	1.65	1.59	1.53	1.47	1.39
120	3.92	3.07	2.68	2.45	2.29	2.17	2.09	2.02	1.96	1.91	1.83	1.75	1.66	1.61	1.55	1.55	1.43	1.35	1.25
∞	3.84	3.00	2.60	2.37	2.21	2.10	2.01	1.94	1.88	1.83	1.75	1.67	1.57	1.52	1.46	1.39	1.32	1.22	1.00

Degrees of Freedom for the Denominator (ν_2)